# THE PETROLOGY AND GEOCHEMISTRY OF THE FITCHBURG PLUTONIC COMPLEX, CENTRAL MASSACHUSETTS

BY DAVID E. MACZUGA

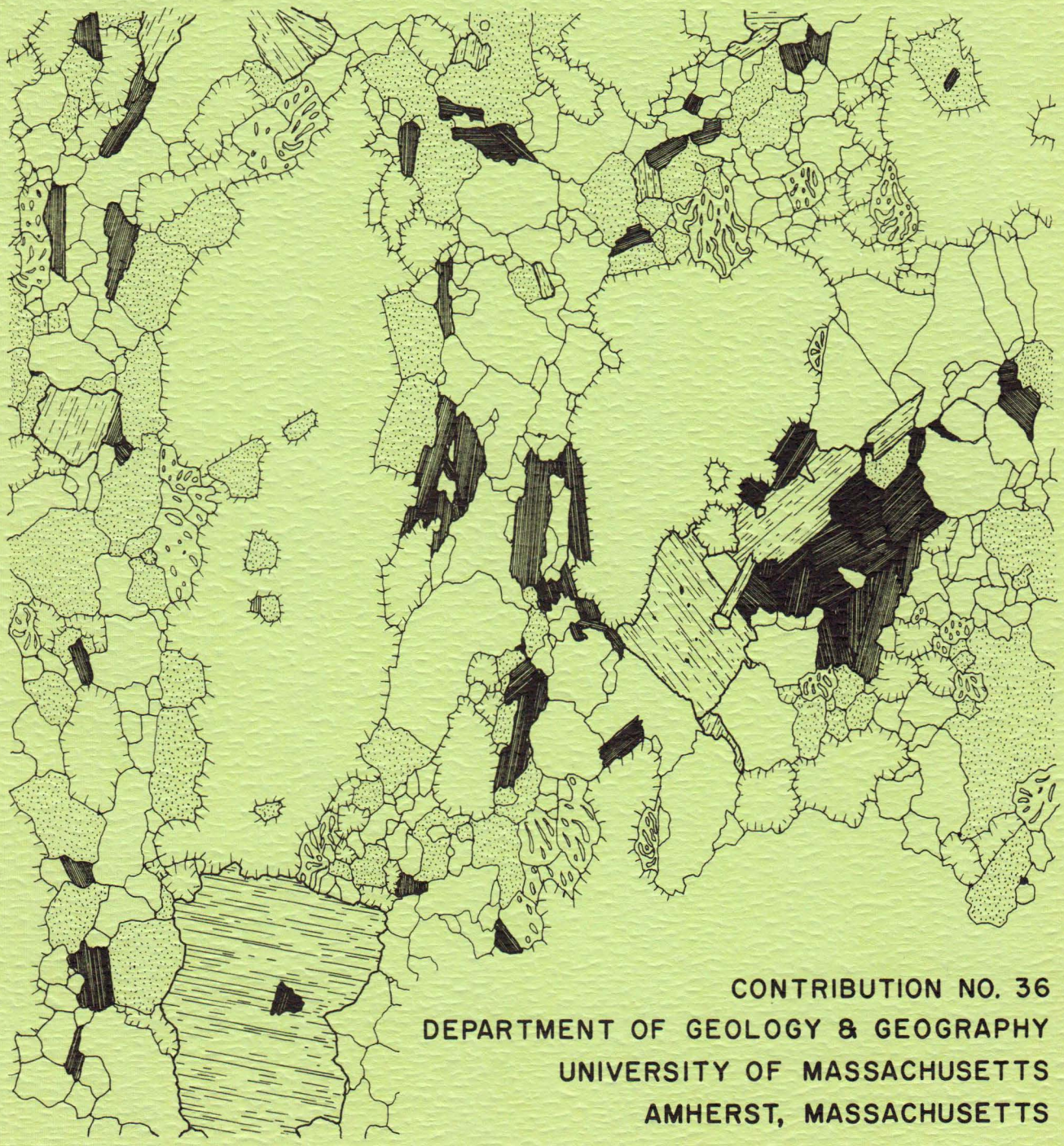

CONTRIBUTION NO. 36
DEPARTMENT OF GEOLOGY & GEOGRAPHY
UNIVERSITY OF MASSACHUSETTS
AMHERST, MASSACHUSETTS

# THE PETROLOGY AND GEOCHEMISTRY OF THE FITCHBURG PLUTONIC COMPLEX, CENTRAL MASSACHUSETTS

by

David E. Maczuga

Contribution No. 36

Department of Geology

University of Massachusetts

Amherst, Massachusetts

April, 1981

# TABLE OF CONTENTS

TABLE OF CONTENTS
(Continued)

TABLE OF CONTENTS
(Continued)

# ILLUSTRATIONS

ILLUSTRATIONS
(Continued)

# TABLES

ABSTRACT

The Devonian Fitchburg Plutonic Complex is a series of syntectonic sheets and late tectonic masses of varied composition, located on the eastern margin of the central Massachusetts metamorphic high. The complex occupies a broad, late tectonic, N-S trending, structural syncline together with Silurian and Lower Devonian metamorphosed sedimentary rocks of the Merrimack synclinorium. During the Acadian the complex was involved in several phases of severe deformation and metamorphism, reaching sillimanite-staurolite grade in the eastern portion, sillimanite-muscovite-K-spar grade in the center, and sillimanite-muscovite grade in the western portion.

Field work and modal analyses have established three major lithic types within the complex, a foliated biotite granodiorite-tonalite gneiss, a foliated biotite-muscovite granite-granodiorite gneiss, and a massive to weakly foliated biotite-muscovite granite. A structurally lower plutonic sheet of foliated biotite granodiorite-tonalite gneiss (granodiorite gneiss) is exposed on both east and west limbs of the major syncline. Twenty samples were analyzed, and they are composed of 29-48% andesine, 0-16% K-feldspar, 18-28% quartz, 16-42% biotite, and 0-4% muscovite with accessory sphene, allanite, clinozoisite, apatite, zircon, ilmenite, and magnetite. Whole rock chemical analyses of these samples show a range of compositions, with Wt% $SiO_2$=57-64, molar $(Fe^{2+}+Mn)/(Fe^{2+}+Mn+Mg)$=0.47-0.59, and molar $Al_2O_3/(K_2O+Na_2O+CaO)$=0.92-1.12. Within the granodiorite gneiss there are three large inclusions of massive, coarse-grained tonalite, from which three samples were col-

lected. They are composed of 37-41% andesine, 17% quartz, 30-32% biotite, and 1-4% hornblende, with accessory clinozoisite, apatite, and ilmenite. The whole rock chemistry of the inclusions is relatively homogeneous with Wt% $SiO_2$=54, $(Fe^{2+}+Mn)/(Fe^{2+}+Mn+Mg)$=0.52-0.54, and $Al_2O_3/(K_2O+Na_2O+CaO)$=0.88-0.94. An upper plutonic sheet of foliated biotite-muscovite granite-granodiorite gneiss (granite gneiss) is composed of 24-44% oligoclase-andesine, 6-32% K-feldspar, 25-28% quartz, 8-20% biotite, and 4-9% muscovite with accessory zircon, apatite, allanite, and ilmenite. Whole rock analyses of seven samples from the granite gneiss unit show a range of compositions with Wt% $SiO_2$=63-71, $(Fe^{2+}+Mn)/(Fe^{2+}+Mn+Mg)$=0.52-0.62, and $Al_2O_3/(Na_2O+K_2O+CaO)$=1.07-1.14. These sheets are cut by more irregular masses of massive to weakly foliated, probably late tectonic biotite-muscovite granite (granite), composed of 23-33% oligoclase, 17-32% K-feldspar, 27-32% quartz, 5-11% biotite, and 4-7% muscovite with accessory apatite, zircon, allanite, and ilmenite. Whole rock analyses of eight samples from the granite show Wt% $SiO_2$=69-73, $(Fe^{2+}+Mn)/(Fe^{2+}+Mn+Mg)$=0.54-0.70, and $Al_2O_3/(Na_2O+K_2O+CaO)$=1.09-1.20.

The tectonic regime, the felsic character, the peraluminous nature, and the high potassium content of the complex indicates that these rocks were derived from partial melting of rocks rich in quartzo-feldspathic components and probably micas. Temperature constraints imposed by phase relations in the system Q-Ab-Or-An-$H_2O$ and other petrologic criteria indicate the source for the granodiorite and granite gneisses was remote; thus, a source in subducted continental crust is postulated. The granodiorite gneiss and the granite gneiss appear to be partial melts of simi-

lar source materials, the granodiorite representing a more extensive partial melt relative to the granite gneiss. The tonalite inclusions in the granodiorite gneiss appear to be accumulations of early crystals from the granodiorite magma. The granite may have formed by minimum melting of source materials similar to the granite gneiss and the granodiorite gneiss, or it may be the product of *in situ* melting of the granite gneiss.

Local chemical variation is observed in the units of the complex, but no single mechanism for the generation of variation adequately explains the observed pattern of chemical behavior. Subsequent to emplacement of the granodiorite gneiss and the granite gneiss, Acadian metamorphism reached its peak in this area at sillimanite-muscovite and locally sillimanite-muscovite-K-spar grade conditions, and apparently caused local partial melting in the granodiorite gneiss at Wachusett Mountain and in the granite gneiss at Crow Hills. By a minimum melt-restite segregation process (White and Chappell, 1977), chemical variation may have been generated in these gneisses. This process seems to be the most satisfactory explanation for much of the observed variation within the units, but the pattern of major and minor element variation indicates a complex history in which a number of mechanisms affected the distribution of the elements.

# INTRODUCTION

Location. The Fitchburg plutonic complex is a series of igneous sheets and irregular masses of varied composition, exposed over an area of approximately 400 square kilometers (155 sq. mi.) in the central part of Massachusetts. The complex lies approximately 55 km (34 mi.) east of Amherst and 70 km (44 mi.) west of Boston. Portions of the complex are situated in the eastern sections of the Ashburnham, Gardner, Wachusett Mountain, and Paxton 7 1/2-minute quadrangles and in the Ashby, Fitchburg, Sterling, and Worcester North quadrangles (Figure 1).

In general, the area has broad, rounded hills having a slight N-S elongation and local relief of 60 meters (200 ft.) or less. A notable exception to this is in the west-central part of the complex. Wachusett Mountain rises approximately 300 meters (1000 ft.) above its base to 611.4 meters (2006 ft.) above sea level and is the highest point of elevation in Massachusetts east of the Connecticut River. The Quinapoxet, Stillwater, Whitman, and Nookagec Rivers drain the study area and join the Nashua River, which flows to the northeast and into New Hampshire.

Regional setting. The Appalachian orogenic belt in New England is primarily composed of deformed, metamorphosed, and intruded sedimentary and volcanic rocks of Early Cambrian through Early Devonian age, in the west resting unconformably on billion-year-old Grenvillian basement and in the east on Late Proterozoic rocks. The belt can be divided into several broad tectonic zones with respect to stratigraphy and style of deformation. The study area lies in the Merrimack synclinorium, which is bound on the west by the Bronson Hill anticlinorium and on the east

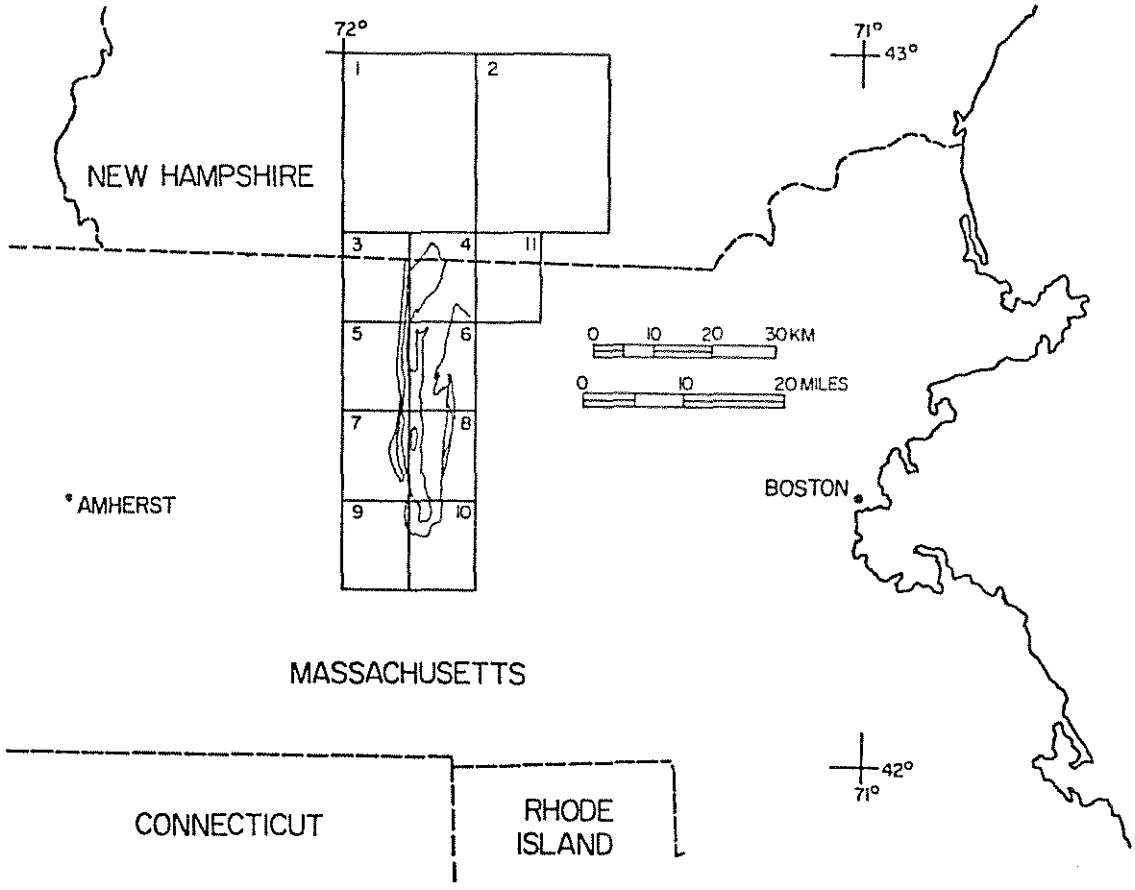


1. Peterborough (Greene, 1970)
2. Milford (Aleinikoff, 1978)
3. Ashburnham (Robinson and Tucker, 1976)
4. Ashby (Peper and Wilson, 1976; Robinson, 1978)
5. Gardner (Tucker and Robinson , 1977)
6. Fitchburg (Peper, 1976)
7. Wachusett Mountain (Fahlquist, 1935; Tucker, 1978)
8. Sterling (Fahlquist, 1935; Grew, 1970; Hepburn, 1976)
9. Paxton (Robinson and Tucker, 1976; Robinson and Belvin, 1977; Belvin and Tollo, 1977)
10. Worcester North (Grew, 1970; Hepburn, 1976; Robinson and Belvin, 1977)
11. Townsend (G.R. Robinson, 1979)

Figure 1. Location map of the Fitchburg plutonic complex area and related geologic mapping.

by the Milford anticlinorium and "Avalon platform" (Zen, 1968; Skehan and others, 1978).

The Bronson Hill anticlinorium is a north-northeast trending belt of approximately twenty en echelon, mantled gneiss domes that extends from the Maine-New Hampshire border to southern Connecticut. The mantling strata, consisting of amphibolites, mica schists, quartzites, and calc-silicate rocks, have been involved in two phases of major recumbent folding prior to the upward gravitational rise of the gneiss domes near the peak of Acadian metamorphism (Thompson and others, 1968).

Plutonic and probable pre-Devonian metamorphic rocks lie in the poorly understood Nashoba block area east of the Merrimack synclinorium. The Milford anticlinorium of southeastern Massachusetts contains metamorphosed rocks of Avalonian and younger age and has an uncertain relationship to the unmetamorphosed Late Precambrian-Cambrian "Avalon platform" further east (Rodgers, 1972).

East of the Bronson Hill anticlinorium lies the Merrimack synclinorium, a belt of predominantly eugeosynclinal, clastic sediments and volcanic debris of high metamorphic grade, extending from west and central Maine through New Hampshire into central Massachusetts and eastern Connecticut. Billings (1956) interpreted it to be a simple synclinorium formed in the Acadian orogeny and consisting solely of Silurian and Devonian strata, but subsequent investigations have revealed additional complexities.

In Maine the synclinorium is a broad, multiply deformed area in which steeply dipping beds and tight folds with vertical axial surfaces are typical (Osberg and others, 1968). In the southern part of the syn-

clinorium, in central Massachusetts (Field, 1975; Tucker, 1977) and eastern Connecticut (Dixon and Lundgren, 1968) a general recumbent style of folding prevails. These recumbent folds have been refolded in the waning stages of the orogeny, resulting in the formation of broad foliation arches and basins. The nappes present in the Bronson Hill anticlinorium to the west may be rooted in the Merrimack synclinorium (Thompson and others, 1968; Field, 1975). Some workers in northeastern Connecticut and south-central Massachusetts (Pease and Peper, 1968; Peper and others, 1975; Pomeroy, 1973; 1975) thought the synclinorium was a westward-dipping homoclinal sequence, juxtaposed against lithologically dissimilar formations as a result of movement along major west dipping faults of the Clinton-Newbury, Bloody Bluff, and Bone Mill Brook systems.

Correlation of the lithologies present in the Merrimack synclinorium in Massachusetts (Peper and Pease, 1975; Field, 1975; Tucker, 1977) can be made with sequences described in south and central Maine (Osberg, 1979), southeast New Hampshire (Billings, 1956), and eastern Connecticut (Dixon, 1968) as well as with many of the units present in the Bronson Hill anticlinorium to the west (Robinson, 1967; Field, 1975).

Acadian (Devonian) intrusive rocks of varied composition form syntectonic, concordant and quasi-concordant lensoid sheets and late- to post-tectonic masses in the metamorphosed sedimentary rocks, accounting for a significant portion of the rocks exposed in the Bronson Hill anticlinorium-Merrimack synclinorium area. In central Massachusetts in the zone of most intense Acadian regional metamorphism and deformation, the

intrusive rocks belong to two apparently contemporaneous suites; peraluminous, biotite-muscovite and/or garnet-bearing leucogneisses on one hand and biotite-, sphene-, epidote-, or hornblende-bearing gneisses on the other. These have been thought of as similar to the S and I granitoids, respectively, of Chappell and White (1974; White and Chappell, 1977), where S-type granitoids are derived from sedimentary source materials and I-type granitoids are derived from igneous source materials.

Purpose of study. Recent work in the Merrimack synclinorium of central Massachusetts, known to be one of the most geologically complex and least studied regions in the northern Appalachians, has concentrated on mapping of the contacts of metamorphosed sedimentary rocks and understanding the major and minor structural features. Due to this emphasis, there is a general lack of petrologic data pertaining to the abundant plutonic rocks.

A detailed sampling program of the lithologies present in the Fitchburg complex was undertaken as part of an ongoing regional research program in central Massachusetts. To provide a quantitative characterization of the complex, detailed thin section petrography, whole rock major element analysis by X-ray fluorescence spectroscopy, and electron microprobe analysis of important co-existing mineral phases have been done on fresh, representative samples collected from selected localities of importance to the study. Data generated in this study will allow for discussion concerning operative igneous and metamorphic processes, place constraints on possible source materials, and contribute to a data base for regional tectonic interpretation.

Previous work. Emerson (1890) originally interpreted the rocks of the Fitchburg complex to be a series of granitic sheets intruded into strata on both limbs of an open syncline. Later (Emerson, 1917) he distinguished two major lithologic units within the pluton, although he did not map them separately: a) a leucocratic, medium-grained, muscovite-biotite granite and b) a dark gray, medium-grained, biotite granodiorite. Dale (1923) described commercial quarrying operations in the biotite-muscovite granite at Rollstone Hill, Fitchburg and in the biotite granodiorite at South Monoosnoc Hill, Leominster. Fahlquist (1935) studied the geology of the Quabbin Aqueduct Tunnel, which passes through the southern part of the complex.

Peper and Wilson (1978) did reconnaissance bedrock geologic mapping of the Fitchburg and Ashby quadrangles. Hepburn (1976) did detailed bedrock geologic mapping of the Sterling quadrangle. Tucker (1978) has done detailed mapping and structural analysis of the Wachusett Mountain area and reconnaissance bedrock geologic mapping of the Gardner quadrangle (Tucker and Robinson, 1977, unpublished data). The geologic mapping of the Worcester North quadrangle was done by Grew, (1970), Hepburn (1976), and Robinson and Belvin (1977). Aleinikoff (1978) distinguished three discrete units in what had been previously mapped as the "Fitchburg pluton" in the central part of the Milford, New Hampshire quadrangle. Peter Robinson (unpublished reconnaissance data, 1978) reinterpreted previous mapping by G. R. Robinson (1978) of the Townsend, Massachusetts quadrangle and by Peper and Wilson (1978) of the eastern section of the Ashby quadrangle in the light of Aleinikoff's conclusions.

Present work. During the summer of 1978, specimens of the various units of the Fitchburg plutonic complex were obtained from the Fitchburg, Sterling, Wachusett Mountain, and Worcester North quadrangles. Forty-four samples were collected and prepared for analytical techniques which were employed to gain a quantitative characterization of the complex.

Acknowledgements. This report is submitted in partial fulfillment of the requirements for the degree of Master of Science in Geology at the University of Massachusetts, Amherst. R. D. Tucker provided the impetus for the project and Peter Robinson oversaw its evolution while serving as principal advisor. J. M. Rhodes and S. A. Morse provided helpful suggestions and guidance. Electron microprobe data were graciously furnished by J. C. Schumacher, K. T. Hollocher, and C. K. Shearer. Information on opaque minerology was furnished by P. T. Panish. Summer subsistence, thin section preparation, manuscript preparation, and other expenses were defrayed by National Science Foundation Grant EAR 79-11207 (to Robinson), United States Geological Survey Grant 14-03-0001-G-400 (to Robinson), and a Grant from the Society of the Sigma Xi. To these people and institutions I extend my deep appreciation and grateful acknowledgement.

## GENERAL GEOLOGY

The "Fitchburg pluton", located on the eastern margin of the central Massachusetts metamorphic high, is actually a complex series of igneous sheets and masses of varied composition, intruded into metamorphosed sedimentary rocks of probable Silurian and Lower Devonian age. Reconnaissance and detailed mapping by Grew (1970), Hepburn (1976), Peper and Wilson

(1978), Tucker (1978), and Tucker and Robinson (1977, 1978, unpublished data) have substantiated the original interpretation of Emerson (1890) concerning the synclinal nature of the complex and contributed to the understanding of the complex stratigraphic and structural relationships in the area.

Plutonic units of the Fitchburg complex. Lithologic refinements (Hepburn, 1976; Peper, 1976; Tucker, 1978) and modal analysis (this study) have established three major units in the Fitchburg complex (Figure 2):

I. Moderately to strongly foliated, dark gray, fine-to medium-grained biotite granodiorite-tonalite gneiss with accessory sphene, allanite epidote, zircon, apatite, ilmenite, magnetite, and pyrite. Moderately foliated varieties of this unit predominate in a series of sill-like lenses on the east side of the major syncline. Here the unit is generally even-grained and uniform at the outcrop scale. The estimated thickness of the sill on the east limb of the syncline at South Monoosnoc Hill (Figure 3) is 335 m (1100 ft). In the more continuous sill on the west limb of the major syncline, this unit is strongly foliated. Here there is substantial variation in grain size, mafic mineral content, and amount of pegmatitic material. The unit is commonly pervaded by medium- to course-grained feldspar megacrysts and/or pegmatitic stringers which can constitute a significant portion of the rock. Zones of leucogneiss also are present. Detailed stratigraphic measurements on the west flank of Wachusett Mountain (Figure 3) yield a thickness of 155 m (508 ft). Several large inclusions of massive, dark gray, coarse-grained, hornblende-biotite tonalite with accessory allanite, epidote, zircon, apatite,

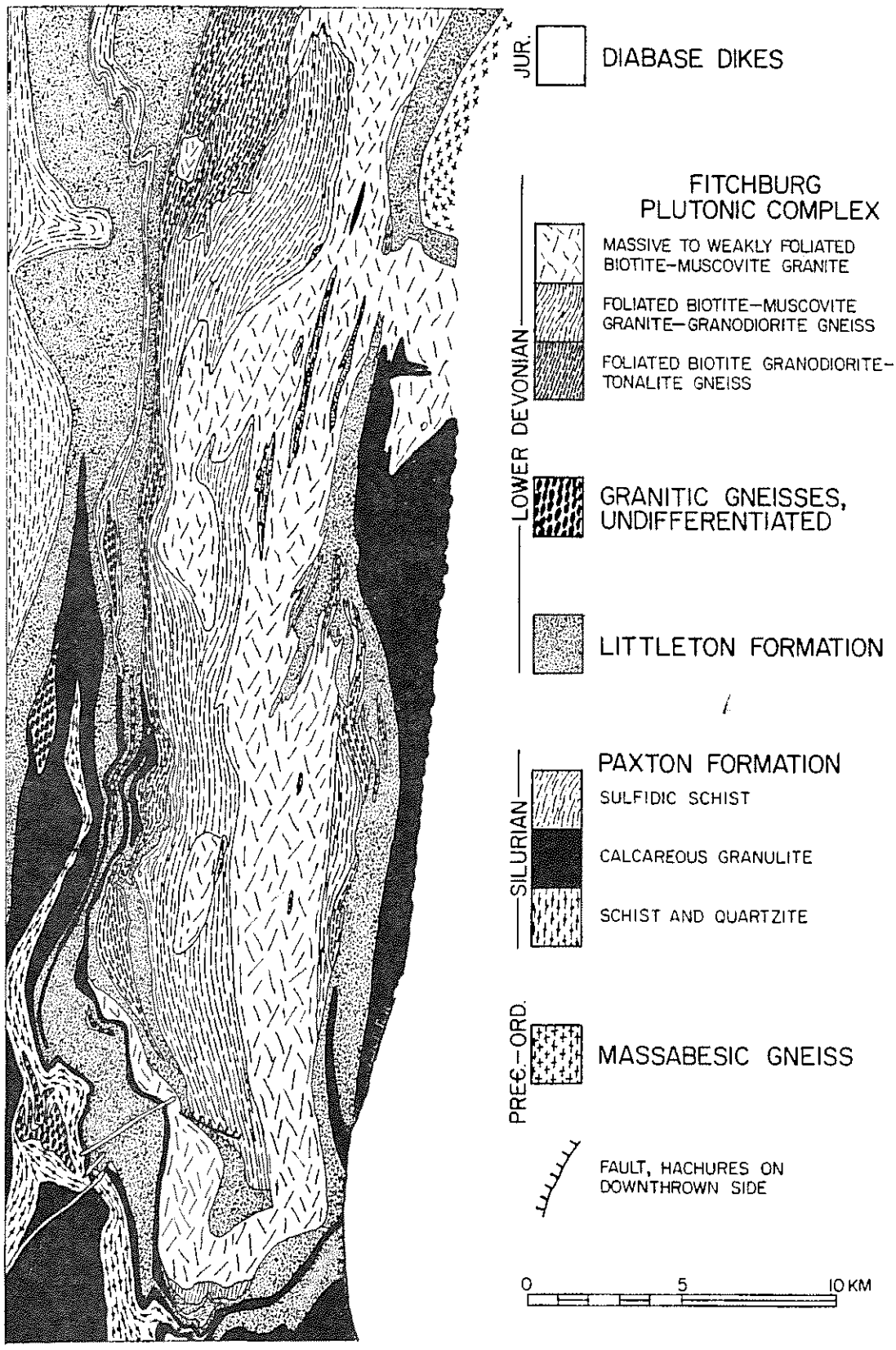


Figure 2. General geologic map of the Fitchburg plutonic complex.

ilmenite, and pyrite occur within the biotite granodiorite-tonalite gneiss on the west limb of the syncline.

II. Moderately to strongly foliated, gray, fine- to medium-grained, biotite-muscovite granite-granodiorite gneiss with accessory zircon, apatite, and ilmenite. Megascopic variation in grain size, mafic mineral content, and amount of pegmatitic stringers occurs at the outcrop scale. This unit forms a long and commonly wide sill on the western side and a much less extensive lens-like body on the east side of the complex.

III. Massive to weakly foliated, leucocratic, medium- to coarse-grained, biotite-muscovite granite with accessory zircon, apatite, and ilmenite and common tourmaline pegmatite. Megascopically, these rocks are uniform at the outcrop scale. This unit extends the length of the complex, occupying the central part of the major syncline.

Numerous xenoliths of the Lower Devonian Littleton Formation included in the various units attest to their igneous origin and maximum age.

Relationships northeast of the study area. The petrology, U-Th-Pb geochronology, and remapping of the Milford, New Hampshire 15-minute quadrangle were done by Aleinikoff (1978). A NE-SW trending swath through the center of the quadrangle, previously mapped as the Fitchburg pluton by Billings (1956), was divided on the basis of composition and cross-cutting relationships into three distinct units: 1) a gray, quartz-plagioclase-biotite (sillimanite) paragneiss (zircon age 646 m.y.); 2) a pink to white, quartz-K-feldspar-plagioclase-biotite-muscovite orthogneiss (zircon age 470 m.y.); and 3) a gray, fine-grained, biotite-muscovite gran-

ite (zircon age 275 m.y.).

Peter Robinson (1978, unpublished reconnaissance data) used the recommendations of Aleinikoff to complete a reinterpretation of earlier mapping by G. R. Robinson (1979) of the Townsend, Massachusetts quadrangle and Peper and Wilson (1978) of the eastern section of the Ashby, Massachusetts quadrangle. Robinson concludes that: a) The Precambrian paragneiss and Ordovician orthogneiss occupy a northeast-trending, upright anticline which plunges gently southwest in the Townsend area. The rocks appear similar to the Monson Gneiss and related rocks of the Bronson Hill anticlinorium and occupy a structural position analogous to the Willimantic Dome of southeastern Connecticut. b) The major syncline containing the Fitchburg plutonic complex in Massachusetts lies entirely west of the gneiss anticline; therefore, the northern extent of the Fitchburg complex into New Hampshire has not been determined. c) The rocks of the paragneiss-orthogneiss complex and the Late Paleozoic granite are distinctive in appearance and are not easily confused with the Devonian granitoid rocks of the Fitchburg complex.

Structural and metamorphic history. The deformational history of central Massachusetts, as interpreted by Robinson (1967), Field (1975), and Tucker (1977, 1978) deals primarily with Acadian deformation, which occurred as four distinct, major phases in this area. The first major episode involved major, westward-directed, recumbent folds on the scale of tens of kilometers. Several plutonic sheets, including the structurally lower biotite granodiorite-tonalite gneiss and the structurally higher, foliated, biotite-muscovite granite-granodiorite gneiss of the Fitchburg

complex appear to have been emplaced before or during this stage in the form of quasi-concordant, lensoid sheets. Recumbent back-folding of the initial isoclinal folds occurred in the second stage, which probably corresponded to the peak of metamorphism in the area. The third stage of folding resulted in the formation of the gneiss domes in the Bronson Hill anticlinorium to the west, as well as related, smaller scale folds and lineations in the east. The fourth stage produced a series of broad, N-S trending, structural anticlines and synclines including the syncline in which the Fitchburg plutons are now situated.

The emplacement of the massive to weakly foliated biotite-muscovite granite may be interpreted to be concurrent with or subsequent to the last major deformational episode due to its relatively undeformed nature, irregular distribution, and apparent cross cutting relationship with the biotite granodiorite-tonalite and the biotite-muscovite granite-granodiorite gneiss. A zircon date of 412 m.y. on samples from Malden Hill, Holden, and a zircon date of 382 m.y. on samples from Rollstone Hill, Fitchburg have been determined on this unit (R.E. Zartman, pers. comm., 1977).

On the western margin of the complex, sillimanite-muscovite grade metamorphism prevails. Local inclusions in the center of the complex contain sillimanite-muscovite-K-spar grade assemblages (P. Robinson, pers. comm., 1979). On the eastern margin, a steep metamorphic gradient is present (Figure 3). The metamorphic grade drops abruptly from sillimanite-muscovite grade near the pluton, through sillimanite-staurolite and andalusite-staurolite, to garnet grade as one proceeds eastward and topographically downhill. This relationship is interpreted to be the result of eastward-directed recumbent folding of a pre-existing contact aureole

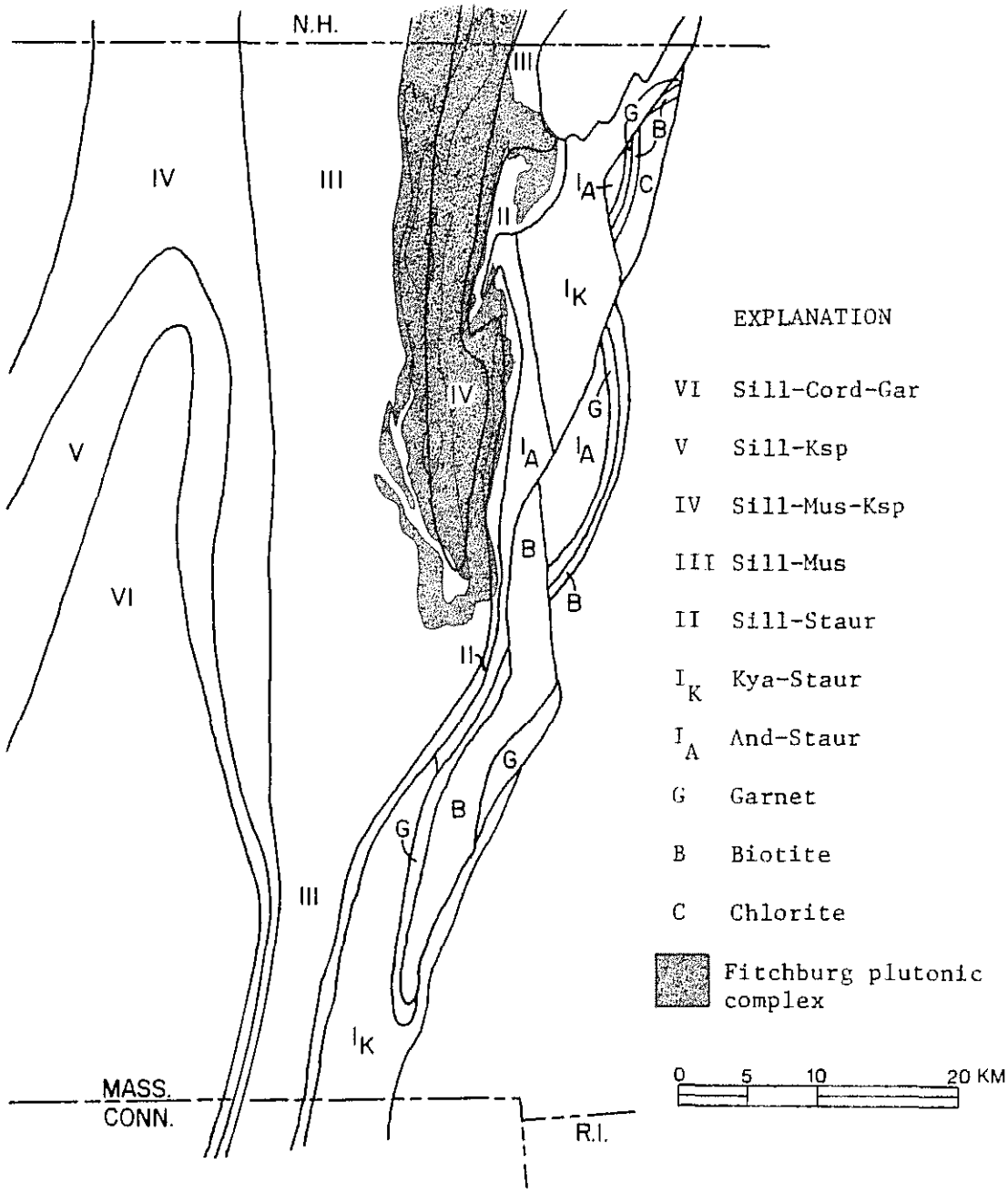


Figure 3. Regional Acadian metamorphic isograd map of central Massachusetts, southern New Hampshire, and northern Connecticut (Peter Robinson, pers. comm., 1980). Area in the northeast corner of the map labelled "Pca" is the contact metamorphic aureole of a Pennsylvanian granite body which overprints earlier Acadian metamorphism.

during continued regional metamorphism.

## PETROGRAPHY

### General Considerations

Sampling procedure. One of the purposes of this study is to quantify the variation within the units of the Fitchburg complex. The generally weathered nature of accessible bedrock in the area renders most rock unsuitable for geochemical study. As a consequence, sampling was primarily confined to road cuts and quarries where relatively fresh samples could be obtained. Under these circumstances statistically valid sampling of the complex was not possible. Samples were taken of as many textural variants as deemed necessary and helpful to the study. Thus, frequency in any parameter may not be particularly meaningful. The variation found in the foliated biotite granodiorite-tonalite gneiss at Wachusett Mountain is thought to be representative since specimens were collected over the entire stratigraphic thickness of the unit.

Preparation of modes. Standard petrographic thin-sections were prepared from each of the forty-four specimens collected for the study. Microscopic examination and modal analysis of the specimens were performed to permit determination of interrelationships among the various mineral species, to allow precise application of nomenclature, and to make possible correlation between actual mineralogy and whole rock chemical variation. To facilitate counting and to insure correct identification of

plagioclase, potassium feldspar, and quartz, all thin sections were etched with hydrofluoric acid vapor and stained with a saturated solution of sodium cobaltinitrite before covering. Thin sections prepared in this manner have bright yellow potassium feldspar, dull, grainy plagioclase, and clear quartz, which are readily distinguished from each other.

Over two thousand points per specimen were counted; thus, modal mineralogy values are within ± 2% at the 95% confidence level for most mineral abundances, according to Van Der Plas (1965). The area over which the points were counted was chosen using the recommendations of Chayes (1956) such that one standard petrographic thin section was used for the finer-grained specimens and as many as three sections were counted in the coarser-grained specimens.

## Foliated Biotite Granodiorite-Tonalite Gneiss

In the broad structural syncline containing the "Fitchburg plutons", the biotite granodiorite-tonalite gneiss sheet is interpreted to have a structurally lower position, relative to the biotite-muscovite granite-granodiorite gneiss. Samples of the foliated biotite granodiorite-tonalite gneiss were taken primarily from two locations, South Monoosnoc Hill on the east limb and Wachusett Mountain on the west limb of the syncline (Figure 4). Figure 5 shows plotted modes of all specimens collected from the unit mapped as foliated biotite granodiorite gneiss by Peper (1976), Hepburn (1976), and Tucker (1978), including the hornblende-biotite tonalite inclusions from the west side. Samples of the foliated biotite granodiorite-tonalite gneiss will here be referred to as the granodiorite gneiss.

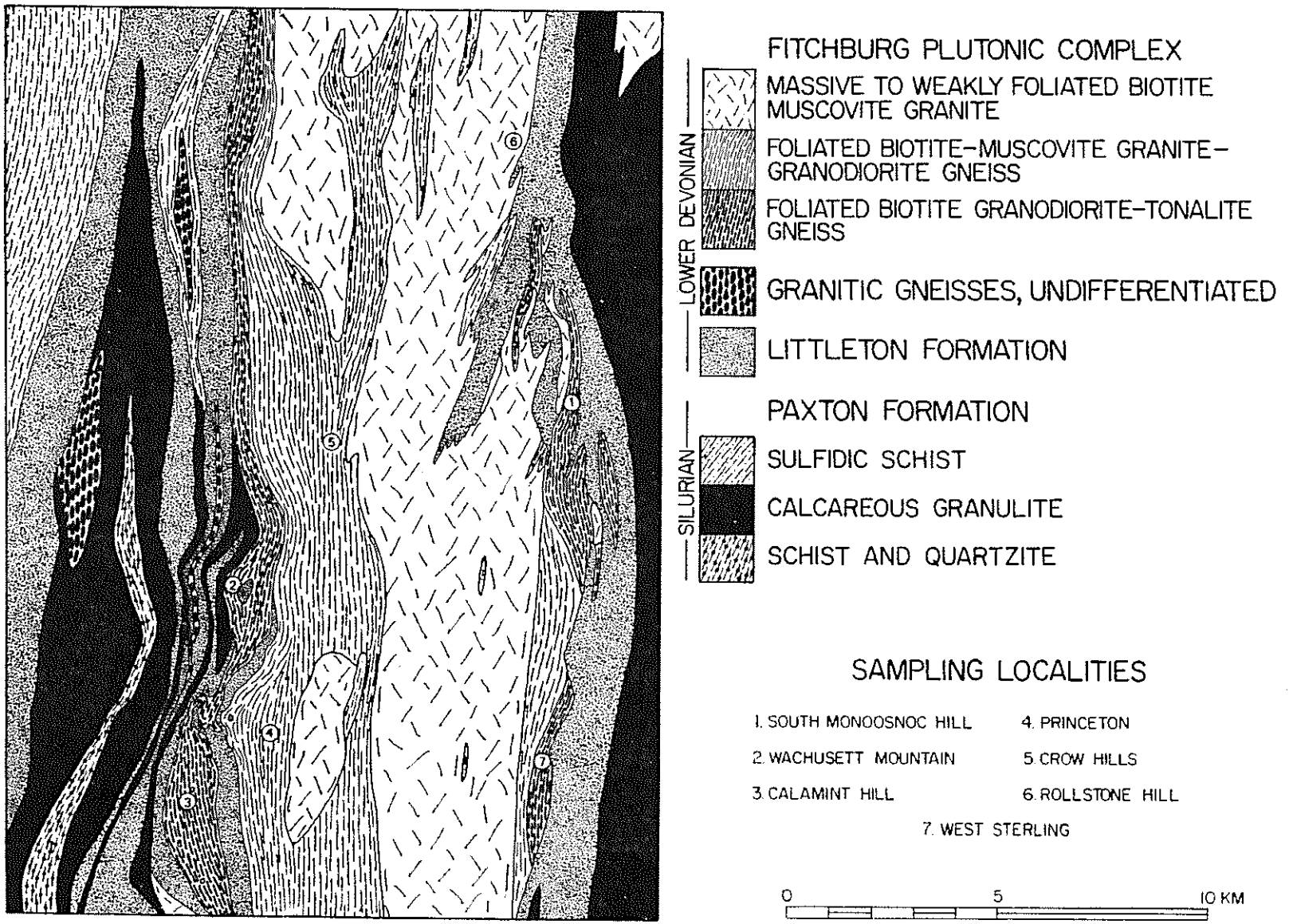


Figure 4. General geologic map indicating major sampling localities in the Fitchburg plutonic complex.

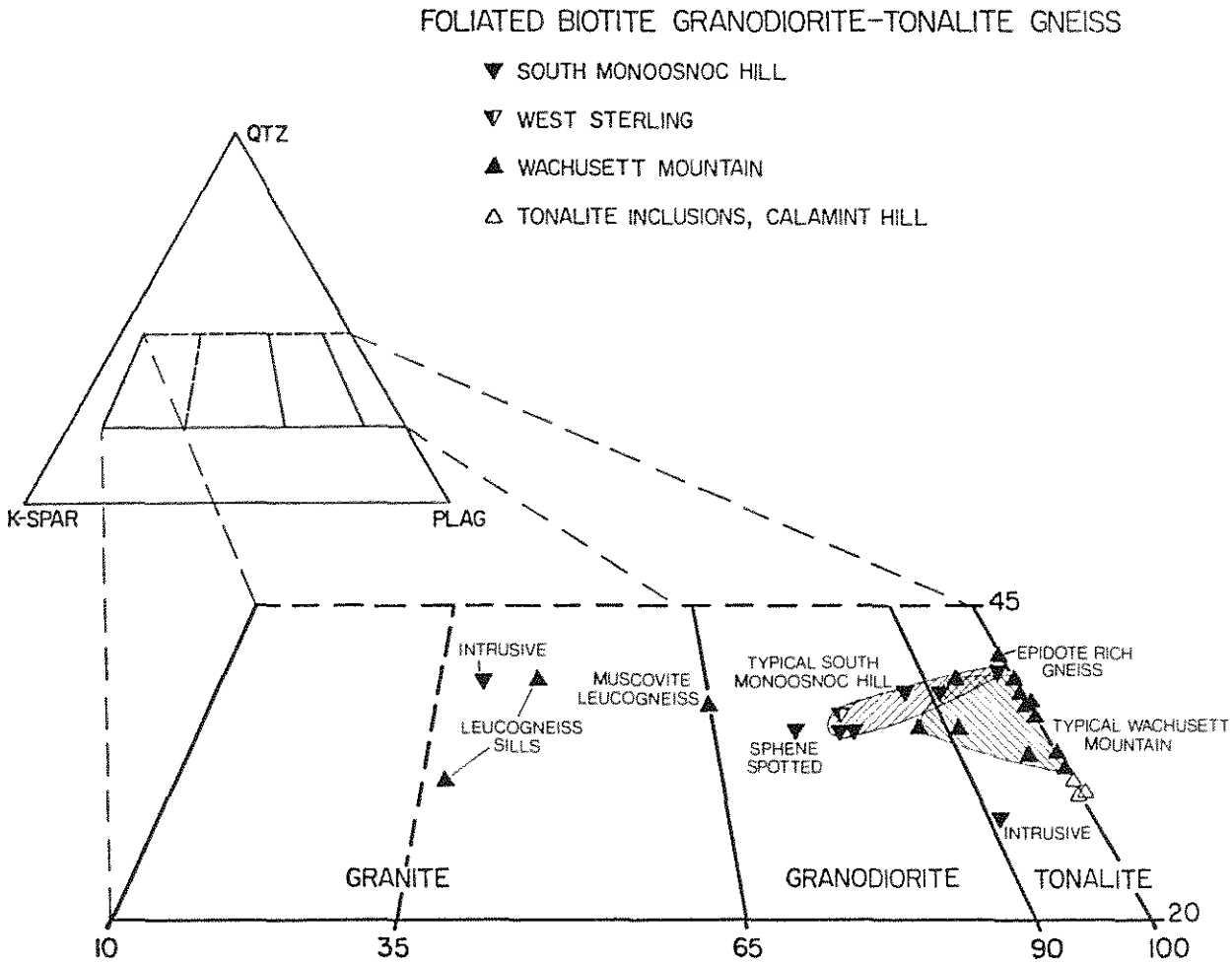


Figure 5. Plot based on modes of samples collected from the foliated biotite granodiorite-tonalite gneiss. Diagram modified from Streckeisen (1973).

Eastern belt: South Monoosnoc Hill and West Sterling. On the eastern slope of South Monoosnoc Hill, approximately 3.2 km (2 mi.) west of Leominster, lies the abandoned Leavitt quarry (Figure 4). Operated from 1890 to 1916, the quarry furnished stone which was used for buildings, curbing, and foundations (Dale, 1923). All that remains is an access road and a forty-five by ninety meter excavation which exposes abundant bedrock and has numerous large blocks of gneiss strewn throughout.

The predominant lithology at South Monoosnoc Hill is a dark gray, fine-grained, moderately foliated, biotite granodiorite-tonalite gneiss, exemplified by samples MF-8, 9, 12, 14, and 15 (Table 1). Sample MS-1 was taken from the east limb of the major syncline in the vicinity of West Sterling (Figure 4). Although it is more foliated, the rock is mineralogically and texturally similar to the typical biotite granodiorite-tonalite gneiss at South Monoosnoc Hill. The major mineral content ranges from 32.4 to 40.2% plagioclase, 0.1 to 8.7% potassic feldspar, 21.9 to 24.9% quartz, and 28.6 to 31.9% biotite. The ratio of plagioclase to total feldspar (100 Pl/(Pl+Ksp) ranges from 79 to 99. Accessory minerals include sphene, muscovite, allanite, clinozoisite, zircon, apatite, magnetite, and ilmenite with secondary chlorite, sericite, pyrite, and calcite. Sillimanite-staurolite grade regional metamorphism has taken its toll on the original igneous texture of this unit, resulting in a partially recrystallized, granoblastic texture with triple point grain junctions, moderate biotite foliation, and development of metamorphic minerals such as clinozoisite (Figure 6).

Table 1. Point-counted modes (over 2000 points) for the granodiorite gneiss, Eastern Belt, South Monoosnoc Hill (Fitchburg quadrangle) and West Sterling (Sterling quadrangle).

| | COMMON GNEISS | | | | | | SPHENE SPOTTED | INTRUSIVE TONALITE | INTRUSIVE GRANITE |
|---|---|---|---|---|---|---|---|---|---|
| | MF-8 | MF-9 | MF-12 | MF-14 | MF-15 | MS-1 | MF-7 | MF-11 | MF-16 |
| Quartz | 21.9 | 22.8 | 26.4 | 24.9 | 23.9 | 22.6 | 25.6 | 20.3 | 29.2 |
| Plagioclase | 32.9 | 32.8 | 40.2 | 35.4 | 36.1 | 32.4 | 34.8 | 48.0 | 18.5 |
| (mol.% An)* | 38-26 | 43-22 | 38-22 | 44-22 | 45-22 | 48-28 | 37-20 | 46-22 | 48-22 |
| Potassic Feldspar | 8.3 | 8.7 | 0.1 | 5.1 | 3.7 | 8.5 | 12.6 | 4.9 | 27.2 |
| Myrmekite | 0.6 | 0.5 | - | 0.1 | - | 0.6 | 0.4 | 4.9 | 4.4 |
| Biotite | 29.3 | 28.7 | 28.6 | 28.9 | 30.6 | 31.9 | 22.0 | 15.6 | 14.6 |
| Muscovite | 1.3 | 0.7 | 0.5 | 2.8 | 1.2 | 0.1 | 0.3 | 3.7 | 3.1 |
| Sphene | 3.4 | 3.7 | 1.7 | 1.5 | 3.1 | 2.7 | 2.0 | 0.9 | 0.9 |
| Allanite | 0.4 | 0.3 | 0.3 | 0.2 | 0.3 | 0.2 | 0.4 | 0.2 | - |
| Clinozoisite | tr | tr | - | - | - | - | 0.2 | tr | - |
| Opaque Minerals | 0.2 | 0.1 | 0.8 | 0.2 | 0.2 | 0.1 | 0.1 | 0.7 | 0.2 |
| Apatite | 1.3 | 1.4 | 0.9 | 0.6 | 0.7 | 0.5 | 0.9 | 0.4 | 0.5 |
| Zircon | 0.3 | 0.3 | 0.5 | 0.2 | 0.2 | 0.3 | 0.7 | 0.3 | 0.2 |
| Chlorite | tr | - | - | tr | - | - | - | tr | 1.2 |
| Calcite | - | tr | - | - | - | - | tr | - | tr |
| 100 Pl/(Pl+Ksp) | 80 | 79 | 99 | 87 | 91 | 79 | 73 | 91 | 40 |
| 100 Qz/(Qz+Fsp) | 35 | 35 | 40 | 38 | 38 | 36 | 35 | 28 | 39 |

* Determined by Michel-Levy extinction angle method, using determinative figure 123, p. 333, Deer Howie, and Zussman (1966).

Table 1, continued. Hand specimen descriptions, Eastern belt, South Monoosnoc Hill and West Sterling.

The abandoned Leavitt quarry on South Monoosnoc Hill can be reached by turning left at the western termination of Exchange Street in Leominster and proceeding approximately 0.8 miles on the unimproved road which leads to the quarry. Samples were taken primarily from loose blocks within the quarry.

MF-8 Weakly foliated, fine- and even-grained, dark-gray, feldspar-quartz-biotite-sphene gneiss. Small rusty patches surround the sulfide minerals.

MF-9 Moderately foliated, fine- to medium-grained, dark-gray, feldspar-quartz-biotite-sphene gneiss.

MF-12 Weakly foliated, very fine-grained, dark-gray, saccaroidal textured, feldspar-quartz-biotite granulite.

MF-14 Moderately foliated, fine-grained, dark-gray, feldspar-quartz-biotite gneiss. This specimen was collected from gneiss in place at the 650 ft. contour along the quarry road, just above the lower contact with country rocks.

MF-15 Moderately foliated, fine-grained, dark-gray, feldspar-quartz-biotite-sphene gneiss. Sphene appears to be contained in small concentrations of felsic components. This specimen was collected from discrete inclusions within the lithology of which MF-16 is a sample.

MS-1 Well foliated feldspar-quartz-biotite-sphene gneiss. This sample is from West Sterling and was collected on Beaman Road 0.9 miles east of the southern intersection of Beaman Road and state highway 140.

MF-7 Generally fine-grained, dark-gray, feldspar-quartz-biotite gneiss. Coarse-grained sphene is contained by 7.0 mm spheroidal masses of feldspar and quartz, giving the rock a spotted appearance.

MF-11 Weakly foliated, fine- to medium-grained, gray, feldspar-quartz-biotite gneiss. Numerous medium-grained, feldspar megacrysts are present and together with biotite, define the weak foliation. This rock type appears to be intrusive into the common gneiss.

MF-16 Weakly foliated, medium-grained, leucocratic, feldspar-quartz-biotite gneiss. This lithology is clearly intrusive into the typical biotite granodiorite gneiss.


Figure 6. Sketch from a thin section of granodiorite gneiss from South Monoosnoc Hill, sample MF-8. P=Plagioclase, Q=Quartz, K=Potassic Feldspar, B=Biotite, M=Muscovite, S=Sphene, black=opaque minerals.

Plagioclase forms subhedral to anhedral, elongate grains ranging in size from 0.2 to 1.5 mm and averaging 0.6 mm. It is compositionally zoned in a continuous, normal manner from $An_{45}$ to $An_{20}$, as optically determined by the Michel-Levy extinction angle method (Deer, Howie, and Zussman, 1966, Figure 123). Plagioclase commonly has a particularly sodic rim ($An_5$, Michel-Levy method) or is myrmekitically intergrown with quartz where adjacent to potassic feldspar. A minor number of plagioclase grains are different in appearance from the average grains. These grains have cores which contain numerous inclusions of an undetermined phase and/or exhibit uneven extinction characteristics. Some sericitic alteration occurs in plagioclase, particularly in the more calcic cores.

Quartz occurs as anhedral grains which range in size from 0.1 to 0.6 mm, and average 0.3 mm. Quartz exhibits undulatory extinction and commonly forms elongate aggregates of polygonal grains averaging 0.8 mm in length. The potassium feldspar is microcline as indicated by the presence of tartan twinning and $2V_x$ of approximately $85^o$. It forms anhedral to interstitial grains ranging in size from 0.2 to 1.0 mm and averaging 0.6 mm.

Strongly pleochroic biotite, with X = pale brown-yellow and Y = Z = dark orange-brown to dark brown, forms subhedral grains which range in size from 0.1 to 1.3 mm and average 0.7 mm. The subparallel arrangement of biotite defines a moderate foliation that is not readily apparent in thin section. In some samples, fine-grained biotite is poikilitically enclosed by sphene. Iron-rich chlorite is a common alteration product of biotite, particularly where the biotite is enclosed by sphene. Minor primary-appearing muscovite is intimately intergrown with biotite.

The grain size of sphene varies among the different samples, ranging from 0.1 to 2.0 mm. It occurs as fine grains disseminated throughout the specimen, as rims surrounding ilmenite, and as 0.7 to 2.0 mm grains or aggregates commonly enclosing biotite or plagioclase poikilitically. Sphene is slightly pleochroic with X = pale brown and Z = light brown, and polysynthetic twins (221) have been observed. Fine-grained secondary calcite is associated with sphene and plagioclase.

Allanite forms 0.4 mm euhedral to anhedral grains commonly associated with biotite. Allanite is partially metamict, surrounded by the characteristic radial cracks, and pleochroic, with X = light brown and Z = brown to orange brown. The grains are zoned, the cores of the grains being more highly colored and birefringent, and commonly displaying a concentric growth pattern. Commonly, thin clinozoisite rims form on allanite where in contact with biotite and mimic the morphology of allanite.

Zircon and apatite have two morphologies, occuring as fine, approximately 0.2 mm slender prisms and more equant, stubby grains. Both are widely disseminated.

The opaque minerals found in this unit include oxides, sulfides, and an arsenide. Fine-grained ilmenite is rimmed by sphene, representing various stages of replacement. Pyrite and pyrrhotite form fine, euhedral to anhedral simple grains or composite grains with other sulfides or oxides. Pyrite appears to be replacing magnetite, and pyrite is being replaced by pentlandite, pyrrhotite, and chalcopyrite. The arsenide, possibly maucherite $[(Ni, Co)_{<3} As_2]$, is found as rare inclusions within the pyrrhotite.

Although modally similar to the typical granodiorite gneiss, MF-7 has a textural difference. Here, in addition to disseminated, fine-grained, anhedral sphene, 1.0 to 2.0 mm sphene poikilitically encloses euhedral to subhedral plagioclase. Surrounding the sphene, plagioclase, quartz, and potassic feldspar form pronounced leucocratic, polycrystalline areas which are devoid of biotite. Textural relationships of sphene intermediate to this and to that described earlier have been observed in several of the specimens. MF-11 has more plagioclase and less biotite than the other samples. Laths of 1.3 mm plagioclase are abundant in this sample, which appears to intrude the common gneiss. The mode of sample MF-16 shows that this specimen is a granite with 100 Pl/(Pl+Ksp) = 40. This rock is clearly intrusive into the typical granodiorite gneiss, although the mineral assemblage is similar.

Western belt: Wachusett Mountain. The road to the summit of Wachusett Mountain (Figures 4 and 7) cuts through a virtually uninterrupted stratigraphic sequence of the granodiorite gneiss; although modes show that here it is predominantly a tonalite gneiss (Figure 5). A detailed description of the lithologies, a measured section (Figure 8), and sampling were done for this sequence.

In the most common rock type (MW-12, 13, 15, 16, 19, 20, 21, 22, 23, 24, 25) megascopic variation is found, but in general the gneiss is dark gray, strongly foliated, and fine-grained. Although these rocks are mineralogically very similar to those found at South Monoosnoc Hill, there are extensive modal variations (Table 2). Quartz ranges from 17.9 to 25.3%, biotite ranges from 26.3 to 38.6%, and plagioclase ranges from

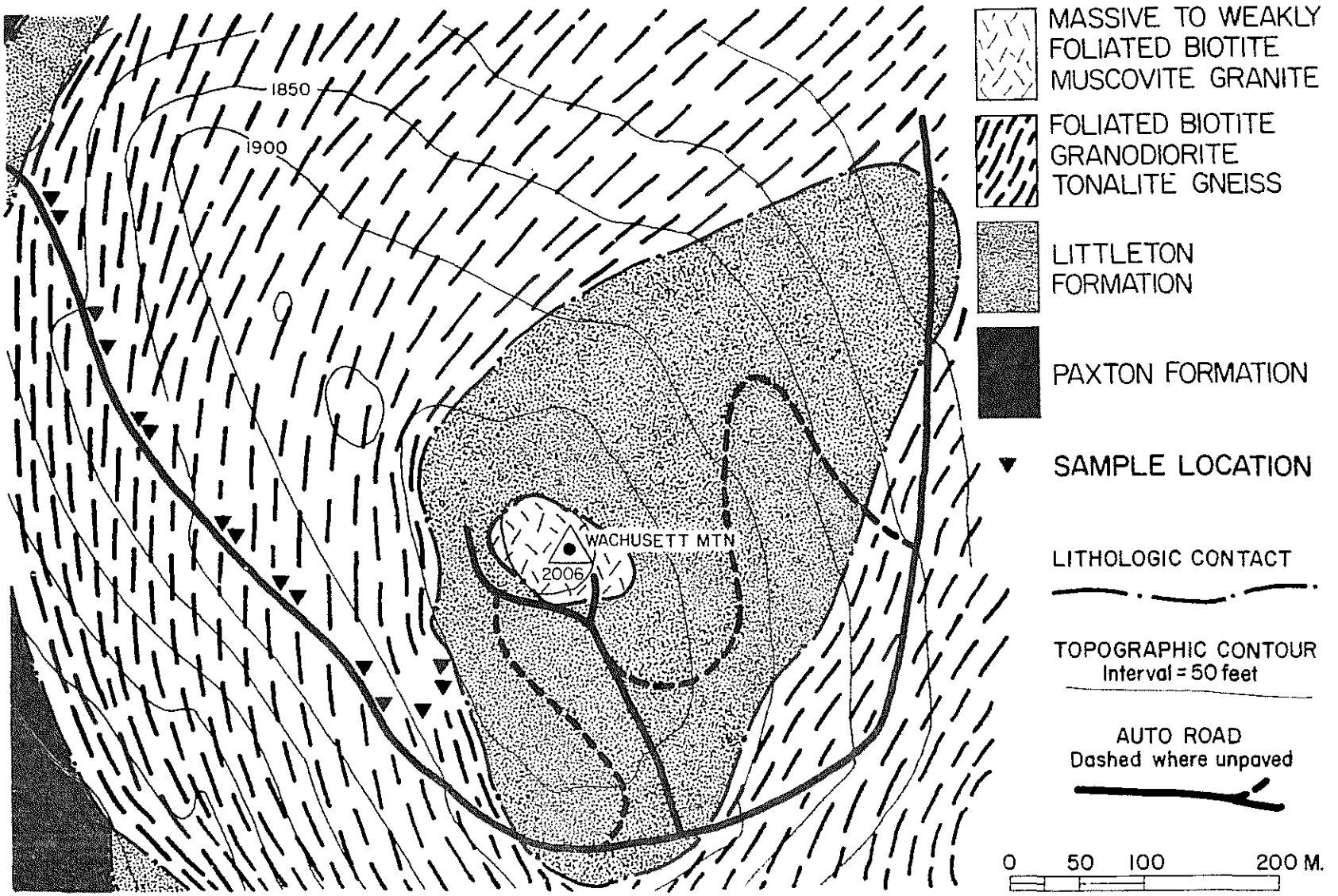


Figure 7. Sample location map for the granodiorite gneiss on Wachusett Mountain. Geology by R.D. Tucker.

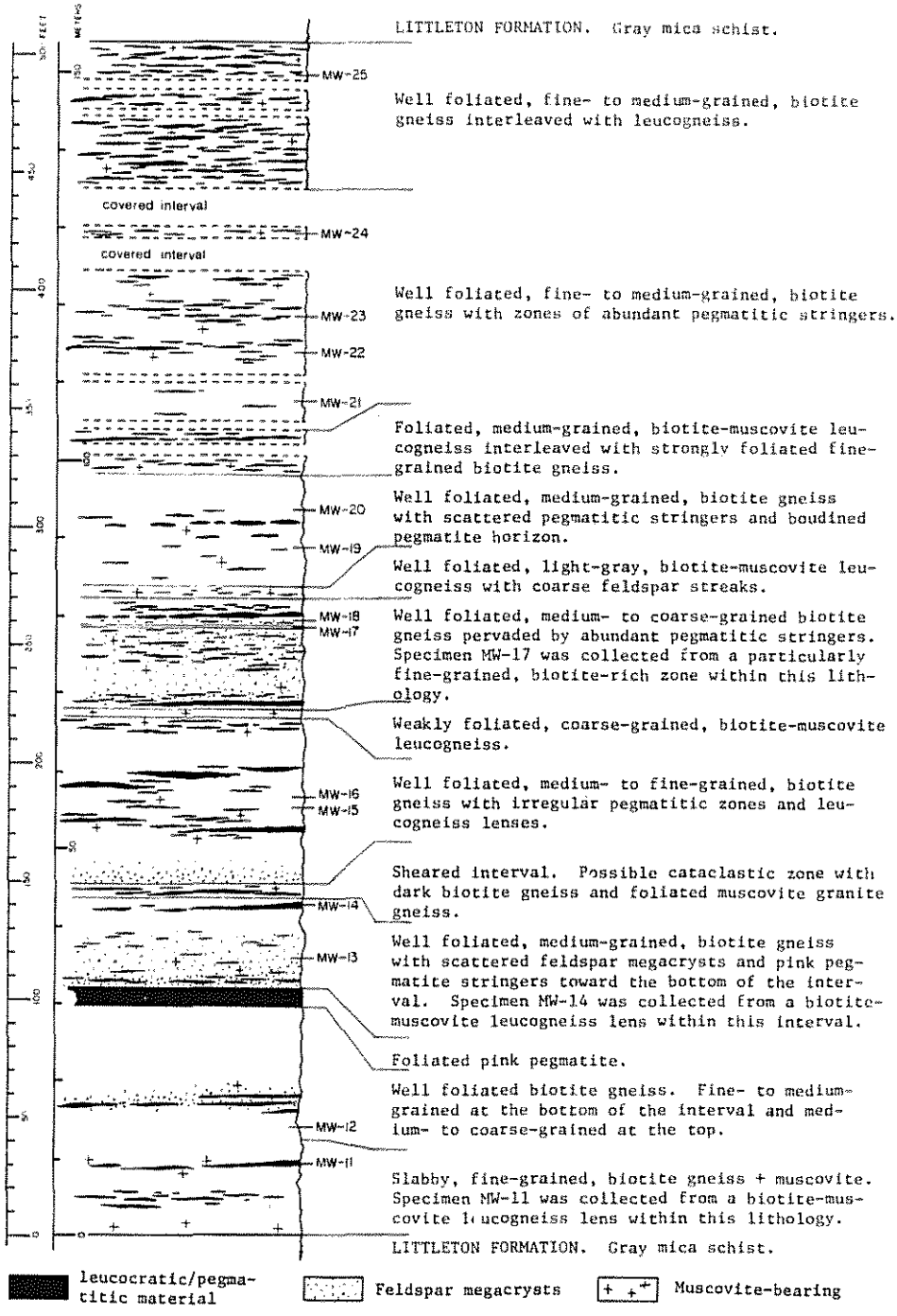


Figure 8. Measured section and description for complete sequence of biotite granodiorite-tonalite gneiss on Wachusett Mountain Road.

Table 2. Point-counted modes (over 2000 points) for the granodiorite gneiss, Western Belt, Wachusett Mountain, including tonalite inclusions from Calamint Hill (Wachusett Mountain quadrangle).

| | COMMON GNEISS | | | | | | | | |
|---|---|---|---|---|---|---|---|---|---|
| | MW-12 | MW-13 | MW-15 | MW-16 | MW-19 | MW-20 | MW-21 | MW-22 | MW-23 |
| Quartz | 20.0 | 21.2 | 24.6 | 22.6 | 23.1 | 22.5 | 17.9 | 21.7 | 23.5 |
| Plagioclase | 42.8 | 36.6 | 35.3 | 36.9 | 41.0 | 36.2 | 37.1 | 44.9 | 37.2 |
| (mol.% An)* | 33 | 37 | 38 | 33 | 39 | 37 | 39 | 33 | 38 |
| Potassic Feldspar | - | 3.5 | 2.8 | 5.6 | - | - | - | 0.1 | - |
| Myrmekite | - | 0.2 | 0.1 | tr | - | - | - | - | - |
| Biotite | 32.9 | 32.5 | 30.8 | 30.1 | 31.3 | 35.3 | 38.6 | 28.0 | 35.1 |
| Muscovite | 1.4 | 1.5 | 2.7 | 1.9 | 1.4 | 0.5 | 1.2 | 2.1 | 0.7 |
| Sphene | 0.4 | 0.7 | 0.2 | 0.4 | 0.2 | 1.3 | 1.8 | 0.1 | 0.3 |
| Allanite | 0.7 | 0.4 | tr | - | - | 0.5 | 0.5 | 0.1 | 0.1 |
| Pistacite | 0.2 | - | 1.2 | 0.5 | 0.3 | 0.4 | 0.1 | 0.2 | - |
| Opaque Minerals | 0.2 | 1.2 | 1.2 | 0.8 | 1.5 | 1.4 | 0.8 | 1.2 | 1.7 |
| Apatite | 1.1 | 2.0 | 1.0 | 1.1 | 1.2 | 1.8 | 2.0 | 1.4 | 1.4 |
| Zircon | 0.3 | 0.1 | tr | tr | - | tr | - | 0.2 | - |
| Chlorite | - | - | tr | - | - | - | - | - | - |
| Calcite | tr | - | - | tr | - | tr | tr | - | - |
| 100 Pl/(Pl+Ksp) | 100 | 91 | 93 | 87 | 100 | 100 | 100 | 97 | 100 |
| 100 Qz/(Qz+Fsp) | 32 | 35 | 39 | 35 | 36 | 38 | 33 | 33 | 39 |

* Determined by Michel-Levy extinction angle method, using determinative figure 123, p. 333, Deer, Howie, and Zussman (1966)

Table 2, continued.

| | COMMON GNEISS | | BIOTITE-EPIDOTE-RICH GNEISS | GRANITIC GNEISS SILLS | | MUSCOVITE-RICH GRANITE GNEISS | HORNBLENDE TONALITE INCLUSIONS | | |
|---|---|---|---|---|---|---|---|---|---|
| | MW-24 | MW-25 | MW-17 | MW-11 | MW-14 | MW-18 | MW-4 | MW-5 | MW-8 |
| Quartz | 25.3 | 25.2 | 20.5 | 35.0 | 25.4 | 27.6 | 17.3 | 17.2 | 16.9 |
| Plagioclase | 43.2 | 42.3 | 29.4 | 24.8 | 21.0 | 31.0 | 40.2 | 41.1 | 37.0 |
| (mol.% An) | 32 | 38 | 48 | 28 | 32 | 31 | 46-28 | 43-28 | 45-28 |
| Potassic Feldspar | - | - | - | 29.4 | 36.1 | 16.3 | - | - | - |
| Myrmekite | - | - | - | 1.8 | 1.8 | 0.5 | 0.2 | - | - |
| Biotite | 26.3 | 26.3 | 41.8 | 7.5 | 13.4 | 17.0 | 31.8 | 30.2 | 30.6 |
| Hornblende | - | - | - | - | - | - | 3.1 | 4.4 | 1.4 |
| Muscovite | 3.0 | 4.6 | 1.3 | 1.0 | 0.2 | 3.9 | - | - | 0.5 |
| Sphene | - | - | 1.3 | - | tr | 0.6 | tr | 0.1 | tr |
| Allanite | - | - | 0.2 | - | tr | - | tr | 0.2 | 0.2 |
| Pistacite | - | - | 2.8 | - | 0.4 | 0.6 | 2.1 | 2.6 | 2.6 |
| Opaque Minerals | 1.1 | 0.7 | 1.2 | 0.2 | 1.0 | 0.9 | 2.6 | 2.6 | 3.1 |
| Apatite | 0.9 | 0.8 | 1.5 | 0.3 | 0.6 | 1.0 | 2.1 | 2.6 | 2.6 |
| Zircon | 0.1 | - | tr | - | 0.1 | 0.1 | tr | tr | 0.1 |
| Chlorite | - | 0.1 | - | tr | tr | 0.4 | tr | tr | 7.2 |
| Calcite | tr | - | - | - | - | - | - | tr | 0.1 |
| 100 Pl/(Pl+Ksp) | 100 | 100 | 100 | 46 | 37 | 65 | 100 | 100 | 100 |
| 100 Qz/(Qz+Fsp) | 37 | 37 | 41 | 39 | 31 | 37 | 30 | 30 | 31 |

* Determined by Michel-Levy extinction angle method, using determinative figure 123, p. 333, Deer, Howie, and Zussman (1966).

Table 2, continued. Hand specimen descriptions, Western belt, Wachusett Mountain and vicinity.

These samples were collected along a traverse through the granodiorite gneiss. The number in parentheses after the sample number indicates the number of running meters along the traverse above the basal contact at which the samples were collected.

MW-11 (27 m) Massive, strongly foliated, lineated, light-gray, feldspar-quartz-biotite-muscovite leucogneiss. Feldspar forms medium-grained augen.

MW-12 (51 m) Massive, strongly foliated, dark-gray, fine-grained, feldspar-quartz-biotite gneiss.

MW-13 (124 m) Flaggy, strongly foliated, dark-gray, predominantly fine-grained, feldspar-quartz-biotite gneiss. Numerous medium- to coarse--grained feldspar augen pervade the sample.

MW-14 (155 m) Massive, strongly foliated, gray, fine-grained, feldspar-quartz-biotite leucogneiss.

MW-15 (223 m) Massive, strongly foliated, dark-gray, fine-grained, feldspar-quartz-biotite-muscovite-epidote gneiss. Fine grains of pyrite are present. Rusty weathering.

MW-16 (232 m) Massive, strongly foliated, dark-gray, predominantly fine-grained, feldspar-quartz-biotite-epidote gneiss. Medium-grained feldspar megacrysts are present but rare.

MW-17 (337 m) Strongly foliated, dark-gray, very fine-grained, feldspar-quartz-biotite gneiss with particularly abundant epidote. This specimen was collected from a 20 cm wide zone in the midst of gneiss from which sample MW-18 was collected.

MW-18 (338 m) Flaggy, strongly foliated, gray, fine- to medium-grained, feldspar-quartz-biotite-muscovite gneiss. Pervasive medium- to coarse-grained leucocratic patches and stringers comprise a significant portion of the rock.

MW-19 (389 m) Massive, strongly foliated, lineated, dark-gray, fine-grained, feldspar-quartz-biotite gneiss.

MW-20 (427 m) Flaggy, strongly foliated, lineated, dark-gray, fine-grained, feldspar-quartz-biotite gneiss.

MW-21 (512 m) Massive, strongly foliated, lineated, dark-gray fine-grained, feldspar-quartz-biotite gneiss.

Table 2, continued.

MW-22 (543 m) Massive, strongly foliated, dark-gray, fine- to medium-grained, feldspar-quartz-biotite gneiss. Medium-grained leucocratic stringers and megacrysts of feldspar and quartz are present.

MW-23 (591 m) Massive, strongly foliated, dark-gray, fine-grained, feldspar-quartz-biotite gneiss.

MW-24 (611 m) Massive, strongly foliated, dark-gray, predominantly fine-grained, feldspar-quartz-biotite gneiss. Medium- to coarse-grained feldspar megacrysts and aggregates of megacrysts are present.

MW-25 (642 m) Massive, strongly foliated, dark-gray, fine-grained, feldspar-quartz-biotite gneiss.

## Tonalite Inclusions

All three specimens of the hornblende-biotite tonalite inclusions were collected in the vicinity of Calamint Hill.

MW-4 Massive, dark-gray, medium- to coarse-grained, feldspar-quartz-biotite rock. Biotite forms large 1 cm poikilitic grains which give the rock a patchy appearance.

MW-5 Massive, weakly foliated, dark-gray, medium-grained, feldspar-quartz-biotite gneiss. It was collected approximately 20 ft away from sample MW-4.

MW-8 Massive, dark-gray, medium- to coarse-grained, feldspar-quartz-biotite rock with rare biotite patches.

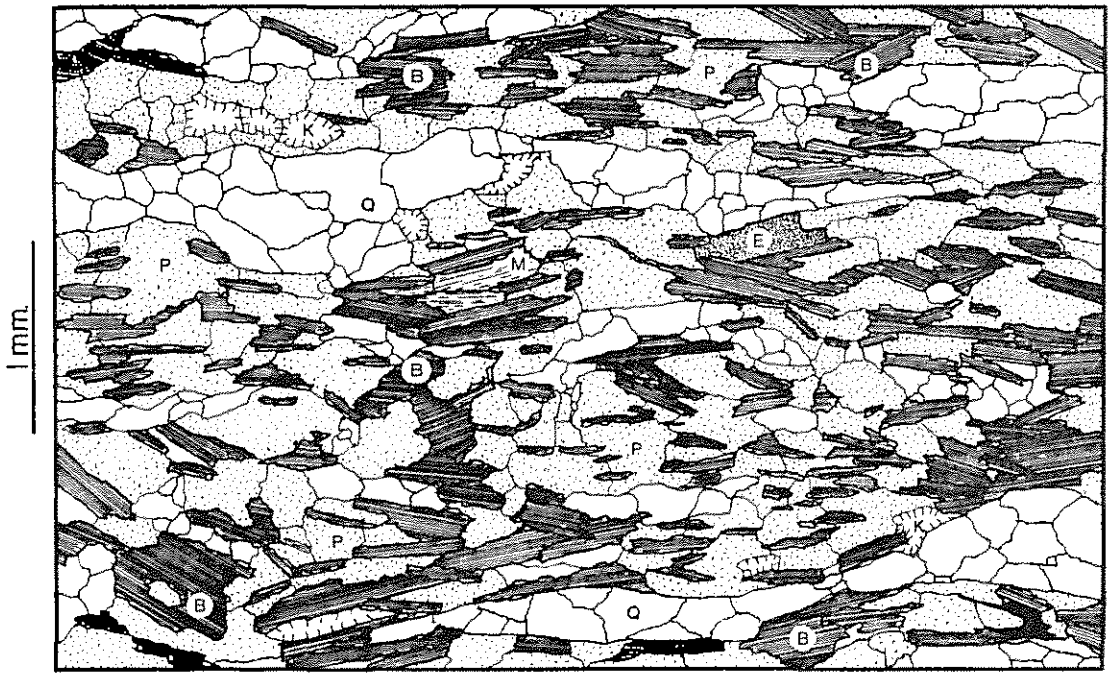


Figure 9. Sketch from a thin section of granodiorite gneiss from Wachusett Mountain, sample MW-15. P=Plagioclase, B=Biotite, Q=Quartz, K=Potassic feldspar, M=Muscovite, E=Epidote, black=opaque minerals.

35.3 to 44.9%. The ratio of plagioclase to total feldspar ranges from 87 to 100. Accessory minerals include potassium feldspar, pistacite, allanite, sphene, muscovite, apatite, zircon, ilmenite, and secondary chlorite, pyrite, rutile, and calcite.

The rocks in the Wachusett Mountain area have undergone sillimanite-muscovite grade metamorphism. As a result, the granodiorite gneiss has developed a more extreme metamorphic texture relative to the sillimanite-staurolite grade gneiss at South Monoosnoc Hill. The gneiss has a strongly foliated and recrystallized fabric readily apparent in thin section (Figure 9). The fabric is defined by the subparallel arrangement of biotite flakes as well as elongate aggregates of feldspar and quartz. Although subsequent recrystallization has probably obliterated much of the evidence, some amount of cataclasis is noted in samples MW-13, 14, 17, 20, and 22. Here, elongate zones of minute, 0.05 to 0.3 mm feldspar, quartz, and biotite grains trend subparallel to the foliation in contrast to the generally even-grained, 0.3 to 1.0 mm grain size distribution commonly observed.

Plagioclase forms 0.05 to 4.0 mm equant to elongate, anhedral grains averaging 0.8 mm in size. Plagioclase ranges from $An_{32}$ to $An_{39}$ (Michel-Levy method). Twin lamellae are deformed, and minute rectangular potassium feldspar antiperthites have been observed. In samples containing discrete potassium feldspar, plagioclase is myrmekitically intergrown with quartz. Elongate to rodded, 0.1 to 1.3 mm anhedral quartz grains, averaging 0.4 mm in size, have undulatory extinction. Commonly, polycrystalline aggregates of quartz averaging 4.0 mm in length are aligned

parallel to the dominant biotite foliation. Biotite forms subparallel, subhedral, 0.1 to 1.2 mm grains having an average size of 0.7 mm. Biotite is pleochroic, with X = pale yellow green to pale yellow brown and Y = Z = dark brown green to dark brown, but orange-brown varieties of biotite have been observed (MW-24 and 25). Biotite is locally altered to iron-rich chlorite.

Potassium feldspar with incipient microcline twinning, typically forms 0.1 to 1.0 mm anhedral grains averaging 0.4 mm in size, but rare porphyroblasts as large as 2.5 mm have been observed.

Allanite, morphologically identical to that found at South Monoosnoc Hill is present. The properties of slight pleochroism with X = colorless and Z = light green yellow and a $2V_x = 85^o$ were used to identify the fine-grained, subhedral epidote in these rocks as pistacite (Tröger, 1971).

Sphene forms fine, anhedral grains and thin rims on ilmenite. It is not so abundant as at South Monoosnoc Hill nor does it have the common poikilitic habit observed there. Zircon occurs as minute, euhedral grains and as larger, rounded grains, some with thin rims of epidote. Apatite forms fine, euhedral grains and larger rounded masses.

Anhedral ilmenite typically has thin irregular sphene rims. Polyphase patches of ilmenite, rutile, and hematite are present within many ilmenite grains and probably are secondary in origin. Pyrite forms fine, euhedral to subhedral grains which, in some instances, appear to be replaced by magnetite.

Sample MW-17 is distinguished from the common gneiss because it is

particularly fine- and even-grained as well as relatively biotite- and epidote-rich. This sample was collected from a 20 cm wide zone within the rock type from which sample MW-18 was collected. MW-18 has a similar mineral assemblage to the common gneiss, but modally, it is on the granite-granodiorite classification boundary. Fine- to medium-grained polycrystalline feldspar and quartz augen dominate the specimen. MW-11 and 14 are discrete sills of strongly foliated granitic gneiss having distinctly lower biotite contents than the common gneiss.

Modal analyses have shown that there are mineralogical differences between the common gneiss at South Monoosnoc Hill and the common gneiss at Wachusett Mountain. In general, the common gneiss at South Monoosnoc Hill contains more K-feldspar, sphene, muscovite, and zircon and less biotite and plagioclase than the common gneiss at Wachusett Mountain.

Hornblende tonalite inclusions: Calamint Hill. In the vicinity of Calamint Hill, Princeton, two of the three large tonalite inclusions located in the granodiorite gneiss were sampled (Figure 4). The petrography of these inclusions is based on point-counted, chemically analysed specimens MW-4, 5, and 8 and observations from slides obtained from R. D. Tucker.

The major mineral content (Table 2) varies from 37.0 to 41.1% plagioclase, 16.7 to 17.3% quartz, and 30.6 to 31.8% biotite. Varietal minerals are hornblende, 1.4 to 4.4%; clinozoisite, 2.1 to 2.6%; and apatite, 2.1 to 2.6%. Accessory minerals include actinolite, allanite, sphene, zircon, and ilmenite with secondary chlorite, muscovite, pyrite, and calcite.

A variety of textures is present among samples of hornblende-biotite tonalite collected within a small, restricted area. Coarser-grained specimens tend to have a relict igneous texture with euhedral to subhedral, medium-grained plagioclase, interstitial, fine- to medium-grained quartz, subhedral, medium- to coarse-grained biotite, and subhedral, fine- to medium-grained hornblende (Figure 10). Correlated with a decrease in general grain size is an increasingly recrystallized, metamorphic texture. The texture of the recrystallized tonalite is dominated by fine-grained, subhedral biotite which defines a moderate foliation, amidst anhedral, equant to elongate, fine- to medium-grained plagioclase and quartz. Hornblende was not present, but no analysis of the recrystallized tonalite inclusion is available to determine if the absence of hornblende is due to a difference in bulk composition relative to the other tonalite inclusions.

Plagioclase forms 0.3 to 3.5 mm grains averaging approximately 1.2 mm in size. Relict igneous varieties are euhedral to subhedral, have normal zoning from $An_{45}$ to $An_{28}$ (Michel-Levy method) and commonly have minute, oriented inclusions of epidote concentrated in their cores. Despite the absence of potassium feldspar, plagioclase is myrmekitically intergrown with quartz. Recrystallized plagioclase is anhedral, virtually unzoned ($An_{37}$, Michel-Levy method) and commonly free from inclusions.

Quartz forms anhedral to interstitial, 0.1 to 1.0 mm grains which average 0.4 mm in size. Although clearly interstitial in the igneous varieties, it is granoblastic in the recrystallized types.

In the igneous varieties, biotite forms 0.2 to 7.0 mm poikilitic grains complexly intergrown with plagioclase, quartz, and/or hornblende.


Figure 10. Sketch from a thin section of hornblende tonalite inclusion, sample MW-4, from the granodiorite gneiss. P=Plagioclase, Q=Quartz, B=Biotite, H=Hornblende, E=Epidote, black=opaque minerals.

Epidote, apatite, and opaques are common inclusions. Biotite is strongly pleochroic with X = pale yellow brown, and Y = Z = dark brown green to brown. Pleochroic hornblende, with X = pale green-brown, Y = brown-green, and Z = blue-green, forms medium to fine subhedral grains, some of which rim pale green actinolite. The fibrous habit and nature of its occurrence suggest that actinolite is an alteration product of clinopyroxene.

Fine-grained, euhedral to subhedral clinozoisite commonly rims fine-grained, euhedral allanite. Some clinozoisite forms complex symplectic intergrowths with quartz. Sphene occurs as fine anhedral grains associated with biotite or as rims around ilmenite. Fine-grained euhedral prisms of apatite are commonly included in biotite and rimmed by ilmenite.

Ilmenite forms fine, simple grains and composite grains with sulfides. Contacts between ilmenite and included pyrite or chalcopyrite (rare) range from sharp to intermediate with zones of two and three phase mosaics of ilmenite, hematite, and rutile separating the two phases. Pyrite occurs as discrete grains with some amount of hematite/goethite alteration.

## Foliated Biotite-Muscovite Granite-Granodiorite Gneiss

The foliated biotite-muscovite granite-granodiorite gneiss forms a structurally higher sheet relative to the granodiorite gneiss in the broad structural syncline. Fresh samples of the gneiss were collected from two localities, along Mountain Road in Princeton and from Crow Hills (Figure 4).

A plot based on modes of all specimens from these localities is shown in Figure 11. Samples from this unit actually span the fields of granite, granodiorite, and tonalite. Samples of the foliated biotite-muscovite granite-granodiorite gneiss will here be referred to as the granite gneiss.

In general this rock type is foliated biotite-muscovite leucogneiss which varies in grain size, mafic mineral content, and amount of pegmatitic stringers at the outcrop scale. Within the rock type (Table 3, sample MF-21 excluded), the major mineral content ranges from 22.5 to 43.7% plagioclase, 5.9 to 31.8% potassium feldspar, 23.1 to 27.8% quartz, 6.0 to 19.7% biotite, and 2.7 to 8.5% muscovite. The ratio of plagioclase to total feldspar ranges from 41 to 88. Accessory minerals include apatite, zircon, allanite, sphene, clinozoisite, and ilmenite with secondary chlorite, pyrite, and calcite. In general, the specimens exhibit a granoblastic texture with felsic minerals forming equant to elongate grains and aggregates, and micas defining a moderate foliation (Figure 12).

Plagioclase forms 0.2 to 5.0 mm equant to elongate grains which average 1.0 mm in size. Polysynthetic twinning is poorly developed, and patchy extinction is common. Well twinned rims on plagioclase form where adjacent to potassium feldspar and have a composition of approximately $An_3$ (Michel-Levy). Antiperthitic patches of potassium feldspar are present in many plagioclase grains. Plagioclase is sericitically altered to varying degrees and is myrmekitically intergrown with quartz.

Quartz forms 0.1 to 2.0 mm anhedral grains which average 0.7 mm in

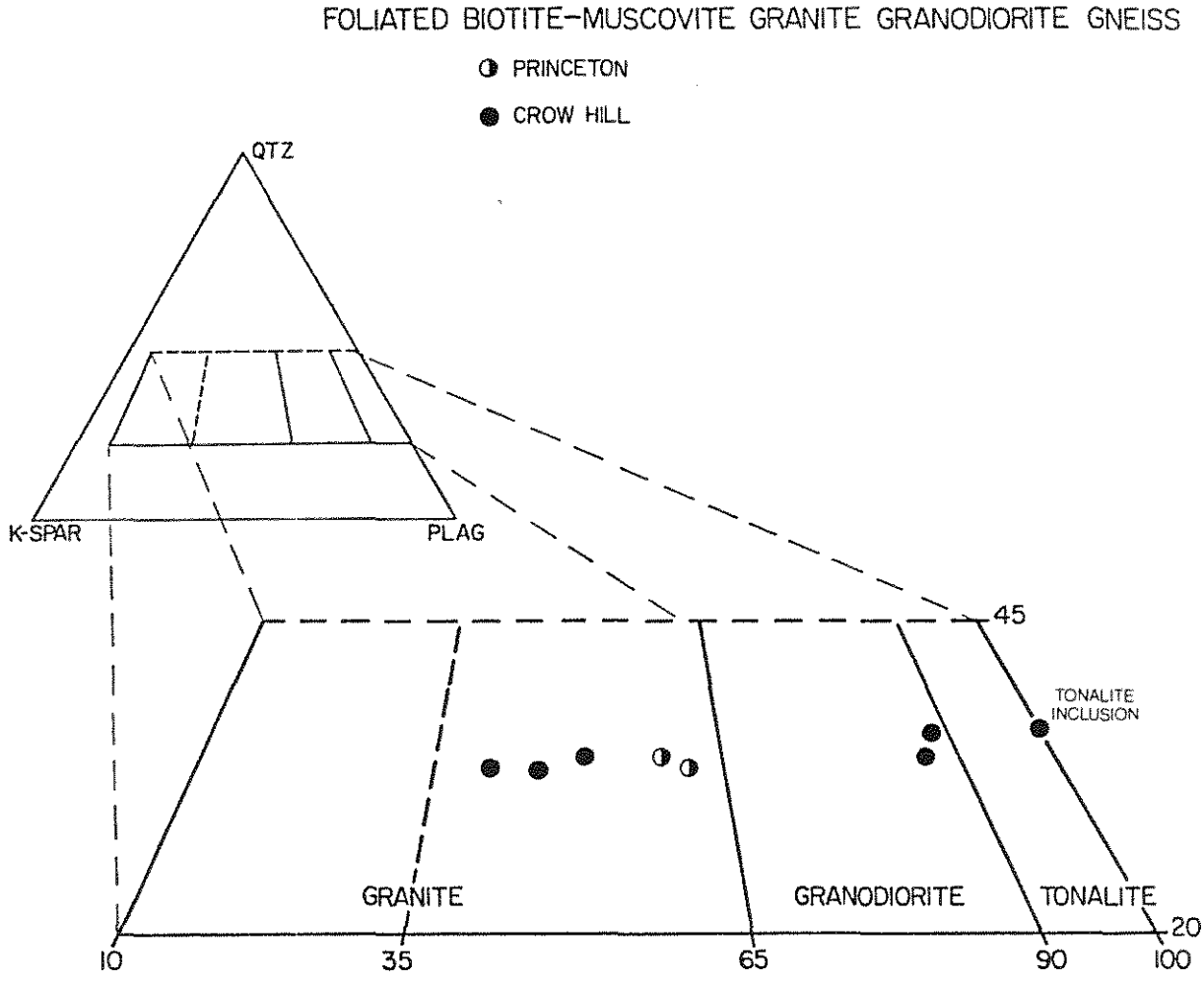


Figure 11. Plot based on modes of samples of foliated biotite-muscovite granite-granodiorite gneiss. Diagram modified from Streckeisen (1973).

Table 3. Point-counted modes (over 2000 points) for the granite gneiss, Princeton (Wachusett Mountain quadrangle) and Crow Hills (Fitchburg quadrangle).

| | PRINCETON | | CROW HILLS | | | | | |
|---|---|---|---|---|---|---|---|---|
| | GRANITE | | GRANITE | | | GRANODIORITE | | TONALITE |
| | MW-1 | MW-2 | MF-24 | MF-25 | MF-27 | MF-22 | MF-29 | MF-21 |
| Quartz | 24.4 | 27.2 | 27.8 | 27.3 | 27.7 | 28.4 | 24.8 | 23.1 |
| Plagioclase | 31.3 | 31.3 | 27.7 | 22.5 | 26.1 | 43.7 | 41.9 | 40.7 |
| (mol.% An)* | 29 | 23 | 24 | 25 | 25 | 24 | 29 | 35 |
| Potassic Feldspar | 19.3 | 21.7 | 26.2 | 31.8 | 30.3 | 5.9 | 6.0 | - |
| Myrmekite | 2.2 | 3.1 | 3.0 | 1.2 | 1.9 | 2.2 | 0.5 | - |
| Biotite | 14.4 | 13.1 | 7.7 | 7.9 | 6.0 | 15.1 | 19.8 | 31.5 |
| Muscovite | 6.6 | 2.7 | 7.1 | 8.5 | 7.5 | 4.0 | 5.2 | - |
| Sphene | 0.3 | - | - | - | - | - | - | 0.9 |
| Allanite | tr | - | tr | - | - | - | 0.1 | 0.4 |
| Clinozoisite | - | - | - | - | - | - | - | 0.4 |
| Opaque Minerals | 0.5 | 0.6 | 0.1 | 0.4 | 0.2 | 0.4 | 1.1 | 0.4 |
| Apatite | 0.6 | 0.2 | 0.3 | 0.2 | 0.2 | 0.3 | 0.6 | 2.3 |
| Zircon | tr | tr | tr | tr | - | - | tr | 0.3 |
| Chlorite | 0.4 | - | tr | 0.2 | tr | - | tr | - |
| Calcite | tr | - | tr | - | - | - | tr | - |
| 100 Pl/(Pl+Ksp) | 62 | 59 | 51 | 41 | 46 | 88 | 87 | 100 |
| 100 Qz/(Qz+Fsp) | 33 | 34 | 34 | 33 | 33 | 36 | 34 | 36 |

* Determined by Michel-Levy extinction angle method using determinative figure 123, p. 333, Deer, Howie, and Zussman (1966).

Table 3, continued. Hand specimen descriptions for the granite gneiss, Princeton and Crow Hills.

MW-1 Well foliated, medium-grained, biotite-muscovite granite gneiss. There is a variable nature to the unit at this outcrop. This sample was collected from a roadcut on Mountain Road, 1.1 miles north of the intersection of state highways 62 and 31 and Mountain Road.

MW-2 Foliated, fine- to medium-grained, biotite-muscovite granite gneiss. This lithology is uniform over the entire outcrop. This sample was collected from a roadcut on Mountain Road 0.2 miles north of the intersection of state highways 62 and 31 and Mountain Road.

The following samples were collected from the large, south-facing cliff at the southern-most mound of Crow Hills. Crow Hills can be reached by traveling approximately 2.3 miles south on state highway 31 after its intersection with Route 2.

MF-24 Foliated, fine- to medium-grained, biotite-muscovite granite gneiss. This sample comes from a relatively uniform section of rock on the west end of the cliff face at the 1100 foot contour.

MF-25 Foliated, fine- to medium-grained, biotite-muscovite granite gneiss. Sampled from the same horizon as MF-24 but in the central part of the cliff face approximately 30 meters to the east of MF-24.

MF-27 Well foliated, fine- to medium-grained, biotite-muscovite granite gneiss. Leucocratic augen and pegmatitic stringers are present in varying proportions. Taken from the eastern edge of the cliff face on the 1160 foot contour.

MF-22 Well foliated, medium-grained, biotite-muscovite granodiorite gneiss. Abundant pegmatitic stringers are present in the outcrop. This is the host gneiss for sample MF-21, taken from the same location.

MF-29 Well foliated, medium-grained, biotite-muscovite granodiorite gneiss. Occurs in a mixed lithology with coarse pegmatite. Collected on the east edge of the cliff face at the 1100 foot contour.

MF-21 Foliated, very fine-grained, biotite tonalite gneiss, distinctively different from the typical gneiss present at this locality. It was collected from the top-central part of the cliff at the 1200 foot contour.

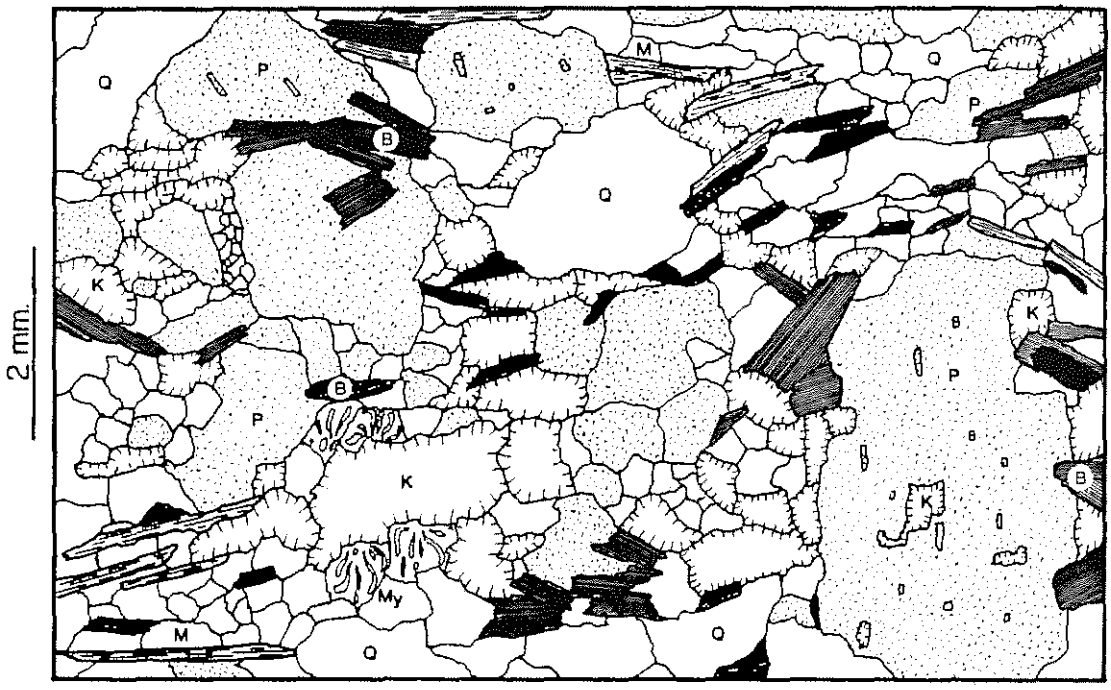


Figure 12. Sketch from a thin section of granite gneiss, sample MW-2. P=Plagioclase, Q=Quartz, K=Microcline, My=Myrmekite, B=Biotite, M=Muscovite, black=opaque minerals.

size. Quartz displays undulatory extinction and commonly forms elongate aggregates averaging 3.0 mm in length.

The micas, together with elongate aggregates of feldspar and quartz, define a moderate foliation. Strongly pleochroic biotite, with X = pale yellow brown, Y = Z = dark brown to red brown, forms 0.1 to 1.5 mm subhedral grains which average 0.5 mm in size. Iron-rich chlorite is a common alteration product of biotite. Muscovite occurs as 0.1 to 1.3 mm subhedral grains which average 0.5 mm in size. Some grains appear to be primary, being intimately intergrown with biotite and concordant with the dominant foliation while others appear to be secondary, being markedly discordant with the general regional foliation.

Apatite and zircon form fine-grained, euhedral to anhedral grains, disseminated throughout the specimen. Rare allanite occurs as fine, euhedral grains, grains interstitial to biotite, and as minute grains rimming some zircons.

Opaque minerals are commonly associated with biotite. Fine-grained ilmenite forms elongate grains included by biotite and paralleling its cleavage. Some ilmenite grains are partly or completely replaced by sphene or secondarily altered to rutile. Pyrrhotite and pyrite form simple subhedral to anhedral grains and pentlandite can form simple grains or composite grains with pyrrhotite.

MF-21 is distinguished from the common granite gneiss by its melanocratic appearance and by its resemblance to the granodiorite gneiss at Wachusett Mountain. It is a fine-, even-grained, strongly foliated tonalite gneiss with accessory sphene, allanite, and clinozoisite.

Massive to Weakly Foliated Biotite-Muscovite Granite

Due to its relatively undeformed nature, irregular distribution, and apparent cross-cutting relationships with the granodiorite gneiss and the granite gneiss, the massive to weakly foliated biotite-muscovite granite is thought to have been emplaced concurrent with or subsequent to the last major deformational episode. Samples of the massive to weakly foliated granite were collected from a number of sites: Rollstone Hill, Fitchburg; along Mountain Road, Princeton; Malden Hill, Holden; and West Sterling (Figure 4). From 1865 to 1919, various operators ran individual quarries at different sites on Rollstone Hill, Fitchburg, furnishing granite for buildings, curbing and paving (Dale, 1923). Here five samples were collected from the large amount of outcrop exposed during quarrying operations. Two samples were collected at different locations on Malden Hill, and single samples were taken from the other two localities.

Modes of all specimens collected from the mapped unit (Peper and Wilson, 1978; Hepburn, 1976) of massive to weakly foliated biotite-muscovite granite are shown in Figure 13. Samples of this unit plot in the granite, granodiorite, and quartz syenite fields. Samples of the massive to weakly foliated biotite-muscovite granite will here be referred to as the granite. The granite appears to be uniform in texture and mineral content over large areas. Pegmatite commonly containing black tourmaline is present. The predominant rock type is a medium- to coarse-grained, massive to weakly foliated, biotite-muscovite granite. The weak foliation is primarily defined by the orientation of feldspar and quartz

aggregates and secondarily by slight planar preferred orientation of mica (Figure 14).

Within the common granite (Table 4, MF-1 to 5; MWN-2; MW-3), the major mineral content ranges from 21.4 to 29.3% plagioclase, 28.9 to 32.4% potassium feldspar, 27.2 to 31.9% quartz, 2.6 to 7.3% muscovite, and 2.3 to 8.3% biotite. Accessory minerals include allanite, apatite, zircon, and ilmenite, and secondary chlorite.

Plagioclase forms subhedral to anhedral grains ranging from 0.1 to 3.2 mm and average 2.0 mm in size. Fine-grained, subhedral grains are commonly included in potassic feldspar. The average composition of plagioclase for this unit, determined by the Michel-Levy method is $An_{24}$. Partial rims of more albite-rich plagioclase ($An_2$, Michel-Levy) occur on grains adjacent to potassic feldspar. Plagioclase is commonly myrmekitically intergrown with quartz and sericitically altered.

Microcline is identified by abundant tartan twinning. It occurs as 0.1 to 9.0 mm subhedral to anhedral to interstitial grains, averaging 4.5 mm in size. The larger grains commonly contain euhedral to subhedral inclusions of plagioclase and biotite.

Quartz forms 0.1 to 6.0 mm anhedral to interstitial grains averaging 1.0 mm in size. Quartz has undulatory extinction and typically forms polycrystalline aggregates averaging 4.0 mm in length.

Strongly pleochroic biotite, with X = pale yellow brown, Y = Z = dark red brown, forms 0.1 to 2.0 mm subhedral grains averaging 0.8 mm in size. Fine-grained euhedral to subhedral biotite is found as inclusions in larger microcline grains. Iron-rich chlorite is observed as an alteration product of some biotite grains. Muscovite forms 0.3 to 5.0 mm

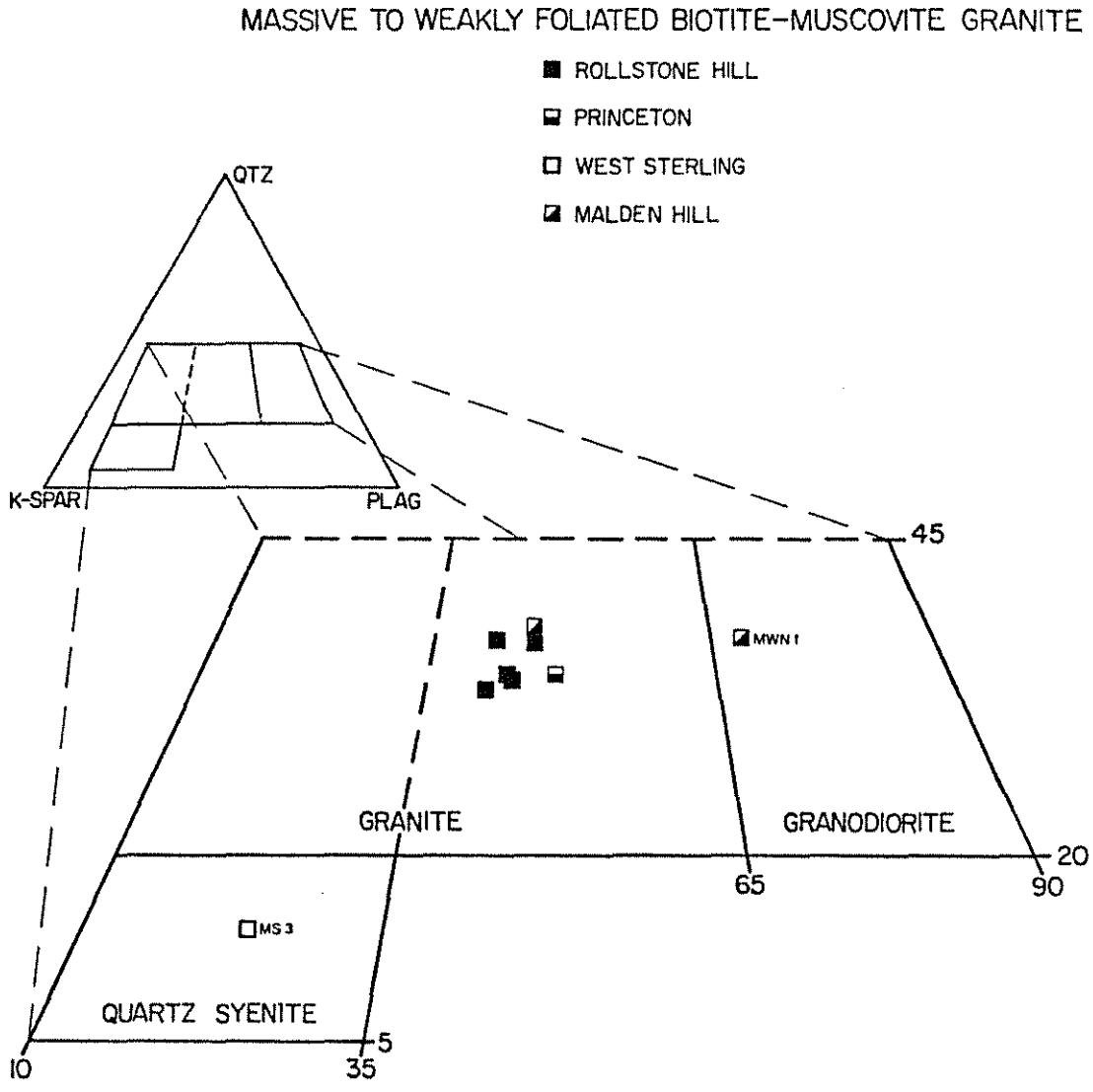


Figure 13. Plot based on modes from samples of the massive to weakly foliated biotite-muscovite granite. Diagram modified from Streckeisen (1973).

Table 4. Point-counted modes (over 2000 points) for the granite.

| | | | | | | GRANO-DIORITE | | | QUARTZ SYENITE |
|---|---|---|---|---|---|---|---|---|---|
| | MF-1 | MF-2 | MF-3 | MF-4 | MF-5 | MWN-1 | MWN-2 | MW-3 | MS-3 |
| Quartz | 27.2 | 28.2 | 27.5 | 29.7 | 31.5 | 29.7 | 31.9 | 31.5 | 11.7 |
| Plagioclase | 22.8 | 23.1 | 22.5 | 21.4 | 25.0 | 35.1 | 24.3 | 29.3 | 17.8 |
| (mol.% An)* | 23 | 22 | 22 | 22 | 24 | 22 | 29 | 22 | 20 |
| Potassic Feldspar | 30.8 | 31.0 | 32.4 | 29.6 | 28.9 | 16.2 | 28.4 | 31.2 | 57.1 |
| Myrmekite | 6.1 | 5.0 | 3.8 | 4.5 | 4.3 | 2.8 | 3.9 | 2.9 | 4.6 |
| Biotite | 8.3 | 7.9 | 8.0 | 6.9 | 5.8 | 11.4 | 4.5 | 2.3 | 5.2 |
| Muscovite | 4.0 | 4.0 | 5.1 | 7.3 | 3.9 | 4.4 | 6.5 | 2.6 | 3.1 |
| Sphene | - | - | - | - | - | - | - | - | - |
| Allanite | 0.1 | - | - | tr | 0.1 | - | - | - | - |
| Clinozoisite | - | - | - | - | - | - | - | - | - |
| Opaque Minerals | 0.2 | 0.3 | 0.3 | 0.3 | 0.2 | tr | tr | 0.1 | 0.1 |
| Apatite | 0.3 | 0.3 | 0.2 | 0.2 | 0.2 | 0.3 | 0.4 | tr | 0.2 |
| Zircon | 0.1 | 0.2 | 0.1 | 0.1 | 0.1 | tr | 0.1 | 0.1 | 0.1 |
| Chlorite | - | - | - | tr | - | tr | tr | - | 0.1 |
| Calcite | - | - | tr | - | - | tr | - | - | - |
| 100 Pl/(Pl+Ksp) | 43 | 43 | 41 | 42 | 46 | 68 | 46 | 48 | 24 |
| 100 Qz/(Qz+Fsp) | 34 | 43 | 33 | 37 | 37 | 37 | 38 | 34 | 14 |

* Determined by Michel-Levy extinction angle method, using determinative figure 123, p. 333, Deer, Howie, and Zussman (1966).

Table 4, continued. Hand specimen descriptions for the granite.

MF-1 through 5, Rollstone Hill. These samples are taken from essentially the same outcrop. They are massive to weakly foliated, medium- to coarse-grained, leucocratic, biotite-muscovite granite. Muscovite forms flakes distinctly larger than biotite. Alignment of potassium feldspar grains forms a weak mineral lineation. The samples were collected from nearly continuous exposure in an abandoned quarry on Rollstone Hill, Fitchburg.

MWN-1, Malden Hill. Same general appearance as granite at Rollstone Hill, except it is more foliated. Modally it is a granodiorite. This sample was collected from exposure along the Asnebumskit Brook, beneath the bridge on Mills Street, approximately 400 ft. north of its junction with Quinapoxet Road in the town of Holden.

MWN-2, Malden Hill. Same general appearance as granite at Rollstone Hill, except it is more foliated. This sample was collected from exposure on Malden Street approximately 800 ft. west of its junction with Goodale Street and Lee Street in the town of West Boylston.

MW-3, Princeton. Weakly foliated, medium- to coarse-grained granite. Biotite and muscovite are present but in lesser quantities than at other localities. This sample was collected from a roadcut on Mountain Road 0.2 miles north of the intersection of state highways 62 and 31 and Mountain Road.

MS-1, West Sterling. Coarse-grained, biotite-muscovite-tourmaline quartz syenite. It is leucocratic and contains much less quartz than other specimens. The alignment of coarse-grained potassium feldspar megacrysts forms a moderate mineral lineation. This sample was collected from a roadcut on Beaman Road 0.9 miles east of the southern intersection of Beaman Road and state highway 140.

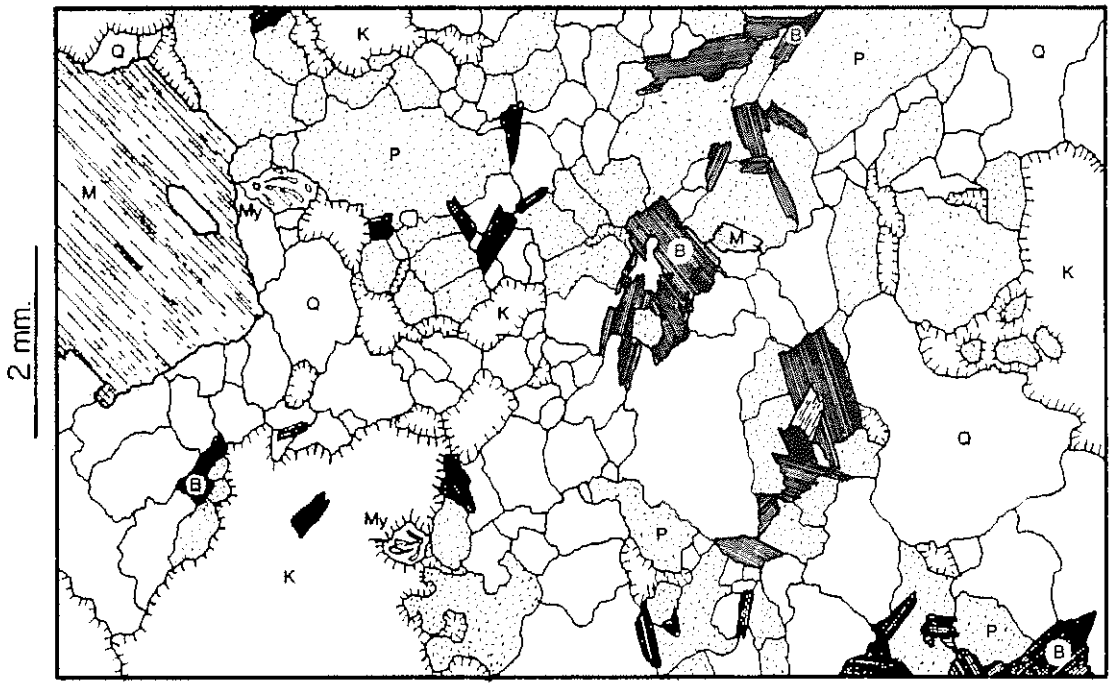


Figure 14. Sketch from a thin section of granite, sample MF-2. P=Plagioclase, Q=Quartz, K=Microcline, My=Myrmekite, B=Biotite, M=Muscovite, black=opaque minerals.

subhedral grains averaging 2.5 mm in size. Some grains have inclusions of apatite, zircon, and/or ilmenite.

Fine-grained, euhedral to subhedral zircon and apatite occur as inclusions in biotite and muscovite. Fine-grained allanite occupies an interstitial position to biotite. Fine-grained, anhedral to subhedral ilmenite is associated with biotite.

Although very similar in appearance to the granite at Rollstone Hill, sample MWN-1 is modally a granodiorite. The principal difference between the two rock types is that plagioclase occurs as larger, as well as more abundant crystals in MWN-1 relative to the Rollstone Hill granite.

Sample MS-3 is distinguished from the common granite in that it is a quartz syenite, being particularly leucocratic and relatively quartz poor. Abundant, coarse-grained, subhedral microcline megacrysts define a moderately developed mineral lineation which roughly parallels the intrusive contact of this rock type into granodiorite gneiss.

Discussion

The rocks of the Fitchburg complex have been divided into three major units by previous workers. There is substantial mineralogic variation within the units, as has been illustrated in the plots of the modes. A greater amount of this variation is found in the rocks of higher metamorphic grade on the western side of the complex relative to those of the eastern side.

Figure 15a is a plot of modal quartz, combined feldspars, and colored minerals (includes biotite, hornblende, sphene, epidote, allanite, and opaque minerals) for all samples of the Fitchburg complex. This plot

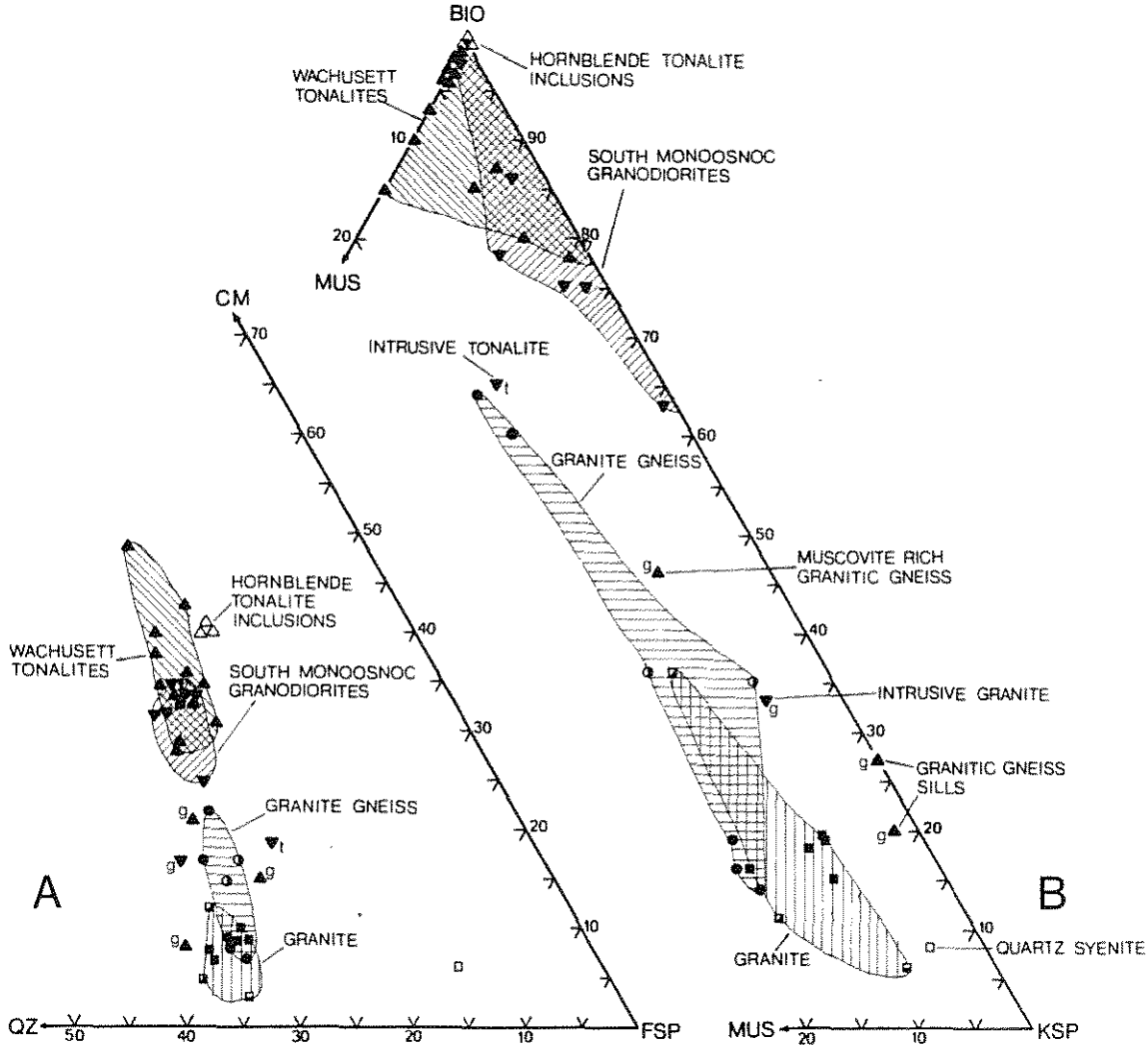


Figure 15a and b. Plots of some modal data for all samples of the Fitchburg complex. Symbols are the same used in the modal plots.

15a. Plot of quartz (QZ), combined feldspars (FSP), and colored minerals (CM). Colored minerals include biotite, hornblende, sphene, epidote, allanite, and opaque minerals.

15b. Plot of biotite (BIO), muscovite (MUS), and K-feldspar (KSP) normalized to the sum of all three.

illustrates the variation in color index. The samples fall into groups plus a few dikes and inclusions as indicated. The quartz syenite sample from West Sterling (MS-3) is the point which falls away from the other samples.

Figure 15b is a plot of modal biotite, K-spar, and muscovite. The samples of the complex plot roughly in two groups: one rich in biotite and one rich in K-feldspar. The granodiorite gneiss has a low muscovite content, and the granite gneiss and the granite have relatively high muscovite contents. This plot also illustrates the differences between the granodiorite gneiss and the various leucocratic rocks which intrude it.

## MINERALOGY

Mineral analyses. The chemistry of major, coexisting minerals was determined with the ETEC Autoprobe at the Department of Geology, University of Massachusetts, Amherst. Representative samples of each unit of the Fitchburg complex were chosen for major mineral analyses as follows: MF-8, granodiorite gneiss, South Monoosnoc Hill; MW-15, granodiorite gneiss, Wachusett Mountain; MW-4, tonalite inclusion, Calamint Hill; MW-2, granite gneiss, Princeton; MF-2, granite, Rollstone Hill. Probe sections were cut and polished from the same rock chip which provided the thin section.

Plagioclase. In the Fitchburg complex, plagioclase occurs in a variety of textures, forming euhedral, anhedral, or recrystallized

granoblastic grains. Plagioclase spans a range of compositions which are predominantly oligoclase to andesine, but albite is present locally.

The relict igneous plagioclase in the sillimanite-staurolite grade granodiorite gneiss at South Monoosnoc Hill is subhedral and zoned. The plagioclase composition in sample MF-8 from South Monoosnoc Hill is $An_{27}Ab_{72}Or_1$ (Table 5). Plagioclase in the sillimanite-muscovite grade granodiorite gneiss at Wachusett Mountain is granoblastic in texture and homogeneous in composition, indicating that a more thorough recrystallization of plagioclase has occurred in samples from Wachusett Mountain than in those from South Monoosnoc Hill as a result of different metamorphic grade.

Relict igneous, euhedral, zoned plagioclase occurs in massive parts of the tonalite inclusions from Calamint Hill. In sample MW-4, which was taken from a massive part of a tonalite inclusion, microprobe analyses of a zoned plagioclase yield a core composition of $An_{46}Ab_{57}Or_0$ and a rim composition of $An_{36}Ab_{63}Or_1$ (Table 5). Unzoned granoblastic plagioclase is found in foliated portions of the tonalite inclusions. Thus, as was previously noted in the case of the granodiorite gneiss, recrystallization of plagioclase results in the loss of igneous crystal habit and homogenization of compositional zoning.

The averages of microprobe analyses of plagioclase in sample MW-2, granite gneiss, and MF-2, granite, are both $An_{21}Ab_{78}Or_1$ (Table 5).

In each of the major units of the complex, partial rims of albite-rich plagioclase can be found on those portions of plagioclase which are contiguous with potassium feldspar. The average of microprobe analyses

Table 5. Average microprobe analyses of plagioclase feldspar.

| | MF-8 | MW-4A | MW-4B | MW-2 | MF-2A | MF-2B |
|---|---|---|---|---|---|---|
| $SiO_2$ | 60.15 | 57.42 | 50.09 | 62.98 | 62.81 | 68.52 |
| $Al_2O_3$ | 24.62 | 27.64 | 26.44 | 23.37 | 23.39 | 19.44 |
| CaO | 5.97 | 9.32 | 7.62 | 4.44 | 4.43 | .17 |
| $Na_2O$ | 8.67 | 6.14 | 7.14 | 9.14 | 9.21 | 11.60 |
| $K_2O$ | .17 | .08 | .10 | .22 | .26 | .15 |
| Total | 99.58 | 100.60 | 100.39 | 100.15 | 100.10 | 99.88 |
| Formulae based on 8 oxygens: | | | | | | |
| Si | 2.691 | 2.556 | 2.620 | 2.783 | 2.778 | 2.996 |
| Al | 1.300 | 1.451 | 1.385 | 1.218 | 1.221 | 1.003 |
| | 3.991 | 4.007 | 4.005 | 4.001 | 3.999 | 3.999 |
| Ca | .286 | .445 | .363 | .210 | .211 | .008 |
| Na | .753 | .531 | .627 | .783 | .791 | .985 |
| K | .010 | .004 | .006 | .013 | .015 | .008 |
| | 1.049 | .980 | .996 | 1.006 | 1.017 | 1.001 |
| An | 27.3 | 45.4 | 36.4 | 20.9 | 20.7 | .8 |
| Ab | 71.8 | 54.2 | 63.0 | 77.8 | 77.8 | 98.4 |
| Or | .9 | .4 | .6 | 1.3 | 1.5 | .8 |
| number of analyses[1] | 1 | 2 | 3 | 4 | 2 | 2 |

MF-8 granodiorite gneiss, South Monoosnoc Hill
MW-4A core, tonalite inclusion, Calamint Hill
MW-4B rim, tonalite inclusion, Calamint Hill
MW-2 granite gneiss, Princeton
MF-2A granite, Rollstone Hill
MF-2B partial rim, granite, Rollstone Hill

of one such rim on plagioclase in sample MF-2 is $An_1Ab_{98}Or_1$ (Table 5). These rims are absent on the same plagioclase grains where they adjoin quartz, plagioclase, or other mineral species. The spatial distribution of these rims and the near end-member composition of the potassium feldspar (see below) suggest an exsolution origin for this feature. It appears that albitic plagioclase, initially present as a component of the original alkali feldspar, has exsolved from potassium feldspar and coalesced onto adjoining plagioclase grains, forming the partial rims.

Potassium feldspar. Potassium feldspar occurs as a discrete phase in all of the major units but does not occur in the tonalite inclusions. In all instances, a large $2V_x$ and tartan twinning identify the potassium feldspar as microcline. Despite the morphological differences in the various units, average microprobe analyses from the representative samples are similar: MF-8, grandiorite gneiss, South Monoosnoc Hill, $Or_{91}Ab_7An_0Cn_2$; MW-2, granite gneiss, Princeton, $Or_{92}Ab_7An_0Cn_1$; MF-2, granite, Rollstone Hill, $Or_{92}Ab_7An_0Cn_1$ (Table 6), although the Cn content of MF-8 is significantly greater. This correspondence suggests a similarity in conditions during potassium feldspar equilibration.

Minute, rectangular potassium feldspar exsolution lamellae are found in some plagioclase antiperthite grains in the granodiorite gneiss at Wachusett Mountain and in the granite gneiss. They are irregularly distributed within individual grains and present sporadically within a given thin section.

Biotite. Biotite is the most important mafic mineral in the rocks of the Fitchburg complex. It occurs primarily as fine- to medium-grained,

Table 6 Average microprobe analyses of potassium feldspar.

| | MF-8 | MW-2 | MF-2 |
|---|---|---|---|
| $SiO_2$ | 63.17 | 63.88 | 64.29 |
| $Al_2O_3$ | 18.87 | 18.68 | 18.90 |
| CaO | .02 | .00 | .01 |
| $Na_2O$ | .81 | .71 | .81 |
| $K_2O$ | 15.66 | 16.10 | 15.62 |
| BaO | 1.25 | .39 | .31 |
| Total | 99.55 | 99.94 | 100.05 |

Formulae based on 8 oxygens:

| | | | |
|---|---|---|---|
| Si | 2.957 | 2.971 | 2.975 |
| Al | 1.040 | 1.025 | 1.032 |
| | 3.998 | 3.996 | 4.007 |
| Ba | .023 | .007 | .006 |
| K | .936 | .956 | .923 |
| Na | .073 | .069 | .072 |
| Ca | .001 | .000 | .000 |
| Total | 1.033 | 1.032 | 1.001 |
| Or | 90.6 | 92.6 | 92.2 |
| Ab | 7.1 | 6.7 | 7.2 |
| An | 0.1 | 0.0 | 0.0 |
| Cn | 2.2 | 0.7 | 0.6 |
| number of analyses | 2 | 3 | 2 |

MF-8 granodiorite gneiss, South Monoosnoc Hill
MW-2 granite gneiss, Princeton
MF-2 granite, Rollstone Hill

subhedral crystals, commonly containing inclusions of apatite and zircon. In extensively recrystallized rock types, the subparallel arrangement of biotite is the dominant element of the metamorphic foliation.

A relationship between color and composition of biotite has been noted in a number of investigations. Hall (1941) studied the composition and color of metamorphic biotites and concluded that variation in color appears to be related to systematic changes in the Fe-Mg ratio and $TiO_2$ content. In a study of the metamorphic hydration of primary igneous monzodiorite to recrystallized granodiorite gneiss in the Belchertown complex, Ashwal (1974) observed a change in the color of biotite with increased metamorphic hydration. Because other chemical parameters were essentially unchanged, Ashwal concluded that the higher $TiO_2$ content of the primary brown biotite relative to that of the recrystallized green biotite was the most important parameter influencing the color. Although the absolute titanium content is important, the color of biotite appears to be more a function of the $Ti^{4+}$ content with respect to the $Fe^{3+}/Fe$ total ratio (Hayama, 1959). High Ti content coupled with high $Fe^{3+}/Fe$ total appears to correlate with a red color, low Ti content coupled with high $Fe^{3+}/Fe$ total appears to correlate with a green color and intermediate values of these parameters appear to result in the gradation of biotite colors.

In general, the color of biotite in the granodiorite gneiss changes from red brown-brown at South Monoosnoc Hill to brown green-brown at Wachusett Mountain. From the comparison of the average analyses of biotite from sample MF-8, South Monoosnoc Hill, and MW-15, Wachusett Mountain (Table 7),

Table 7. Average microprobe analyses of biotites.

| Sample | MW-4 | MW-15 | MF-8 | MW-2 | MF-2 |
|---|---|---|---|---|---|
| $SiO_2$ | 34.92 | 35.72 | 36.63 | 35.89 | 36.08 |
| $TiO_2$ | 2.28 | 3.26 | 2.24 | 2.53 | 2.76 |
| $Al_2O_3$ | 16.36 | 16.42 | 17.56 | 17.19 | 17.05 |
| $FeO_T$ | 19.84 | 20.84 | 21.48 | 23.72 | 24.86 |
| MnO | .25 | .41 | .60 | .43 | .49 |
| MgO | 11.01 | 9.46 | 8.67 | 5.88 | 5.62 |
| CaO | .00 | n.d. | .00 | .00 | .00 |
| $Na_2O$ | .13 | .00 | .09 | .00 | .03 |
| $K_2O$ | 9.38 | 9.67 | 9.66 | 9.84 | 9.30 |
| NiO | .05 | n.d. | n.d. | .03 | n.d. |
| ZnO | .18 | n.d. | n.d. | .13 | n.d. |
| Total | 94.40 | 95.78 | 96.93 | 95.64 | 96.19 |
| Formulae based on 11 oxygens | | | | | |
| Si | 2.701 | 2.739 | 2.772 | 2.785 | 2.794 |
| Al | 1.299 | 1.261 | 1.228 | 1.215 | 1.206 |
| | 4.000 | 4.000 | 4.000 | 4.000 | 4.000 |
| Al | .194 | .224 | .340 | .358 | .351 |
| Ti | .133 | .188 | .128 | .148 | .161 |
| Ni | .004 | n.d. | n.d. | .002 | n.d. |
| Zn | .010 | n.d. | n.d. | .008 | n.d. |
| Fe | 1.285 | 1.337 | 1.360 | 1.541 | 1.611 |
| Mn | .017 | .027 | .039 | .030 | .032 |
| Mg | 1.270 | 1.082 | .979 | .681 | .649 |
| | 2.913 | 2.858 | 2.846 | 2.768 | 2.804 |
| Ca | .000 | n.d. | .000 | .000 | .000 |
| Na | .019 | .000 | .013 | .000 | .004 |
| K | .926 | .947 | .933 | .973 | .919 |
| | .945 | .947 | .946 | .973 | .923 |
| $\frac{Fe+Mn}{Fe+Mn+Mg}$ | .506 | .558 | .588 | .698 | .717 |
| number of analyses | 4 | 5 | 8 | 3 | 5 |
| COLOR | GN-BR to BR | BR-GN to BR | RED-BR to BR | RED to RED-BR | RED to RED-BR |

MW-4 Tonalite inclusion
MW-15 Granodiorite gneiss, Wachusett Mountain
MF-8 Granodiorite gneiss, South Monoosnoc Hill
MW-2 Granite gneiss, Princeton
MF-2 Granite, Rollstone Hill
n.d.=not determined

it can be seen that the relative enrichment in titanium and magnesium, and depletion in aluminum are the most important chemical readjustments associated with the higher metamorphic grade and coincident color change from red brown to brown green. Although the more red-colored biotite from South Monoosnoc Hill has a lower absolute titanium content relative to the more green-colored biotite from Wachusett Mountain, the ratio of $Fe^{3+}$ to Fe total is probably lower as shown by the rock analysis, probably resolving the apparent discrepancy.

In the massive sections of the tonalite inclusions, biotite forms coarse-grained, poikilitic, brown to green-brown plates, morphologically suggestive of late stage, igneous crystallization. The average of analyses of biotite in sample MW-4, a massive tonalite inclusion, is the most magnesian and least siliceous of the biotites analyzed for this study (Table 7). In more recrystallized specimens, biotite is fine- to medium-grained and defines a moderate foliation.

The biotites from sample MW-2, granite gneiss from Princeton, and MF-2, granite from Rollstone Hill, are chemically very similar (Table 7). The biotites from these two rock types are both red-brown to red in color, and their intimate association with muscovite is common. In that their $TiO_2$ contents are similar to those of the other biotites, the red color suggests a relatively low $Fe^{3+}$ ratio.

As can be seen by comparing all of the biotite analyses in Table 7, there is a systematic increase in the iron-magnesium ratio and silica content. Both of these trends correlate with the general increase in the felsic character of the host rock. The data suggest that biotite accommodates a certain proportion of aluminum, and aluminum in excess of that

proportion goes toward the formation of muscovite. Thus biotite will have the maximum amount of aluminum in the presence to muscovite.

Hornblende. Hornblende is found only in the tonalite inclusions, where it forms medium- to fine-grained subhedral to anhedral crystals. The average of microprobe analyses of hornblende in sample MW-4 is given in Table 8. Comparison of this average analysis with igneous hornblende analyses from the Belchertown complex (Ashwal, 1974) shows that the hornblende from the tonalite inclusions contains more K, Al, Fe, and Ti than the hornblende from the monzodiorite of the Belchertown complex.

Pale green fibrous-appearing amphibole forms roughly equant patches in the cores of some of the hornblende crystals in the tonalite inclusions. Although its fibrous habit hampers precise identification by thin section examination, the amphibole appears to be actinolite and it contains numerous, minute opaque inclusions which could not be optically identified. This combination of habit, occurrence, and chemistry suggests that these actinolite cores were former clinopyroxene grains which have been altered to amphibole.

Muscovite. Muscovite occurs as minor, fine grains, intimately intergrown with biotite in the granodiorite gneiss, and forms fine to coarse plates in the more felsic rocks. Microprobe analyses of muscovite (Table 8) in the representative samples are similar. Their most notable feature is that they are much less aluminous than normal muscovite, due to solid solution with celadonite, the dioctahedral tetrasilicic mica. In the muscovite-celadonite partial solid solution, $(Mg + Fe^{2+})^{VI}Si^{IV}$ substitutes

Table 8. Average microprobe analyses of a hornblende and muscovites.

| | HORNBLENDE | MUSCOVITE | | |
|---|---|---|---|---|
| Sample | MW-4 | MF-8 | MW-2 | MF-2 |
| $SiO_2$ | 42.23 | 47.52 | 47.71 | 47.89 |
| $TiO_2$ | 1.65 | .85 | .90 | .93 |
| $Al_2O_3$ | 10.84 | 30.87 | 30.81 | 30.71 |
| $FeO_T$ | 19.50 | 3.47 | 3.39 | 3.36 |
| MnO | .46 | .00 | .01 | .03 |
| MgO | 8.10 | 1.65 | 1.39 | 1.34 |
| CaO | 11.57 | .00 | .00 | .00 |
| $Na_2O$ | 1.00 | .15 | .22 | .26 |
| $K_2O$ | 1.23 | 11.04 | 10.84 | 10.78 |
| Total | 96.63 | 95.55 | 95.27 | 95.30 |

Formulae based on:

| | 23 oxygens | | 11 oxygens | | |
|---|---|---|---|---|---|
| Si | 6.507 | Si | 3.197 | 3.216 | 3.222 |
| Al | 1.493 | Al | .803 | .784 | .778 |
| | 8.000 | | 4.000 | 4.000 | 4.000 |
| Al | .473 | Al | 1.646 | 1.662 | 1.659 |
| Ti | .191 | Ti | .043 | .045 | .047 |
| *Fe3+ | .088 | Fe | .196 | .190 | .189 |
| Mg | 1.858 | Mn | .000 | .000 | .002 |
| Fe2+ | 2.390 | Mg | .166 | .138 | .135 |
| | 5.000 | | 2.051 | 2.035 | 2.032 |
| Fe2+ | .031 | Ca | .000 | .000 | .000 |
| Mn | .060 | Na | .020 | .033 | .034 |
| Ca | 1.908 | K | .949 | .932 | .926 |
| | 1.999 | | .969 | .965 | .960 |
| Na | .298 | Mol % Mus | 97.9 | 96.6 | 96.5 |
| K | .251 | | | | |
| | .549 | Mol % Par | 2.1 | 3.4 | 3.5 |
| $\frac{Fe^{2+}+Mn}{Fe^{2+}+Mn+Mg}$ | .572 | $\frac{Fe+Mn}{Fe+Mn+Mg}$ | .541 | .579 | .586 |
| $\frac{Fe^{3+}}{Fe^{3+}+Fe^{2+}}$ | .035 | number of analyses | 10 | 7 | 9 |
| Ca/Ca+Na | .865 | | | | |
| number of analyses | 5 | | | | |

*Data corrected for ferric iron on the basis of calculation to 15 cations exclusive of Na,K.

in for $Al^{VI}Al^{IV}$. The celadonite-rich composition of the muscovites is probably due to the fact that they coexist with K-feldspar and plagioclase (Guidotti and Sassi, 1976).

## ROCK CHEMISTRY

Sample preparation. For each of the forty-four samples collected for this study, approximately two kilograms of material were mechanically homogenized by crushing for use in whole rock chemical analyses. Because some of the samples are medium- to coarse-grained, the two kilogram specimen size was chosen, and this should insure representative sampling.

The crushing process involved using a hydraulic rock splitter to break hand specimen size chunks of rock into approximately one centimeter diameter pieces. These pieces were reduced to the size of coarse sand by crushing in a Spex "Shatterbox", equipped with a tungsten carbide grinding vessel. The sample size was reduced to approximately 100 grams by successive splittings, and this was ground again in the Shatterbox to a very fine powder. The various analytical techniques were performed on this finely ground material. By preparing the samples in the preceding manner, sample contamination was restricted to tungsten as well as trace amounts of titanium and cobalt from the tungsten carbide grinding vessel.

Analytical methods. The majority of whole rock chemical data was obtained through X-ray fluorescence spectroscopy. Concentrations of the major elements (Si, Ti, Al, total Fe, Mn, Mg, Ca, K, P) were determined from measurements on prepared glass discs. The glass discs were made by

fusing the sample with lanthanum-doped lithium tetraborate in proportions such that a balance is achieved between sensitivity and elimination of matrix effects (Norrish and Chappell, 1967). The concentrations of trace elements (Rb, Sr, Ga, Y, Pb, Th) were determined from measurements on undiluted pressed powder pellets. Analyses were done in duplicate on separately prepared glass discs or pressed powder pellets, and the results were averaged. The XRF spectrograph was calibrated on both primary synthetic standards and standard rocks, and natural rock standards were analyzed as monitors on each run.

The determination of ferrous iron was done by the cold acid digestion procedure of Wilson (1955) made by combining sample and hydrofluoric acid in the presence of excess ammonium metavanadate. This was titrated against a potassium dichromate solution to determine the amount of excess vanadic ion, which is proportional to the amount of ferrous iron. The remainder, resulting from the subtraction of ferrous iron obtained by titration from total iron obtained by X-ray fluorescence spectroscopy, is the amount of ferric iron.

The concentration of sodium was determined on digested rock solutions using an Instrumentation Laboratory 443 flame photometer. The solution has a lithium internal standard which minimizes instrumental instabilities.

Combined water ($H_2O-$, $H_2O+$) and carbon dioxide were determined on a Hewlitt Packard 185B carbon-hydrogen-nitrogen analyzer. Samples are heated to drive off the volatiles, which are captured by a helium carrier gas and quantitatively analyzed.

General aspects of the analyses. The results of whole rock analyses

for major elements and some trace elements are listed in Table 9. The chemical data from all of the samples collected for the study are listed with their corresponding CIPW norms grouped according to sample locality.

During each run of the spectrograph, U.S. Geological Survey standards W-1 and GSP-1 were analyzed as unknowns for major and trace elements, respectively. The mean, standard deviation, and standard error of these XRF analyses are given in Table 9 as well as the recommended values of Fleischer (1969) for major elements and of Flanagan (1976) for trace elements.

The reason for the generally low whole rock, major element totals is not known with certainty. Approximately fifty percent of the whole rock analyses have totals less than the generally acceptable range of 99 to 101%, most have summations over 98%, but four analyses are lower than 98%. Ample care was taken in the preparation of the samples for the various analytical techniques. The compilation of W-1 analyses from major element XRF runs (Table 9) is in excellent agreement with recommended values, indicating proper calibration and function of the spectrograph. The analyses do not include BaO, which could account for a few tenths of a percent in some rocks, but this obviously does not explain all of the problems. Samples were analyzed in duplicate, but eight pairs of analyses did not have <1% agreement between their respective silica values. Doubt has been cast on the precision and accuracy of the manufacturer who prepared pre-weighed aliquots of lithium tetraborate used in the making of the fused glass discs. Although this suspicion has

Table 9. Whole rock analyses for major elements, some trace elements and calculated CIPW norms for all samples of the Fitchburg complex.

GRANODIORITE GNEISS, SOUTH MONOOSNOC HILL

| Sample | MF-7 | MF-8 | MF-9 | MF-11 | MF-12 | MF-14 | MF-15 | MF-16 |
|---|---|---|---|---|---|---|---|---|
| $SiO_2$ | 60.86 | 60.02 | 60.21 | 62.01 | 60.81 | 61.71 | 59.35 | 67.26 |
| $TiO_2$ | 1.61 | 1.70 | 1.70 | 1.22 | 1.74 | 1.57 | 1.65 | .81 |
| $Al_2O_3$ | 15.16 | 15.23 | 15.28 | 17.72 | 15.44 | 15.45 | 14.97 | 15.42 |
| FeO | 4.88 | 5.35 | 5.43 | 3.18 | 5.61 | 4.91 | 5.36 | 2.77 |
| $Fe_2O_3$ | 1.17 | 1.16 | 1.04 | 1.08 | .87 | 1.28 | .93 | .41 |
| MnO | .15 | .17 | .17 | .10 | .14 | .15 | .17 | .07 |
| MgO | 2.21 | 2.42 | 2.45 | 1.56 | 2.52 | 2.27 | 2.44 | 1.08 |
| CaO | 3.76 | 3.98 | 4.00 | 3.64 | 4.01 | 3.67 | 3.87 | 2.47 |
| $Na_2O$ | 3.07 | 3.02 | 2.99 | 4.12 | 3.34 | 2.76 | 2.86 | 3.02 |
| $K_2O$ | 4.06 | 3.98 | 3.94 | 3.41 | 2.85 | 4.00 | 3.88 | 5.10 |
| $P_2O_5$ | .78 | .85 | .85 | .48 | .88 | .79 | .84 | .33 |
| $H_2O$ | .82 | 1.09 | 1.05 | .90 | .99 | 1.11 | 1.03 | .44 |
| $CO_2$ | .07 | .14 | .16 | .25 | .04 | .09 | .11 | .06 |
| Total | 98.60 | 99.11 | 99.27 | 99.67 | 99.24 | 99.76 | 97.46 | 99.24 |
| Trace Elements (ppm) | | | | | | | | |
| Y | 30 | 33 | 33 | 23 | 31 | 33 | 33 | 16 |
| Sr | 524 | 558 | 549 | 487 | 460 | 479 | 538 | 524 |
| Rb | 158 | 142 | 135 | 221 | 184 | 165 | 153 | 155 |
| Th | 25 | 27 | 27 | 29 | 25 | 32 | 28 | 29 |
| Pb | 41 | 39 | 38 | 40 | 28 | 36 | 36 | 56 |
| Ga | 23 | 23 | 23 | 26 | 24 | 23 | 24 | 20 |
| CIPW Norms | | | | | | | | |
| Qz | 15.73 | 14.72 | 15.09 | 15.35 | 17.29 | 18.78 | 15.33 | 22.66 |
| Or | 23.99 | 23.52 | 23.28 | 20.15 | 16.84 | 23.64 | 22.93 | 30.14 |
| Ab | 25.98 | 25.56 | 25.30 | 34.86 | 28.26 | 23.36 | 24.20 | 25.56 |
| An | 13.62 | 13.86 | 13.84 | 13.66 | 14.47 | 12.99 | 13.57 | 9.93 |
| C | .72 | .87 | 1.03 | 2.25 | 1.56 | 1.82 | 1.09 | 1.29 |
| En | 5.50 | 6.03 | 6.10 | 3.88 | 6.28 | 5.65 | 6.08 | 2.69 |
| Fs | 5.62 | 6.37 | 6.62 | 3.12 | 6.97 | 5.65 | 6.67 | 3.54 |
| Mt | 1.70 | 1.68 | 1.51 | 1.57 | 1.26 | 1.86 | 1.35 | .59 |
| Il | 3.06 | 3.23 | 3.23 | 2.32 | 3.30 | 2.98 | 3.13 | 1.54 |
| Ap | 1.70 | 1.86 | 1.86 | 1.05 | 1.92 | 1.73 | 1.84 | .72 |
| Cc | .16 | .32 | .36 | .57 | .09 | .20 | .25 | .14 |
| | 97.78 | 98.02 | 98.22 | 98.77 | 98.25 | 98.65 | 96.43 | 98.80 |
| $H_2O$ | .82 | 1.09 | 1.05 | .90 | .99 | 1.11 | 1.03 | .44 |
| Total | 98.60 | 99.11 | 99.27 | 99.67 | 99.24 | 99.76 | 97.46 | 99.24 |

Table 9, continued.

| | GRANODIORITE GNEISS | | | | | | | |
|---|---|---|---|---|---|---|---|---|
| | W. STERLING | WACHUSETT MOUNTAIN | | | | | | |
| Sample | MS-1 | MW-11 | MW-12 | MW-13 | MW-14 | MW-15 | MW-16 | MW-17 |
| $SiO_2$ | 60.40 | 71.43 | 59.11 | 59.10 | 65.04 | 60.46 | 61.46 | 57.28 |
| $TiO_2$ | 1.60 | .39 | 1.61 | 1.77 | .71 | 1.50 | 1.44 | 1.93 |
| $Al_2O_3$ | 15.28 | 15.06 | 15.93 | 15.25 | 16.62 | 15.70 | 15.55 | 15.43 |
| FeO | 5.31 | 1.02 | 4.47 | 4.28 | 1.96 | 4.41 | 4.15 | 5.62 |
| $Fe_2O_3$ | .92 | ,50 | 1.87 | 2.13 | 1.17 | 1.67 | 1.69 | 1.36 |
| MnO | .17 | .02 | .16 | .19 | .06 | .14 | .14 | .16 |
| MgO | 2.37 | .45 | 2.72 | 2.89 | .84 | 2.36 | 2.33 | 3.45 |
| CaO | 3.82 | 1.66 | 3.74 | 4.14 | 2.35 | 3.52 | 3.47 | 4.17 |
| $Na_2O$ | 2.94 | 3.15 | 3.42 | 2.88 | 3.07 | 3.56 | 3.58 | 2.86 |
| $K_2O$ | 3.97 | 5.15 | 3.05 | 3.46 | 6.33 | 3.07 | 3.12 | 3.28 |
| $P_2O_5$ | .80 | .09 | .70 | 1.04 | .36 | .70 | .66 | .82 |
| $H_2O$ | .87 | .39 | 1.07 | 1.13 | .52 | 1.11 | 1.02 | 1.43 |
| $CO_2$ | .04 | .04 | .07 | .20 | .04 | .21 | .21 | .08 |
| Total | 98.49 | 99.35 | 97.92 | 98.46 | 99.07 | 98.41 | 98.82 | 97.87 |
| Trace Elements (ppm) | | | | | | | | |
| Y | 33 | 4 | 23 | 34 | 4 | 26 | 26 | 28 |
| Sr | 522 | 641 | 658 | 923 | 879 | 548 | 560 | 685 |
| Rb | 148 | 172 | 148 | 155 | 133 | 181 | 179 | 216 |
| Th | 31 | 15 | 36 | 27 | 6 | 27 | 30 | 22 |
| Pb | 35 | 49 | 28 | 22 | 49 | 29 | 30 | 21 |
| Ga | 23 | 16 | 26 | 24 | 21 | 24 | 24 | 23 |
| CIPW Norms | | | | | | | | |
| Qz | 15.49 | 29.12 | 15.48 | 17.50 | 16.97 | 17.24 | 18.16 | 13.44 |
| Or | 23.46 | 30.44 | 18.02 | 20.45 | 37.41 | 18.14 | 18.44 | 19.38 |
| Ab | 24.88 | 26.66 | 28.94 | 24.37 | 25.98 | 30.13 | 30.29 | 24.20 |
| An | 13.99 | 7.45 | 14.00 | 13.16 | 9.29 | 12.02 | 12.01 | 15.36 |
| C | 1.02 | 1.57 | 1.87 | 1.94 | 1.31 | 2.12 | 1.88 | 1.55 |
| En | 5.90 | 1.12 | 6.77 | 7.20 | 2.09 | 5.88 | 5.80 | 8.59 |
| Fs | 6.66 | .85 | 4.30 | 3.53 | 1.57 | 4.50 | 4.11 | 6.31 |
| Mt | 1.33 | .72 | 2.71 | 3.09 | 1.70 | 2.42 | 2.45 | 1.97 |
| Il | 3.04 | .74 | 3.06 | 3.36 | 1.35 | 2.85 | 2.73 | 3.67 |
| Ap | 1.75 | .20 | 1.53 | 2.27 | .79 | 1.53 | 1.44 | 1.79 |
| Cc | .09 | .09 | .16 | .45 | .09 | .48 | .48 | .18 |
| | 97.62 | 98.96 | 96.85 | 97.33 | 98.55 | 97.30 | 97.80 | 96.44 |
| $H_2O$ | .87 | .39 | 1.07 | 1.13 | .52 | 1.11 | 1.02 | 1.43 |
| Total | 98.49 | 99.35 | 97.92 | 98.46 | 99.07 | 98.41 | 98.82 | 97.87 |

Table 9, continued.

GRANODIORITE GNEISS, WACHUSETT MOUNTAIN

| Sample | MW-18 | MW-19 | MW-20 | MW-21 | MW-22 | MW-23 | MW-24 | MW-25 |
|---|---|---|---|---|---|---|---|---|
| $SiO_2$ | 64.60 | 60.29 | 57.59 | 56.71 | 63.66 | 59.29 | 63.39 | 62.85 |
| $TiO_2$ | 1.02 | 1.73 | 2.02 | 2.09 | 1.45 | 1.85 | 1.44 | 1.40 |
| $Al_2O_3$ | 15.15 | 15.97 | 15.50 | 15.30 | 15.34 | 16.06 | 15.66 | 16.08 |
| FeO | 3.15 | 4.59 | 5.60 | 5.17 | 4.20 | 5.05 | 4.72 | 4.25 |
| $Fe_2O_3$ | 1.06 | 1.71 | 1.78 | 2.39 | 1.76 | 1.97 | .66 | 1.36 |
| MnO | .09 | .16 | .19 | .19 | .11 | .18 | .08 | .14 |
| MgO | 1.63 | 2.51 | 2.81 | 3.22 | 2.00 | 2.67 | 2.28 | 2.42 |
| CaO | 2.79 | 3.72 | 4.53 | 4.57 | 3.37 | 3.89 | 2.94 | 3.09 |
| $Na_2O$ | 3.34 | 3.61 | 3.15 | 2.91 | 3.85 | 3.37 | 3.64 | 3.42 |
| $K_2O$ | 3.93 | 2.76 | 3.00 | 3.25 | 2.40 | 2.93 | 2.67 | 2.86 |
| $P_2O_5$ | .54 | .84 | 1.00 | 1.04 | .67 | .96 | .70 | .68 |
| $H_2O$ | .99 | 1.06 | 1.31 | 1.43 | .92 | 1.16 | 1.21 | 1.18 |
| $CO_2$ | .28 | .12 | .33 | .06 | .07 | .05 | .09 | .04 |
| Total | 98.57 | 99.07 | 98.81 | 98.33 | 99.80 | 99.43 | 99.48 | 99.77 |

Trace Elements (ppm)

| | | | | | | | | |
|---|---|---|---|---|---|---|---|---|
| Y | 16 | 22 | 31 | 31 | 31 | 26 | 24 | 26 |
| Sr | 707 | 552 | 633 | 728 | 362 | 510 | 649 | 659 |
| Rb | 165 | 205 | 166 | 167 | 160 | 200 | 168 | 182 |
| Th | 31 | 26 | 27 | 24 | 34 | 20 | 33 | 28 |
| Pb | 34 | 20 | 23 | 24 | 29 | 24 | 30 | 32 |
| Ga | 22 | 26 | 24 | 24 | 24 | 27 | 23 | 23 |

CIPW Norms

| | | | | | | | | |
|---|---|---|---|---|---|---|---|---|
| Qz | 22.31 | 17.45 | 14.67 | 13.54 | 21.92 | 16.49 | 21.64 | 21.51 |
| Or | 23.23 | 16.31 | 17.73 | 19.21 | 14.18 | 17.32 | 15.78 | 16.90 |
| Ab | 28.26 | 30.55 | 26.66 | 24.62 | 32.58 | 28.52 | 30.80 | 28.94 |
| An | 8.90 | 12.76 | 14.51 | 16.18 | 12.34 | 13.34 | 9.90 | 11.08 |
| C | 2.14 | 2.37 | 1.75 | 1.07 | 1.89 | 2.46 | 3.15 | 3.30 |
| En | 4.06 | 6.25 | 7.00 | 8.02 | 4.98 | 6.65 | 5.68 | 6.03 |
| Fs | 3.39 | 4.46 | 5.83 | 4.42 | 4.07 | 4.93 | 5.89 | 4.63 |
| Mt | 1.54 | 2.48 | 2.58 | 3.47 | 2.55 | 2.86 | .96 | 1.97 |
| Il | 1.94 | 3.29 | 3.84 | 3.97 | 2.75 | 3.51 | 2.73 | 2.66 |
| Ap | 1.18 | 1.84 | 2.19 | 2.27 | 1.46 | 2.10 | 1.53 | 1.49 |
| Cc | .64 | ,27 | .75 | .14 | .16 | .11 | .20 | .09 |
| | 97.58 | 98.01 | 97.50 | 96.90 | 98.88 | 98.27 | 98.27 | 98.59 |
| $H_2O$ | .99 | 1.06 | 1.31 | 1.43 | .92 | 1.16 | 1.21 | 1.18 |
| Total | 98.57 | 99.07 | 98.81 | 98.33 | 99.80 | 99.43 | 99.48 | 99.77 |

Table 9, continued.

| | GRANITE GNEISS | | | | | | | |
|---|---|---|---|---|---|---|---|---|
| | PRINCETON | | CROW HILLS | | | | | |
| Sample | MW-1 | MW-2 | MF-21 | MF-22 | MF-24 | MF-25 | MF-27 | MF-29 |
| $SiO_2$ | 66.43 | 66.33 | 58.41 | 66.66 | 70.93 | 70.97 | 71.59 | 63.05 |
| $TiO_2$ | .85 | .76 | 2.04 | .85 | .57 | .61 | .53 | 1.47 |
| $Al_2O_3$ | 15.16 | 16.51 | 15.45 | 15.26 | 13.95 | 14.60 | 14.37 | 15.92 |
| FeO | 3.13 | 2.67 | 4.50 | 3.36 | 1.46 | 1.48 | 1.35 | 4.36 |
| $Fe_2O_3$ | .71 | .64 | 1.61 | 1.40 | .78 | 1.18 | .69 | 1.53 |
| MnO | .02 | .05 | .18 | .07 | .04 | .02 | .05 | .13 |
| MgO | 1.29 | .94 | 3.40 | 1.78 | .66 | .69 | .59 | 1.83 |
| CaO | 2.25 | 2.23 | 4.58 | 2.44 | 1.18 | 1.33 | 1.05 | 2.93 |
| $Na_2O$ | 2.86 | 3.94 | 2.96 | 3.96 | 2.88 | 2.88 | 2.99 | 3.34 |
| $K_2O$ | 4.66 | 4.58 | 2.86 | 2.66 | 5.20 | 5.34 | 5.35 | 3.34 |
| $P_2O_5$ | .37 | .33 | 1.46 | .51 | .21 | .20 | .24 | .64 |
| $H_2O$ | 1.00 | .55 | 1.30 | .84 | .66 | .71 | .62 | .98 |
| $CO_2$ | .23 | .10 | .09 | .04 | .15 | .20 | .05 | .03 |
| Total | 98.96 | 99.63 | 98.84 | 99.83 | 98.67 | 100.21 | 99.47 | 99.55 |
| Trace Elements (ppm) | | | | | | | | |
| Y | 22 | 13 | 31 | 29 | 17 | 15 | 15 | 25 |
| Sr | 523 | 509 | 2427 | 469 | 387 | 208 | 281 | 484 |
| Rb | 197 | 164 | 187 | 163 | 189 | 179 | 213 | 185 |
| Th | 28 | 10 | 34 | 16 | 49 | 55 | 41 | 49 |
| Pb | 51 | 43 | 32 | 27 | 45 | 43 | 44 | 32 |
| Ga | 20 | 21 | 22 | 24 | 18 | 20 | 19 | 25 |
| CIPW Norms | | | | | | | | |
| Qz | 25.05 | 19.35 | 17.54 | 25.26 | 31.17 | 30.60 | 30.82 | 21.46 |
| Or | 27.54 | 27.07 | 16.90 | 15.72 | 30.73 | 31.56 | 31.62 | 19.74 |
| Ab | 24.20 | 33.34 | 25.05 | 33.51 | 24.37 | 24.37 | 25.30 | 28.26 |
| An | 7.53 | 8.49 | 13.57 | 8.85 | 3.67 | 4.16 | 3.48 | 10.58 |
| C | 2.65 | 1.96 | 2.51 | 2.62 | 2.24 | 2.56 | 2.38 | 2.93 |
| En | 3.21 | 2.34 | 8.47 | 4.43 | 1.64 | 1.72 | 1.47 | 4.56 |
| Fs | 3.79 | 3.21 | 3.90 | 3.74 | 1.17 | .77 | 1.13 | 4.56 |
| Mt | 1.03 | .93 | 2.33 | 2.03 | 1.13 | 1.71 | 1.00 | 2.22 |
| Il | 1.61 | 1.44 | 3.87 | 1.61 | 1.08 | 1.16 | 1.01 | 2.79 |
| Ap | .81 | .72 | 3.19 | 1.11 | .46 | .44 | .52 | 1.40 |
| Cc | .52 | .23 | .20 | .09 | .34 | .45 | .11 | .07 |
| | 97.96 | 99.08 | 97.54 | 98.99 | 98.01 | 99.50 | 98.85 | 98.57 |
| $H_2O$ | 1.00 | .55 | 1.30 | .84 | .66 | .71 | .62 | .98 |
| Total | 98.96 | 99.63 | 98.84 | 99.83 | 98.67 | 100.21 | 99.47 | 99.55 |

Table 9, continued.

| | GRANITE | | | | | | | |
|---|---|---|---|---|---|---|---|---|
| | ROLLSTONE HILL | | | | | MALDEN HILL | | PRINCETON |
| Sample | MF-1 | MF-2 | MF-3 | MF-4 | MF-5 | MWN-1 | MWN-2 | MW-3 |
| $SiO_2$ | 69.70 | 70.20 | 69.92 | 69.35 | 69.99 | 70.30 | 71.50 | 73.28 |
| $TiO_2$ | .52 | .52 | .53 | .53 | .50 | .37 | .27 | .15 |
| $Al_2O_3$ | 14.67 | 14.62 | 14.63 | 14.51 | 14.64 | 15.17 | 15.60 | 14.30 |
| FeO | 1.72 | 1.55 | 1.66 | 1.64 | 1.24 | 1.73 | .91 | .46 |
| $Fe_2O_3$ | .68 | .83 | .81 | .89 | 1.17 | 1.14 | .47 | .26 |
| MnO | .05 | .05 | .05 | .05 | .05 | .04 | .04 | .01 |
| MgO | .42 | .42 | .48 | .45 | .43 | .63 | .27 | .22 |
| CaO | 1.39 | 1.41 | 1.43 | 1.48 | 1.39 | 1.77 | .94 | 1.48 |
| $Na_2O$ | 2.83 | 3.07 | 2.96 | 2.96 | 3.07 | 3.64 | 3.15 | 3.18 |
| $K_2O$ | 5.42 | 5.36 | 5.31 | 5.27 | 5.21 | 3.63 | 5.63 | 4.49 |
| $P_2O_5$ | .25 | .26 | .27 | .25 | .25 | .26 | .22 | .08 |
| $H_2O$ | .68 | .58 | .58 | .58 | .57 | .74 | .77 | .47 |
| $CO_2$ | .05 | .22 | .04 | .06 | .04 | .03 | .08 | .03 |
| Total | 98.38 | 99.09 | 98.67 | 98.02 | 98.55 | 99.45 | 99.55 | 98.41 |
| Trace Elements (ppm) | | | | | | | | |
| Y | 19 | 20 | 18 | 19 | 19 | 18 | 7 | 7 |
| Sr | 145 | 136 | 145 | 147 | 133 | 129 | 132 | 220 |
| Rb | 240 | 251 | 241 | 233 | 248 | 214 | 394 | 290 |
| Th | 42 | 40 | 42 | 40 | 39 | 7 | 16 | 15 |
| Pb | 41 | 40 | 42 | 41 | 39 | 29 | 41 | 67 |
| Ga | 21 | 21 | 22 | 21 | 23 | 20 | 24 | 18 |
| CIPW Norms | | | | | | | | |
| Qz | 28.83 | 28.81 | 28.67 | 28.24 | 29.05 | 30.47 | 29.57 | 34.20 |
| Or | 32.03 | 31.68 | 31.38 | 31.14 | 30.79 | 21.45 | 33.27 | 26.53 |
| Ab | 23.95 | 25.98 | 25.05 | 25.05 | 25.98 | 30.80 | 26.66 | 26.91 |
| An | 5.11 | 4.08 | 5.25 | 5.49 | 5.17 | 7.06 | 2.86 | 6.68 |
| C | 2.28 | 2.27 | 2.09 | 1.92 | 2.05 | 2.66 | 3.27 | 1.76 |
| En | 1.05 | 1.05 | 1.20 | 1.12 | 1.07 | 1.57 | .67 | .55 |
| Fs | 1.83 | 1.39 | 1.60 | 1.49 | .50 | 1.70 | .91 | .40 |
| Mt | .99 | 1.20 | 1.17 | 1.29 | 1.70 | 1.65 | .68 | .38 |
| Il | .99 | .99 | 1.01 | 1.01 | .95 | .70 | .51 | .28 |
| Ap | .55 | .57 | .59 | .55 | .55 | .57 | .48 | .17 |
| Cc | .11 | .50 | .09 | .14 | .09 | .07 | .18 | .07 |
| | 97.70 | 98.51 | 98.09 | 97.44 | 97.98 | 98.71 | 99.08 | 97.94 |
| $H_2O$ | .68 | .58 | .58 | .58 | .57 | .74 | .77 | .47 |
| Total | 98.38 | 99.09 | 98.67 | 98.02 | 98.55 | 99.45 | 99.55 | 98.41 |

Table 9, continued

| | TONALITE INCLUSIONS | | | | AVERAGE XRF ANALYSES * | | | |
|---|---|---|---|---|---|---|---|---|
| Sample | MW-4 | MW-5 | MW-8 | MS-3 | MEAN | ST D | ST ER | RC VL |
| $SiO_2$ | 53.68 | 53.93 | 53.69 | 67.45 | 52.82 | 0.31 | 0.08 | 52.64 |
| $TiO_2$ | 2.35 | 2.51 | 2.52 | .27 | 1.09 | 0.01 | 0.00 | 1.07 |
| $Al_2O_3$ | 15.74 | 15.83 | 16.19 | 16.87 | 15.07 | 0.08 | 0.02 | 14.85 |
| FeO | 6.47 | 7.16 | 7.24 | .85 | - | - | - | - |
| $Fe_2O_3$ | 2.34 | 1.89 | 1.68 | .38 | 11.12 | 0.10 | 0.02 | 11.09 |
| MnO | .23 | .24 | .21 | .02 | .18 | 0.01 | 0.00 | .17 |
| MgO | 3.34 | 3.51 | 3.81 | .21 | 6.62 | 0.04 | 0.01 | 6.62 |
| CaO | 5.30 | 5.57 | 5.29 | .96 | 10.93 | 0.04 | 0.01 | 10.96 |
| $Na_2O$ | 2.67 | 2.94 | 2.83 | 3.50 | - | - | - | - |
| $K_2O$ | 2.48 | 2.80 | 2.78 | 7.80 | .63 | 0.01 | 0.00 | .64 |
| $P_2O_5$ | 1.28 | 1.36 | 1.36 | .18 | .17 | 0.01 | 0.00 | .14 |
| $H_2O$ | 1.15 | 1.13 | 1.50 | .35 | - | - | - | - |
| $CO_2$ | .06 | .01 | .10 | .05 | - | - | - | - |
| Total | 97.47 | 98.88 | 99.20 | 98.99 | | | | |
| Trace Elements (ppm) | | | | | | | | |
| Y | 33 | 32 | 35 | | 23 | 0.52 | 0.15 | 30 |
| Sr | 777 | 765 | 747 | 524 | 236 | 0.74 | 0.21 | 233 |
| Rb | 82 | 84 | 84 | 130 | 251 | 1.47 | 0.42 | 254 |
| Th | 15 | 13 | 13 | 1 | 91 | 0.74 | 0.21 | 104 |
| Pb | 27 | 27 | 27 | 50 | 54 | 0.90 | 0.24 | 51 |
| Ga | 25 | 24 | 25 | 15 | 22 | 0.39 | 0.11 | 22 |

| CIPW Norms | | | | |
|---|---|---|---|---|
| Qz | 11.40 | 8.83 | 9.59 | 14.70 |
| Or | 16.78 | 16.55 | 16.43 | 46.69 |
| Ab | 22.59 | 24.88 | 23.95 | 29.62 |
| An | 18.39 | 19.57 | 17.62 | 3.39 |
| C | 1.53 | .79 | 2.07 | 1.32 |
| En | 8.32 | 8.74 | 9.49 | .52 |
| Fs | 6.49 | 7.89 | 8.14 | .84 |
| Mt | 3.39 | 2.74 | 2.44 | .55 |
| Il | 4.46 | 4.77 | 4.79 | .51 |
| Ap | 2.80 | 2.97 | 2.97 | .39 |
| Cc | .14 | .02 | .23 | .11 |
| Total | 96.30 | 97.75 | 97.70 | 98.64 |
| $H_2O$ | 1.15 | 1.13 | 1.50 | .35 |
| Total | 97.45 | 98.80 | 99.20 | 98.99 |

*XRF analyses were performed on U.S.G.S. standards W-1 for major elements and GSP-1 for trace elements. ST D= standard deviation (N=26 for major elements, N=12 for trace elements), ST ER=standard error of the mean, RC VL= recommended values. Recommended values were taken from Fleischer (1969) for the major elements and Flanagan (1976) for trace elements.

not yet been confirmed, such inconsistencies could result in the observed low totals.

Overall chemistry of the complex. The silica content of the rocks in the complex as a whole ranges from approximately 54 to 73 weight percent. The samples are oversaturated with respect to silica, since all have free quartz in the mode. Figure 16a, b, and c, illustrate the variation of the major elements and some trace elements when plotted against silica.

Silica has been chosen as the independent variable here because a) by accounting for the majority of the total variation in many rock series, the silica content is a reasonable parameter with which to compare the variation of the other elements, and b) alternative functions which use some combination of variables, produce artifically smoothed curves due to the fact that some variables are plotted against themselves (Rhodes, 1969).

For the sake of brevity and convenience, the data from all of the samples collected in this study have been presented in the same figures (Figure 16a, b, c), using the symbols of the modal plots. By presenting the data in this manner it is not intended to imply a consanguinous relationship among the different rock units, although that possibility will be explored in a later section.

In looking at the data a general trend can be identified in most of the major and trace element plots. The strength of these trends varies widely from element to element, ranging from well defined to very diffuse. In that the chemistry and mineralogy of the rocks are inextricably linked, the trends are due to the generally systematic variation in

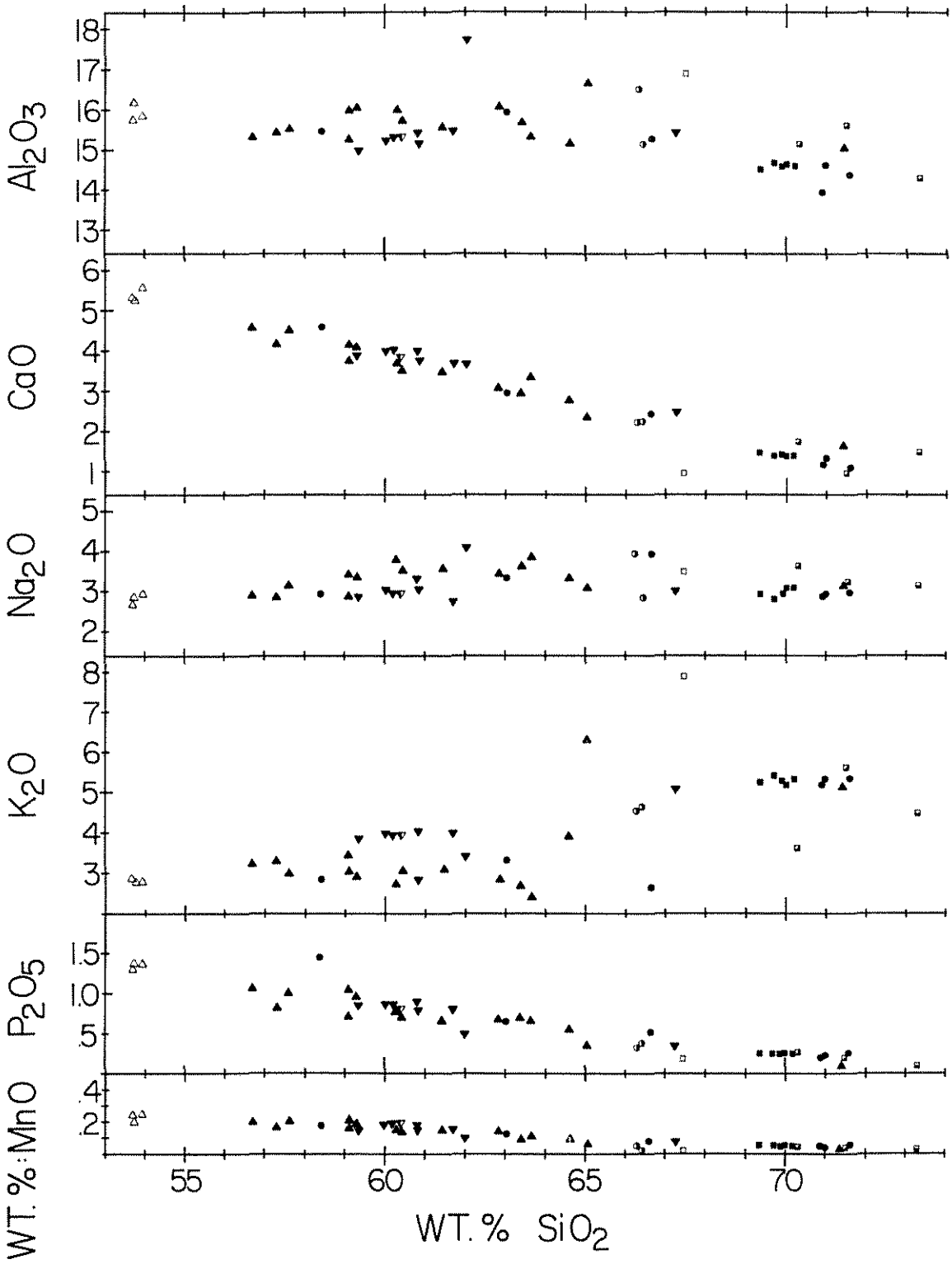


Figure 16. Plot of whole rock chemical data from all samples collected for the study of the Fitchburg complex. a) Wt% $Al_2O_3$, CaO, $Na_2O$, $K_2O$, $P_2O_5$, and MnO against Wt% $SiO_2$.

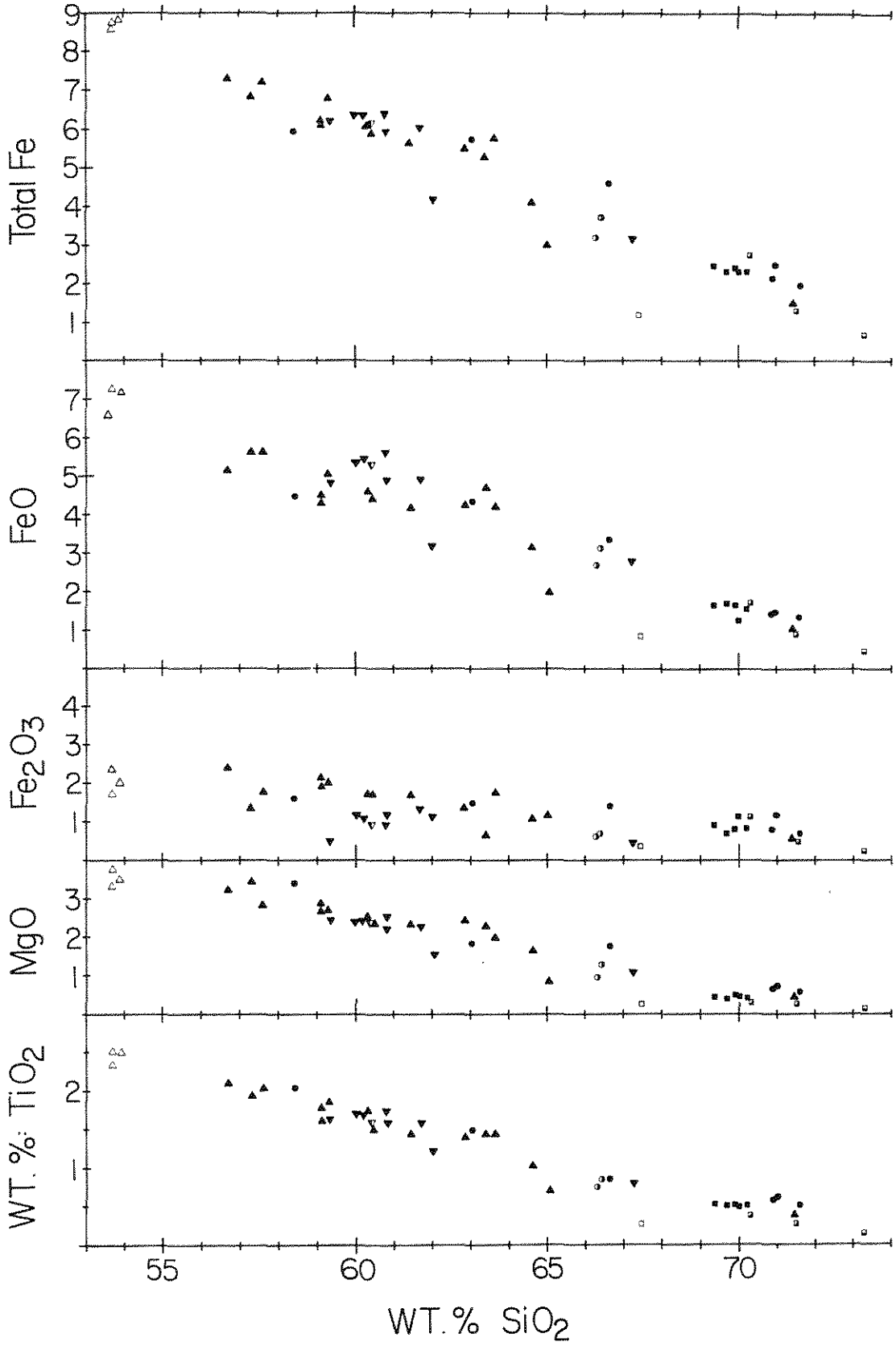


Figure 16b. Wt% Total Fe as FeO, FeO, $Fe_2O_3$, MgO, $TiO_2$ against Wt% $SiO_2$.

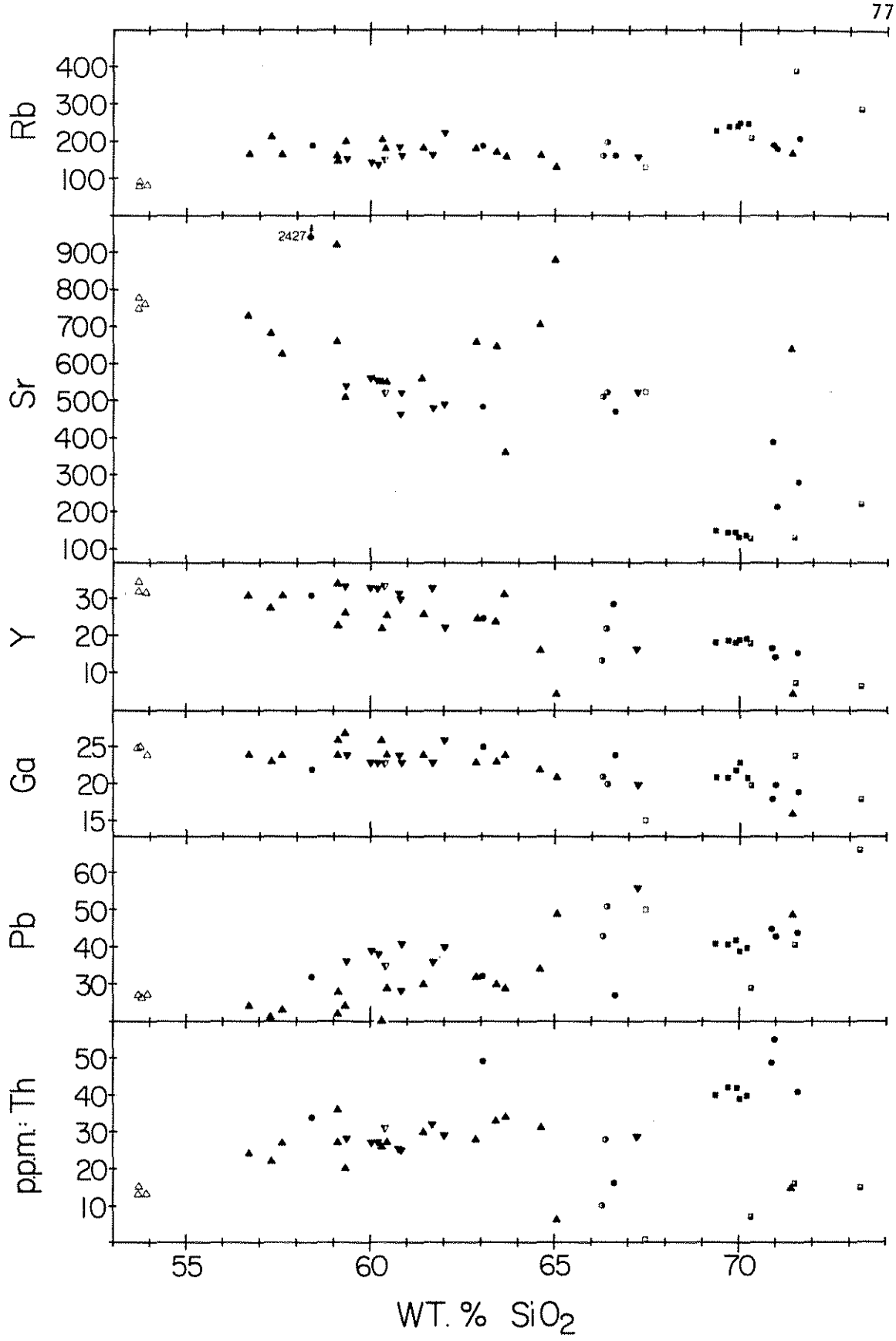


Figure 16c. Rb, Sr, Y, Ga, Pb, Th (ppm) against Wt% $SiO_2$.

mineralogy, which has been observed within and among the different units of the complex and characterized in the section dealing with petrography. Thus the regular variation in the chemistry can be ascribed to the combined effects of change in the plagioclase-potassium feldspar ratio, the continuously variable mafic mineral content, and the compositional differences of some of the major mineral phases.

Figure 17 illustrates how the alkali-lime index (Peacock, 1931) was determined for the units of the Fitchburg complex. The symbols are those used in the chemical plots; the solid shapes represent weight % $Na_2O$ + $K_2O$ and the hollow shapes represent weight % CaO, all plotted against weight % silica. Linear regression lines were calculated from various data sets, and the silica content at the intersection of the total alkali line with the calcium line is the index for a given data set. Using all of the samples of the granodiorite gneiss from both the eastern and western belts, the solid set of regression lines as calculated. The index is 52.5, placing the unit in the alkali-calcic category. When calculations were done using data from the common gneiss types only, the regression line for CaO is no different from the line calculated for all of the samples, but the slope of the total alkali line is much flatter (see broken line, Figure 17). Consequently the index is 49, which falls in the alkalic category. Regression lines were calculated for the granite gneiss with and without sample MF-21, a possible inclusion of granodiorite gneiss within the granite gneiss. The solid hachured lines, which represent the regressions for the granite gneiss including MF-21, yield an index of 55. The broken hachured lines, which represent the regressions for the granite gneiss without MF-21 yield an index of 53.2.

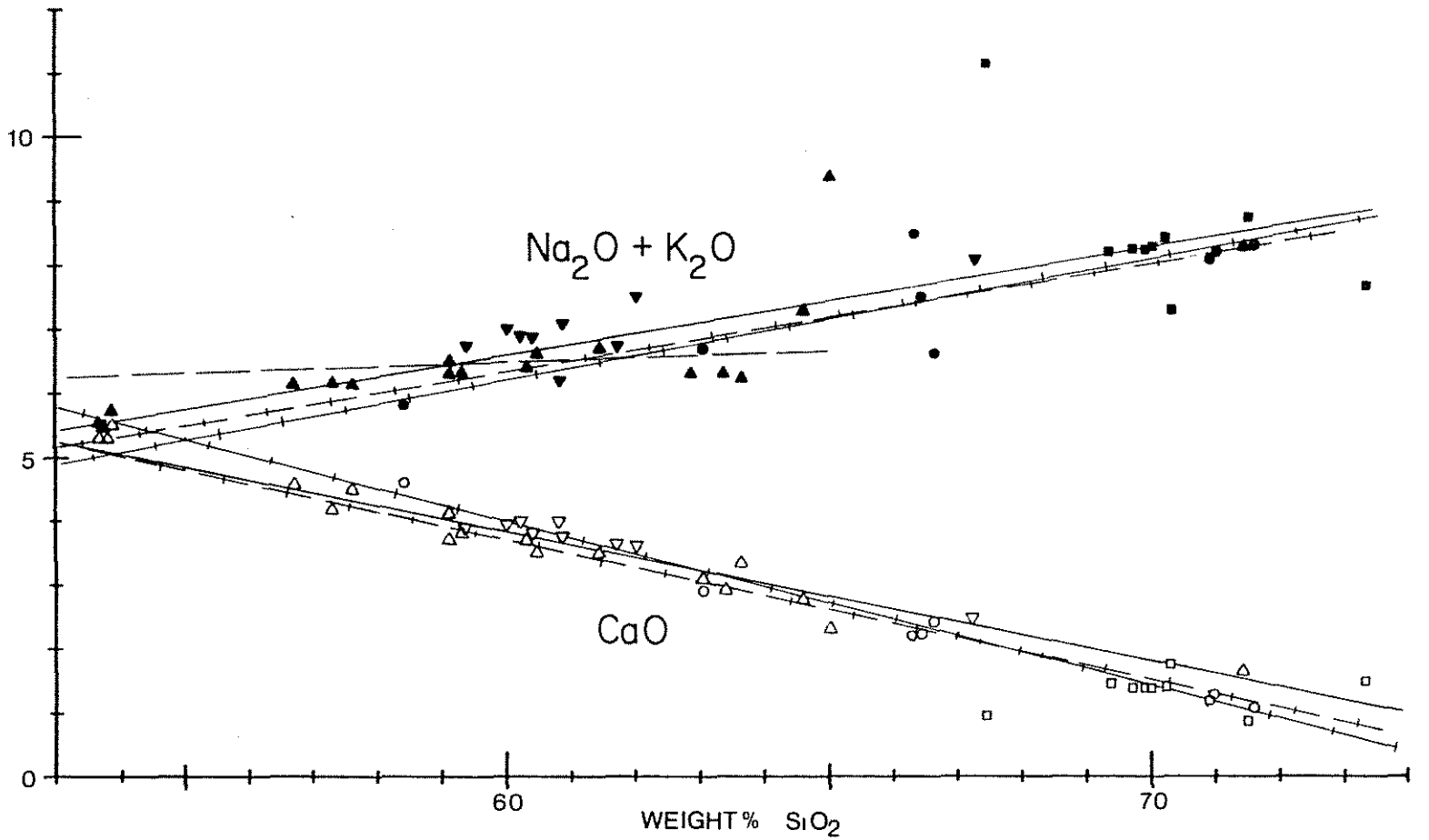


Figure 17. Plot of Wt% CaO (hollow symbols) and Wt% $Na_2O + K_2O$ (solid symbols) against Wt% $SiO_2$, used to determine the alkali-lime index. Explanation of the linear regression lines in text.

Both indices are in the alkali-calcic category. Thus, as the alkali-lime index demonstrates, these rocks are relatively high in alkalis and low in calcium. The granite gneiss index is based on fewer data than that of the granodiorite gneiss, and the extrapolation necessary to obtain the index is somewhat tenuous. Insufficient data are available for making a meaningful estimate of the index for the granite.

All of the samples are peraluminous, having molar $Al_2O_3 > (CaO + Na_2O + K_2O)$ after correction for apatite and calcite. The excess aluminum is expressed in the norm as corundum and is present in the mode primarily as muscovite and extra AlAl substitution in biotite.

The whole rock chemistry of samples from the Fitchburg complex is plotted on an ACF diagram (Figure 18), which has been modified from Winkler (1979). Due to the incompleteness of information on the modes of the various opaque minerals; the Al, Fe, and Mg contents of the biotites; and the K, Al, Fe, and Mg contents of muscovite in each specimen, simplifications have been made. Corrections have not been made for hematite, magnetite, ilmenite, biotite, muscovite, or paragonite, and ferric iron has not been added to the A apex. The samples are represented by the same symbols as used in the modal plots. All samples are peraluminous since they all plot above the plagioclase (An)-hypersthene (Hyp) tie line. Additional tie lines have been drawn from anorthite to muscovite, biotite, or hornblende compositions, indicating coexisting mineral assemblages in the representative samples. The hornblende tonalite inclusions plot below the An-Bio join. The plot illustrates the gradational nature of the rocks, which range from a hornblende-biotite-plagioclase assemblage to biotite-muscovite-plagioclase assemblages.

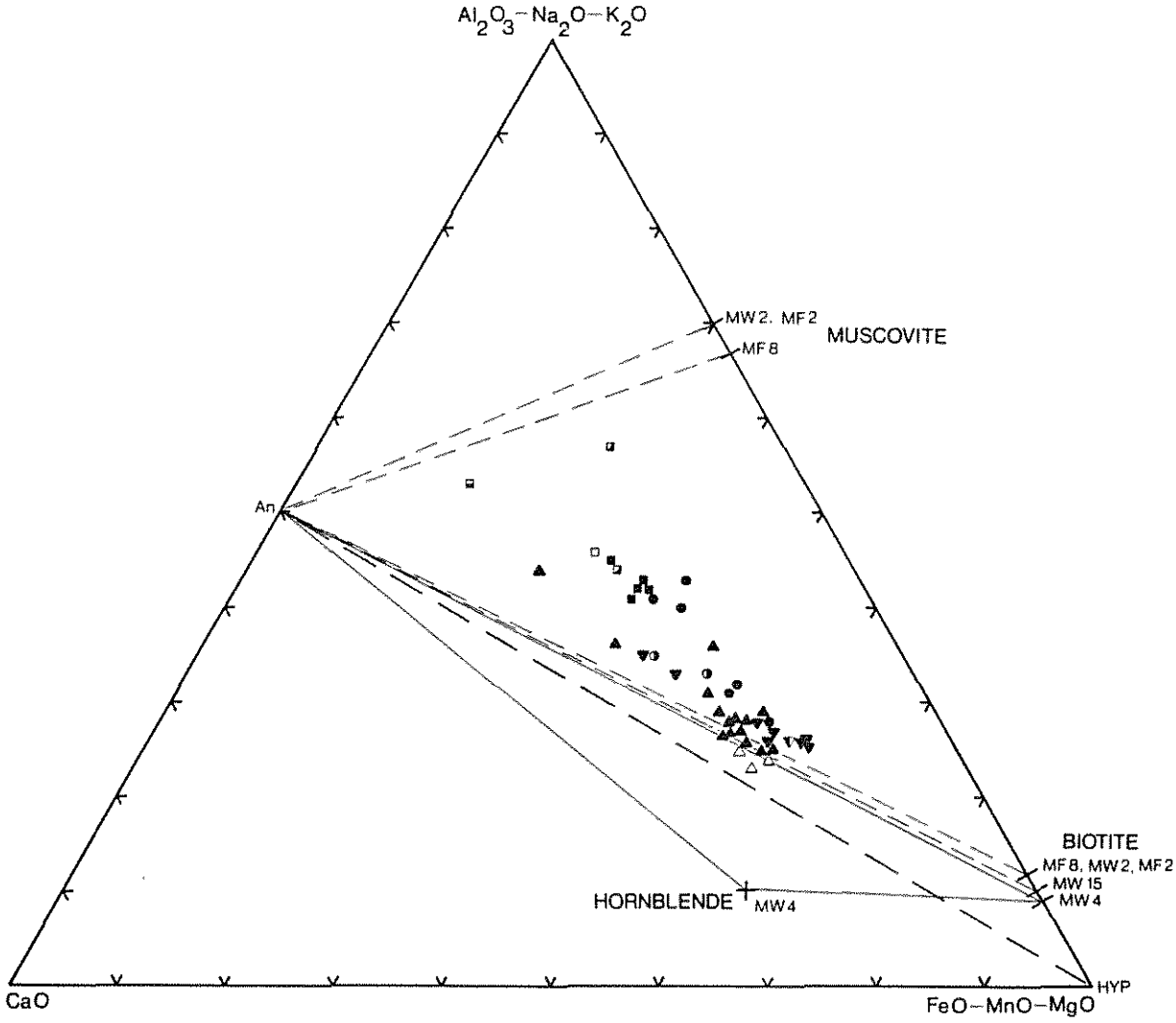


Figure 18. Plot of whole rock chemical data for rocks of the Fitchburg complex on a modified ACF diagram. Heavy dashed line connects anorthite (An) to hypersthene (HYP). All Fitchburg samples plot above this line, indicating that they are all peraluminous. Solid tie lines connect An, biotite, and hornblende compositions in sample MW-4. The light dashed tie lines go from An to biotite compositions in MW-15, MF-8, MW-2, and MF-2 and to muscovite compositions in MF-8, MW-2, and MF-2. Mineral compositions are those listed in Tables 7 and 8.

Granodiorite gneiss. The analyses of samples of the granodiorite gneiss from the eastern belt at South Monoosnoc Hill (Figure 16, solid downward pointing triangles) and West Sterling (Figure 16, half-filled downward pointing triangle) show that the common gneiss is relatively homogeneous in composition with silica contents ranging from 59.35 to 61.71 wt %. The low figure is from the analysis of sample MF-15, which has a particularly low summation and hence is probably low in silica. Porphyritic gneiss of uncertain affinity (MF-11) and a leucogranite (MF-16) clearly intrusive into the common rock type have silica contents of 62.01 and 67.76 wt % respectively (Table 9).

There is a relatively large amount of chemical variation in the granodiorite gneiss from the western belt at Wachusett Mountain (Figure 16, solid upward pointing triangles). The silica contents of the samples, which were collected over the complete stratigraphic thickness of the gneiss, range from 56.61 to 63.39 wt % for the common rock type and up to 71.43% when the more leucocratic samples (MW-11, 14, 18) are included. Although there is regular variation in the gneiss, it is not spatially disposed in a systematic manner. Sampling done at smaller intervals may discern systematic variation at a finer scale, but current work has not found regular chemical zonation to this sill-like body of gneiss. In the commonly occurring gneiss, most individual elements present in the eastern belt occur with closely corresponding abundances at comparable silica contents in the western belt and vary in a more or less linear manner when plotted against silica (Table 9, Figure 16). Departure from this general sort of behavior occurs in the elements K, Na, $Fe^{2+}$, $Fe^{3+}$, Sr, and Pb. Partial melting, which appears to have occurred in the

sillimanite-muscovite grade gneiss from the western belt but not in the sillimanite-staurolite grade gneiss from the eastern belt, probably altered the distribution of elements in the gneiss of the western belt relative to the eastern belt and thus may be responsible for the lack of correspondence.

Tonalite inclusions. The three samples of the tonalite inclusions are the most mafic rocks collected in the complex and are chemically very similar. Whole rock analyses of the samples (Figure 16a, b, c; open upward pointing triangles) yield silica contents of 53.68 to 53.93 wt %, and closely corresponding abundances of each of the major and trace elements (Table 9). Although the total iron contents of the samples are similar, a slight difference occurs in the ferrous-ferric ratios, but this is probably a reflection of the differing degrees of sample freshness. The relative chemical homogeneity of these samples is illustrated in Figure 16a and b, where the data consistently plot in a cluster, save for ferrous and ferric iron. Similarly, the clustering of the data points is tight for the trace elements (Figure 16c), and this degree of coherence is not observed in the other units.

Granite gneiss. Samples collected from the granite gneiss at Crow Hills (Figure 16, solid circles) and Princeton (Figure 16, half-filled circles) span a range of bulk chemistries (Table 9). Silica contents of 58.41 to 71.59 wt % are present, but continuously variable mineralogy and chemistry like that found in the granodiorite gneiss has not been observed. To some extent the absence of systematic chemical/mineralogical variation may be the result of the lack of a statistically valid sampling

program or the collection of too few samples, but the preponderance of rock examined at the two sampling localities is quite leucocratic and would probably fall into the interval of silica contents between 66 and 72 wt %. The more mafic material (MF-29) is volumetrically much less important than the common felsic material, and sample MF-21 is a small lens of material suspected of being an inclusion of the granodiorite gneiss within the granite gneiss. Although modally and chemically very similar to the granodiorite gneiss, its wildly aberrant Sr concentration (2427 ppm) is difficult to relate to the granodiorite gneiss.

As can be seen in the plots, most elements appear to vary in a linear manner. This generalization may be in serious error because there is a distinct lack of data points which would be helpful in corroborating the correlation through such a range of silica contents. Even in areas where sufficient data are present, the correlation appears to be loose for some elements and particularly poor for Pb and Th.

Granite. When considered as a group, there is a fair amount of chemical variation in the samples of the granite (Table 9). Silica contents range from 69.35 to 73.28 wt %, and each of the other elements analyzed show at least that much relative variation. Major and trace element data from samples collected at Rollstone Hill (filled squares), Malden Hill (diagonal, half-filled squares), Princeton (horizontal, half-filled square), and West Sterling (open square) have been plotted against silica in Figure 16a, b, and c. It can be seen that the correlation among the data for the group is good for most major elements, much poorer for the trace elements, and generally comparable to that seen in the other units.

At Rollstone Hill, where five samples were taken at different locations within a single large quarry, and hence, where variability within a single sampling locality in this unit can be assessed most accurately, the analyses yield results which are similar for both major and trace elements. Since there is a positive correlation with the silica content and the major element summations as well as some uncertainty concerning the reasons for the low totals, the chemical similarity of these samples is probably closer than the analyses would indicate.

Because sample MS-3 from West Sterling is a quartz syenite, it has markedly discordant mineralogy and chemistry relative to the other samples collected from the granite. Because of these differences, it is thought that sample MS-3 did not originate by the same process or have the same source as the typical granite. Discussion about the granite has not taken into account information derived from sample MS-3.

## PETROGENESIS

This is the first detailed study of the petrography and geochemistry of the Fitchburg Plutonic Complex and an initial attempt at resolving some of the uncertainties surrounding its genesis. The information generated by this investigation can be used to evaluate hypotheses dealing with the generation of melt, the evolution of melt, and the effects of metamorphism.

A number of hypotheses concerning the petrogenesis of the complex merit consideration. Melt generation may have occurred in the mantle, in subducted continental crust, and/or *in situ* during regional meta-

morphism. A variety of source materials may have been involved. Mechanisms involved in melt evolution may have included fractional crystallization, multistage intrusion, or assimilation of xenolithic materials. Acadian metamorphism subsequent to emplacement has resulted in textural changes and some local partial melting.

Pertinent Work

Before delving into the specific problems concerning the genesis of the Fitchburg complex, it is necessary to consider the data in light of some pertinent work. Strengths and limitations of genetic hypotheses can then be assessed.

Muscovite breakdown curve. A general estimate of conditions during crystallization of the granite can be made utilizing the fact that it contains large plates of primary muscovite. Accordingly, the granite should have existed as a melt in the region of P-T space outlined by the muscovite + quartz breakdown curve (Day, 1973) and the minimum melt curve of granite (Tuttle and Bowen, 1958). Based on this evidence, a minimum pressure of approximately 3 kb and a temperature of approximately 660$^{o}$C is indicated (Figure 19). Earlier work by Evans (1965) placed the breakdown of muscovite at lower temperatures, but the work of Day (1973) is preferred because it was done using pure K end-member starting materials.

Kerrick (1972) worked on the breakdown of muscovite and on granite melting, examining the affect of $CO_2$ in the fluid of the system. In general with increasing $X_{CO_2}$, there is a systematic shift of the muscovite breakdown curve to lower temperatures and of the granite melting curve to higher temperatures. Thus with regard to granitic magmas containing mus-

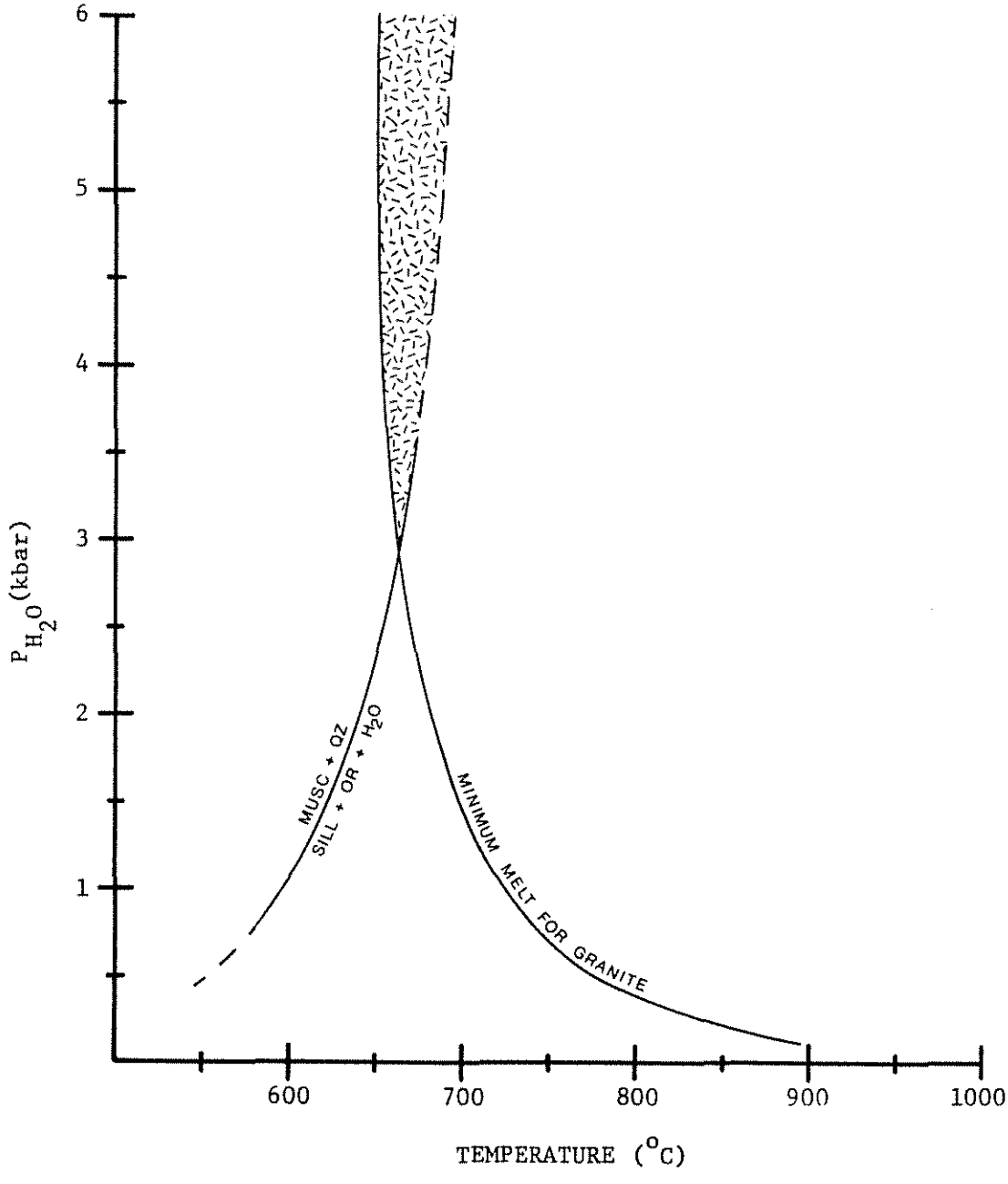


Figure 19. Muscovite-bearing magma should exist as a melt in the shaded area. Muscovite breakdown curve comes from Day (1973). Minimum melt for granite comes from Tuttle and Bowen (1958).

covite, relatively large pressure increases and relatively small temperature increases would be necessary to sustain such a melt with increasing $X_{CO_2}$ in the fluid.

Feldspar geothermometry. An attempt at precise temperature estimates for crystallization can be made for the units of the complex using the two feldspar geothermometer of Stormer (1975). Application of the feldspar compositions found in samples MF-2 of the granite, MW-2 of the granite gneiss, and MF-8 of the granodiorite gneiss (Tables 5 and 6) to the determinative figures yields essentially the same results; temperatures of roughly 400°C are indicated for all specimens at pressures of one through ten kilobars. Even though these determinations are in an area of the plot where reasonable accuracy cannot be assured, these temperature estimates apparently record subsolidus reequilibration and not liquidus temperatures.

System Q-Ab-Or. Figure 20 is a ternary plot of normative quartz, albite, and orthoclase, and samples of the Fitchburg complex composed of 80% or more of these components are plotted. The ternary minimum (*) and ternary eutectic (x) compositions of the water-saturated system are indicated (Winkler, 1979). Although Wyllie (1977) has made a case against the widespread assumption of water-saturation in natural magmas, the presence of hydrous phases and late-stage pegmatites in the rocks of the Fitchburg complex imply fluid saturation, at least in the later stages of solidification. For this system, increased $P_{H_2O}$ shifts the ternary minimum toward the Ab apex (Tuttle and Bowen, 1958; Luth and others, 1964)

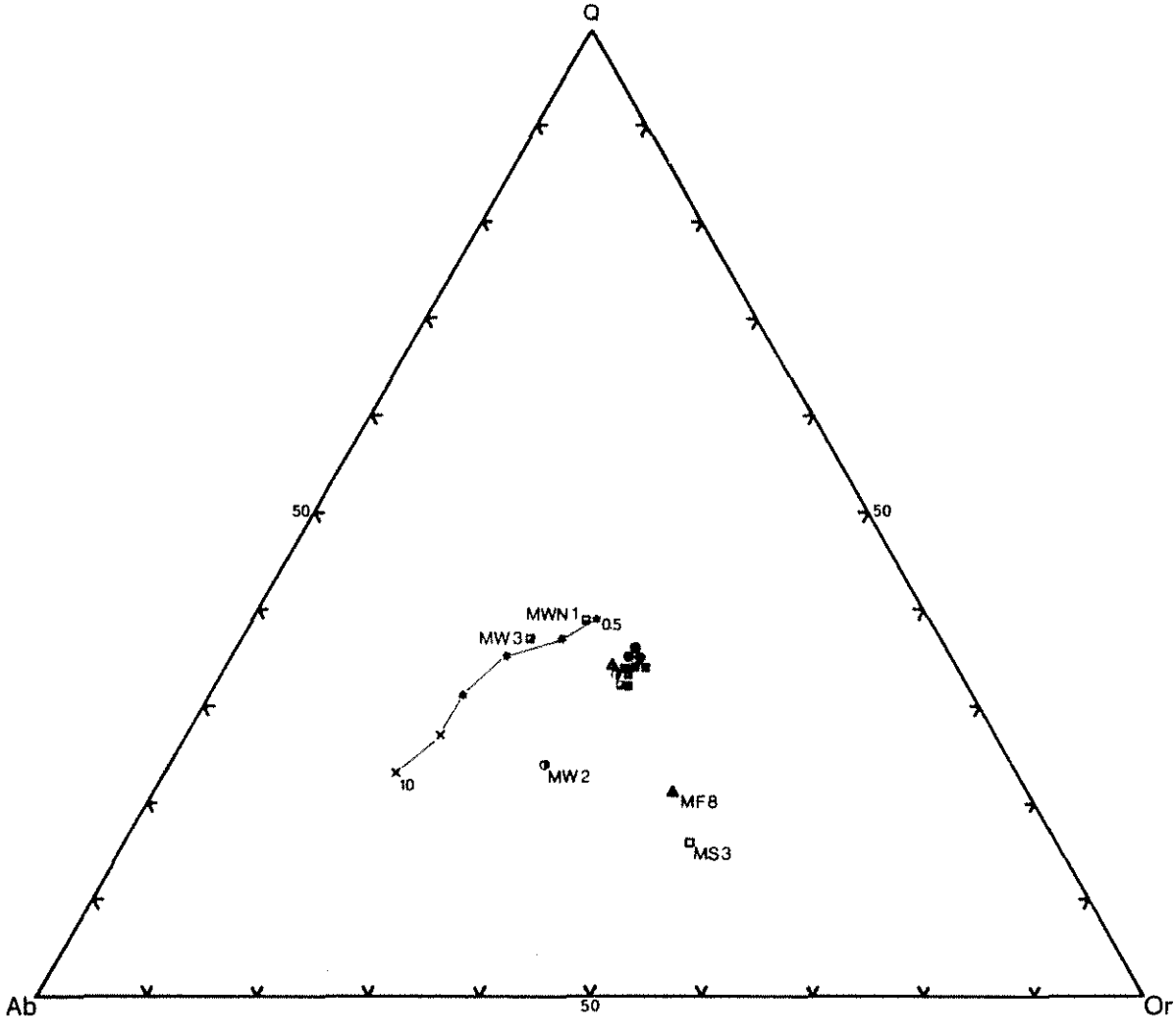


Figure 20. Normative Q-Ab-Or diagram. Samples of the Fitchburg complex composed of ≥80% of these components are plotted. Indicated are the ternary minimum (*) and ternary eutectic (x) compositions for $P_{H_2O}$= 0.5, 1, 2, 4, 5, and 10 kbar (Winkler, 1979).

but addition of normative anorthite component to the system will shift the minima/eutectics toward the Q-Or join (James and Hamilton, 1969).

Only the more leucocratic samples from the Fitchburg complex, primarily those from the granite and granite gneiss, have over 80% normative Q+Ab+Or. Although most samples of the granodiorite gneiss have subordinate to no modal potassium feldspar, they contain significant normative potassium feldspar. Some of these samples contain as much as 42% biotite in the mode, but the $K_2O$ content of the biotite is assigned to potassium feldspar in the norm because the norm calculation assumes that $Fe^{2+}$ and Mg in biotite are in pyroxene. However, with the amount of normative hypersthene in many of these rocks, it is clear that at 5 kbar $P_{H_2O}$, the pertinent liquidus phase would be biotite and not K-feldspar. Thus, rocks can be tonalites according to their modes but granodiorites according to normative mineralogy.

Although they fall away from the experimentally determined minima/eutectics, the cluster of data points displaced from the low $P_{H_2O}$ ternary minima toward the Or apex of the plot in Figure 20 could be construed to indicate some sort of minimum melting. The lack of correspondence to the synthetic system may be due to the fact that the effect of the anorthite component has been neglected, the source rocks have a particularly high normative potassic feldspar plus quartz to plagioclase ratio (James and Hamilton, 1969), or the presence of biotite as a principal mafic phase has not been taken into account.

System Q-Ab-Or-An-$H_2O$. Winkler (1979) states that the system Q-Ab-Or-$H_2O$ is inadequate for dealing quantitatively with the crystalliza-

tion of granites or the anatexis of gneisses, maintaining that the anorthite component of granites and gneisses, though subordinate to the albite component, is much too influential to be ignored. A better approximation of the granite system can be made with the system Q-Ab-Or-An-$H_2O$. This system can be represented by a tetrahedral volume bounded by the four component systems: Q-Ab-An-$H_2O$, Q-Or-An-$H_2O$, An-Ab-Or-$H_2O$, and Q-Ab-Or-$H_2O$, where $H_2O$ is present but not represented (Figure 21). The volume contains three cotectic surfaces where plagioclase + quartz + melt, quartz + alkali feldspar + melt, or plagioclase + alkali feldspar + melt coexist in the presence of a vapor phase. The $P_{H_2O}$ of the system is sufficient such that the plagioclase + alkali feldspar cotectic surface is complete and eutectic throughout. Cotectic line AB, where the surfaces intersect, marks those melt compositions which coexist with plagioclase, quartz, alkali feldspar, and vapor.

Figure 22a and b are anorthite and quartz projections respectively adapted from Winkler (1979) showing the data from the Fitchburg complex, the isobaric cotectic line AB, and isotherms on the cotectic surfaces of the system Q-Ab-Or-An-$H_2O$ at $P_{H_2O}$ = 5 kbar. Figure 22a shows the isotherms on the plag + qz + L + V and the plag + alk fsp + L + V cotectic surfaces projected from the An apex onto the Q-Ab-Or face of the tetrahedron. Figure 22b shows the isotherms on the plag + qz + L + V and the qz + alk fsp + L + V cotectic surfaces projected from the quartz apex onto the An-Ab-Or face of the tetrahedron. The bold face numbers on the isotherms and on the cotectic line are the experimentally determined amounts of anorthite (Figure 22a) or quartz (Figure 22b) component from which the projection emanates. When unconcerned with precise tempera-

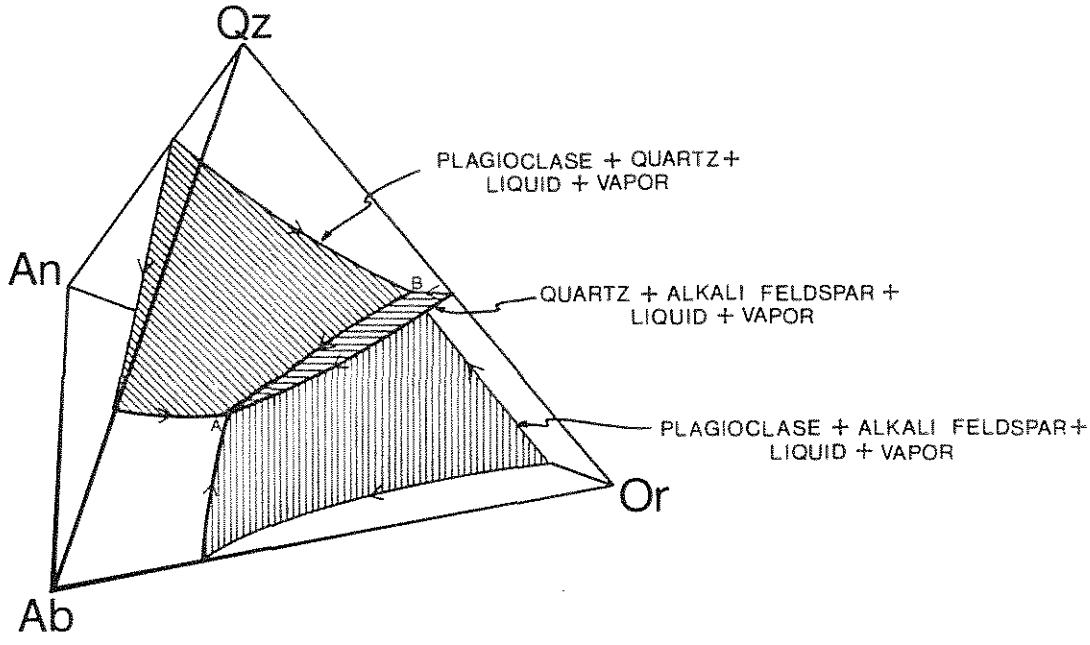


Figure 21. Schematic diagram of the phase relations in the system Q-Ab-Or-An-$H_2O$, where $H_2O$ is present but not represented. Shown are the three cotectic surfaces where plagioclase + quartz + liquid, quartz + alkali feldspar + liquid, and plagioclase + alkali feldspar + liquid coexist in the presence of a vapor phase. Cotectic line AB marks those melt compositions which are in equilibrium with plagioclase + quartz + alkali feldspar + vapor. The $P_{H_2O}$ of the system is sufficient that the plagioclase + alkali feldspar cotectic surface is complete and eutectic throughout.

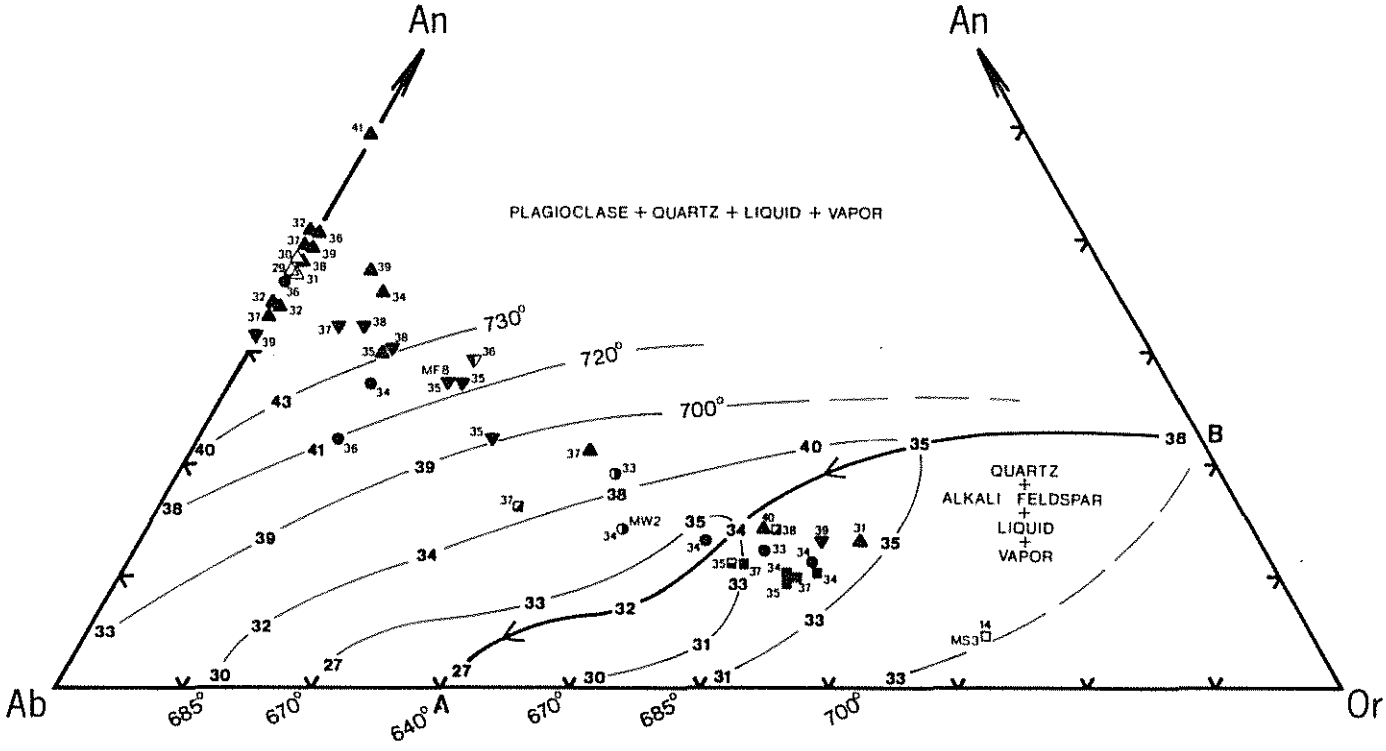


Figure 22b. Plot of modes from the Fitchburg complex on the projection of the isobaric cotectic line AB and the isotherms on the plag + qz + L + V and qz + alk fsp + L + V cotectic surfaces from the Qz apex on to the An-Ab-Or face of the tetrahedron in the system Q-Ab-Or-An-$H_2O$ with water pressure of 5 kbar (Winkler, 1979). Samples are identified by the same symbols used in the chemical plots. Numbers adjacent to the symbols and on the cotectic line and isotherms are the amount of Qz (Qz/(An + Ab + Qz + Or)) in weight percent. See text for further explanation.

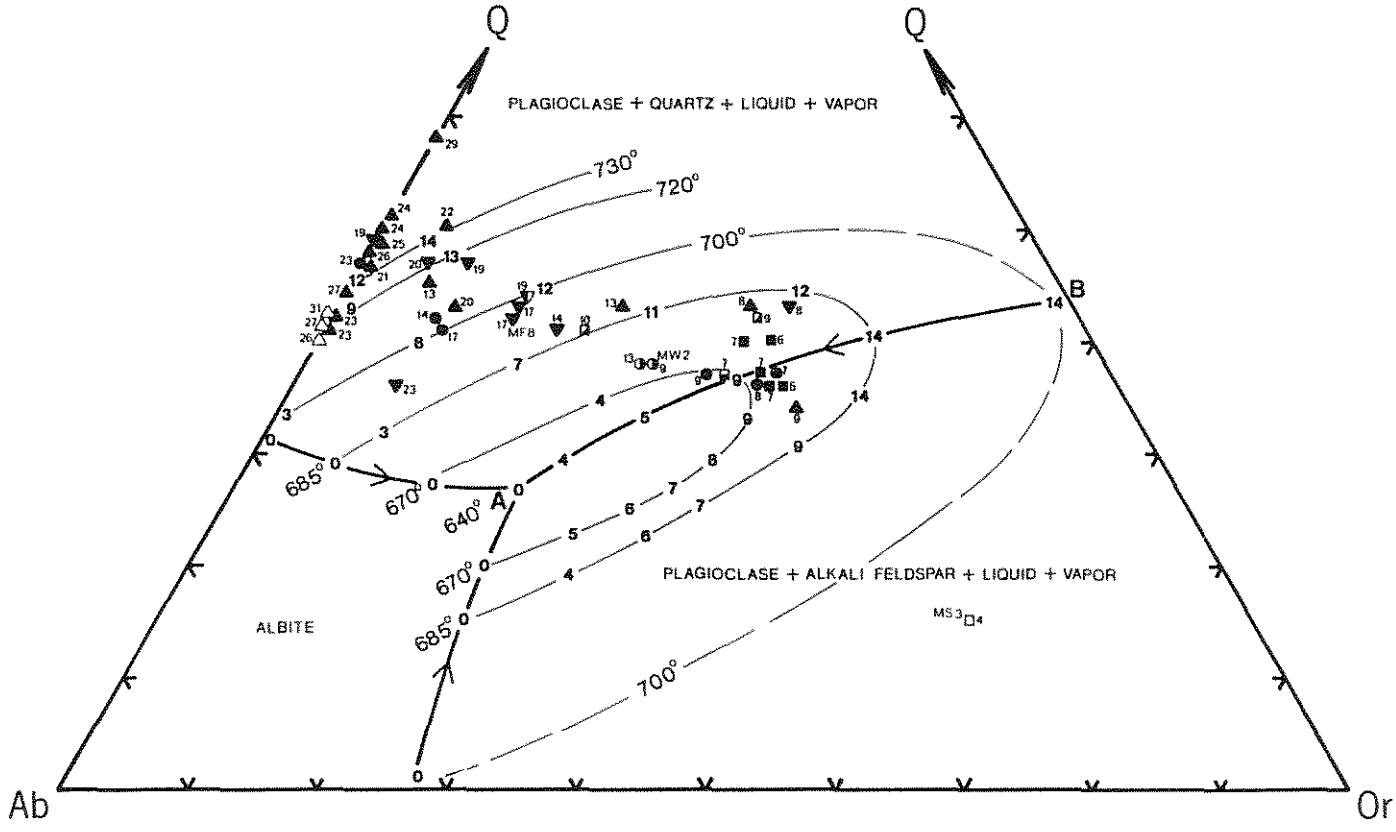


Figure 22a. Plot of modes from the Fitchburg complex on the projection of the isobaric cotectic line AB and the isotherms on the plag + qz + L + V and plag + alk fsp + L + V cotectic surfaces from the An apex on to the Q-Ab-Or face of the tetrahedron in the system Q-Ab-Or-An-$H_2O$ with water pressure of 5 kbar (Winkler, 1979). Samples are identified by the same symbols used in the chemical plots. Numbers adjacent to the symbols and on the cotectic line and isotherms are the amount of An (An/(An + Ab + Qz + Or)) in weight percent. See text for further explanation.

tures, this configuration of isotherms on the cotectic surfaces and the cotectic line can still be used in evaluating melt compositions which have temperatures exceeding the solidus by a few tens of degrees over a range of 3 to 10 kbar.

For melt compositions that are less than 2% of the projected component away from a cotectic surface, temperatures necessary to sustain a melt are probably less than $10^{o}$ higher than those needed for melts which have adjacent compositions but are situated on a cotectic surface. Substantial temperature increases occur with significant departures from the cotectic surfaces, particularly for melt compositions in the plagioclase volume or the quartz volume.

Data for the rocks of the Fitchburg complex are in weight percent and are derived from the modal amounts of plagioclase, quartz, alkali feldspar. An and Ab components of plagioclase were apportioned according to the Michel-Levy determinations (Tables 1-4), and the Or and Ab components of the alkali feldspar were apportioned on the basis of the results from microprobe analyses of the representative samples for each unit (Table 6). Problems with the effect of biotite which occur when representing the samples of the Fitchburg complex in the normative Q-Ab-Or-$H_2O$ system do not exist in this modal treatment of Q-Ab-Or-An-$H_2O$.

The granodiorite gneiss from the eastern belt (South Monoosnoc Hill, solid, downward-pointing triangles; West Sterling, half-filled, downward pointing triangle) and the western belt (Wachusett Mountain, solid, upward pointing triangles) are plotted in Figure 22 a and b. All samples which are modally granodiorite or tonalite plot significantly into the plagioclase volume from 5 to 15% or more away from the plag + qz + L + V cotec-

tic surface. Most of the modal tonalites, primarily from the western belt, are particularly far removed from the cotectic surface and well into the plagioclase volume in a high temperature region of the plot. The hornblende tonalite inclusions (open upward pointing triangles) are located in the same region.

The wide range of compositions found in this unit span a wide range of possible melt temperatures. The location of many of the samples off of the cotectic surface into the plagioclase volume makes meaningful estimation of melt temperatures difficult, but a range from approximately 700$^{o}$ to 800$^{o}$C or higher are indicated.

The granitic samples grouped with the granodiorite gneiss (MF-16, MW-11, 14) plot in the area where the modal granites from the complex are situated. MF-16 and MW-11 plot approximately at 4% excess quartz away from the cotectic line AB near the 670-685$^{o}$C isotherms, and MW-14 plots at approximately 2% excess alkali feldspar from the plag + alk fsp + L + V cotectic surface.

Samples of the granite gneiss from Princeton (half-filled circles) and from Crow Hills (filled circles) span a range of compositions in Figure 22a and b. Samples MW-2 and MW-1 from Princeton plot just off of the plag + qz + L + V cotectic surface into the plagioclase volume with approximately 1 and 4 percent excess plagioclase respectively. The temperature indicated for a melt having a composition of MW-2 is approximately 680$^{o}$C, and due to the excess plagioclase, a significantly higher temperature would be necessary for MW-1 to be completely molten. Another group of granite gneiss samples (MF-24, 25, 27) are disposed around the cotectic line AB either on or immediately adjacent to the plag + qz +L+V

or qz + alk fsp + L + V cotectic surfaces. Melt temperatures of approximately 675°C are indicated. Lastly, there is a group of samples (MF-21, tonalite; MF-22, 29, granodiorite) which plot significantly away from the plag + qz + L + V cotectic surface into the plagioclase volume, having 6 to 10% plagioclase in excess and requiring temperatures of approximately 750° to 800° to be molten.

As illustrated in Figure 22a and b, all but one of the granite samples from Rollstone Hill (solid squared), Malden Hill (diagonal, half-filled squares), and Princeton (horizontal, half-filled square) plot on the qz + alk fsp + L + V cotectic surface or into the quartz volume approximately equidistant from the plag + qz + L + V and the qz + alk fsp + L + V cotectic surfaces near the 670° and 685°C isotherms. The figure indicates that there would be 0 to 4% quartz in excess at temperatures of approximately 670 to 680°C. Thus a melt having the general composition of the granites of the Fitchburg complex could exist at roughly 670 to 680°C with $P_{H_2O}$ = 5 kbar. Sample MWN-1 from Malden Hill is a granodiorite and plots on the plag + qz + L + V cotectic surface on the 685°C isotherm, suggesting that it was entirely molten prior to crystallization.

In evaluating products of minimum or near minimum melting during upper crustal anatexis, high temperatures are not expected. Thus, departure from the cotectic surfaces has been interpreted by Winkler (1979) to indicate that some amount of the felsic constituents, probably residual material from the partially melted source rock, have been incorporated into or were never separated from the melt.

In their investigation of the system An-Ab-Or-Q-$H_2O$, Presnall and Bateman (1973) maintain that the departure of melt compositions from the

plag + qz + L + V cotectic surface into the plagioclase volume indicates the operation of equilibrium fusion rather than fractional fusion as the primary generating process for the Sierra Nevada batholith. Although Presnall and Bateman do not discount the possibility that some residual material could have been incorporated in the magma, it is the existence of melts in the plagioclase volume (and not in equilibrium with quartz) which allows them to reject fractional fusion as a significant contributing process. Because Presnall and Bateman propose a lower crust-upper mantle origin for the magmas and because temperatures present at this boundary are substantially higher than those associated with regional metamorphism, their conclusion concerning the existence of melt compositions well into the plagioclase volume is plausible.

## Generation of Melt

During mid-Paleozoic time, major tectonic events occurred on the eastern edge of the North American craton, culminating in the Acadian orogeny. In central Massachusetts, in the zone of most intense Acadian metamorphism, numerous large bodies of Devonian plutonic rocks occur, including the Hardwick, Coys Hill, Prescott, Belchertown, West Warren, and Fitchburg plutons.

Possible source materials. The tectonic environment, the relatively felsic character, the generally high potassium content, and the peraluminous nature of the Fitchburg complex are strongly suggestive of derivation by anatexis from rocks rich in quartzofeldspathic components and probably micas.

Initially it was thought that the rocks of the Fitchburg complex fit

well into the S-type and I-type granitoid classification system of Chappell and White (1974), where S-type granitoids are the products of partial melting of material exposed to a weathering cycle and I-type granitoids are products of partial melting of igneous source materials. According to theory, the process of weathering will endow sedimentary rocks with a chemistry significantly different from unweathered igneous rocks. Partial melting from either rock type can be identified because the melts inherit distinctive chemical traits from their source materials.

On the basis of mineralogy observed in thin section, the granodiorite gneiss appears to be an I-type granitoid, and the granite gneiss and the granite appear to be S-type granitoids. Upon consideration of the chemical data, separation of the rocks of the Fitchburg complex into these two groups becomes somewhat dubious, because there is a gradational aspect to the chemistry.

Distinguishing parameters, which permit the identification and separation of S and I granitoids were developed during extensive study of the Lachlan fold belt of southeastern Australia. Among the most important considerations which allow the rocks of the Lachlan belt to be divided into S and I granitoids are:

I. Alumina saturation: S-types have > 1% normative corundum and I-types have <1% normative corundum (Chappell and White, 1974). All of the granite and granite gneiss samples, a large majority of the granodiorite gneiss samples, and two of the three hornblende tonalite inclusions have >1% normative corundum, and thus fall into the S-type granitoid category. A few samples of the granodiorite gneiss and one hornblende tonalite inclusion sample have <1% normative corundum and

could be considered I-type granitoids.

II. Whole rock silica content: Most S-types have higher silica contents compared to most I-types (Griffin and others, 1976). The least siliceous S-type granitoid reported from the Kosciusko batholith (Hine and others, 1978) or the Moonbi district, New England batholith (Chappell, 1978) has 65.78% silica, and the majority of S-types have silica contents over 70%. In the Fitchburg complex, samples of the granodiorite gneiss, classified as S-type on the basis of alumina saturation, have silica contents as low as 56.71% and an "S-type" tonalite inclusion has 53.68% silica. Clearly there is a significant difference between the Fitchburg complex and the granitoids of the Lachlan belt on this point.

III. $Na_2O/K_2O$ ratio: S-types have a distinctly lower $Na_2O/K_2O$ ratio when compared to I-types (White and others, 1977; Hine and others, 1978). Figure 23 is a plot of weight % $Na_2O$ vs weight % $K_2O$, and it illustrates another incongruity. The dashed lines are discriminants for the Berridale batholith (White and others, 1977) and the Kosciusko batholith (Hine and others, 1978) which distinctly divide S- from I-type granitoids at the respective localities. Samples from the Fitchburg complex do not obviously group with respect to these discriminants, and those few samples of the granodiorite gneiss which are I-types on the basis of alumina saturation are S-types with respect to the discriminants in Figure 23.

IV. Oxidation state of iron: S-types have lower $Fe^{3+}/Fe^{2+}$ ratios when compared to I-types (Hine and others, 1978; Chappell, 1978). In contrast to that found in the Moonbi district (Chappell, 1978) and the Kosciusko batholith (Hine and others, 1978) the higher ferric-ferrous iron ratios

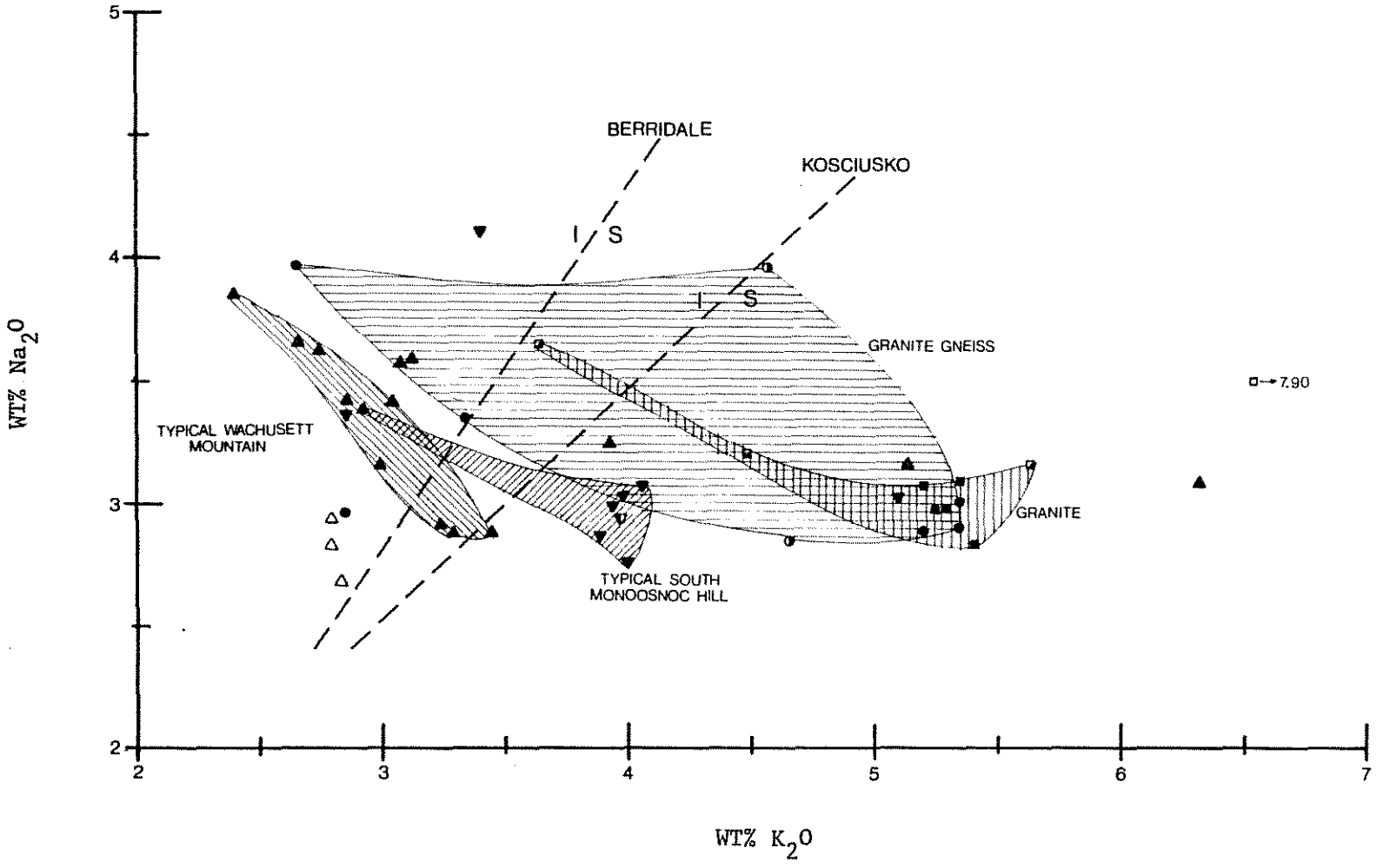


Figure 23. Plot of whole rock $Na_2O$ vs. $K_2O$ (Wt%) for the samples of the Fitchburg complex. Dashed lines are discriminants between S-type and I-type granitoids of the Berridale (White and others, 1977) and the Kosciusko (Hine and others, 1978) batholiths from the Lachlan fold belt of eastern Australia.

are associated with the more felsic rocks, although the variation in the ratios is subtle in the rocks of the Fitchburg complex. The ferric-ferrous iron ratios vary in a broadly diffuse manner.

V. Xenoliths: Although xenoliths or xenocrysts are rare in S-types, those present are commonly pieces of local country rock. Xenoliths and xenocrysts are very common in I-type granitoids and are thought to represent entrained residual material (restite) from partial melting (White and Chappell, 1977; Chappell, 1978). Restite inclusions within the granitoids, as described by White and Chappell (1977) and Chappell (1978) are not observed in the Fitchburg complex. The only inclusions are of country rock near the contacts. In the Lachlan belt, chemical variation appears to be controlled primarily by the relative proportions of melt and restite, but no such correlation is obvious in the rocks of the Fitchburg complex.

Thus on the basis of the above criteria, the rocks of the Fitchburg complex do not fit particularly well into the S-type and I-type granitoid classification but appear to be primarily S-types grading into I-types. Alternative possibilities for the source materials of the complex include the following:

a. Possibly, the source rocks for the complex were not strictly mature sedimentary rocks or igneous rocks and consequently did not have sufficiently distinct chemical traits. A combination of chemistries corresponding to mature sedimentary rocks such as pelite, immature sedimentary rocks such as arkose, and igneous rock could have been the source.

b. Due to the large volume of material necessary to produce a partial melt which results in a body as large as a pluton, it is conceivable that

melting could have incorporated several different lithologies. The melts then coalesced and mixed to produce a range of intermediate type granitoids.

For a system of large scale such as the zone of generation for a granitic pluton, equilibrium should have existed between the melt and the residual source material during anatexis. Thus, the near-liquidus mineralogy of such a melt should correspond to the major minerals in the source at the pressures and temperatures of origin (Wyllie and others, 1976).

Most of the rocks of the complex have undergone some amount of recrystallization subsequent to emplacement, impeding the determination of their paragenetic sequence by textural evidence. In the absence of such evidence, the relationships indicated by the system Q-Ab-Or-An-$H_2O$ (Winkler, 1979) diagrams (Figures 22a and b) can be used to approximate the sequence of crystallization from which information about the source can be inferred.

According to Figures 22a and b, most of the granite samples plot on the qz + alk fsp + L + V cotectic surface or in the quartz volume. At the site of generation, melts of those compositions which are situated on the cotectic surface are still in equilibrium with quartz and alkali feldspar of the source material. Melt compositions are no longer situated on cotectic line AB, indicating that the plagioclase content of the source was exhausted during the melting interval and thus was subordinate to the quartz content and the alkali feldspar content.

It has been noted that the presence of hydrous minerals in a source

can significantly affect the normative orthoclase content of a resulting partial melt (Brown and Fyfe, 1970). If the source rock contained muscovite, a part of the alkali feldspar component of the granitoid could have been derived from the reaction where: muscovite + quartz = potassium feldspar (in melt) + aluminum silicate + $H_2O$. In an anatectic environment, the alkali feldspar component would enter into the melt while the aluminum silicate would largely remain as a residual phase. Similarly, biotite can contribute some alkali feldspar component during anatexis through reactions which, depending on the bulk composition, produce hornblende, cordierite, almandine, ilmenite, and/or magnetite as residual phases and free alkali feldspar component to be incorporated into the melt (Winkler, 1979).

Both the granite gneiss and the granodiorite gneiss units have a wide range of variation that can be seen in Figures 22a and b. The common intermediate to more mafic specimens from each unit lie at various distances into the plagioclase volume, away from the plag + qz + L + V cotectic surface. The more felsic specimens plot in various places, generally near the cotectic line AB. The position of the common intermediate to more mafic types indicate that alkali feldspar and/or micas were subordinate to plagioclase and quartz in the source(s). The mineralogy of the tonalite inclusions indicate hornblende in their source.

Differences between the granodiorite gneiss and the granite gneiss may be the result of:

a. Differences in source materials: Different amounts or absence of alkali feldspar, muscovite, and/or biotite would have had significant affect on the alkali feldspar component of a partial melt, which appears to

be one of the principal differences between the two gneisses. The feldspar to quartz ratio appears to be relatively constant throughout the whole series of rock compositions (Figure 15a).

b. Different degrees of partial melting of the same source: A melt fraction corresponding to the granodiorite gneiss may have been generated under specific temperatures and pressures. In a different, probably lower temperature and pressure regime, a melt which has a higher K content could be generated due to less extensive melting.

c. Some combination of a and b.

Source in the mantle. Because crust-mantle interaction undoubtedly occurred during the Acadian orogeny and because the element versus silica plots (Figure 16 a,b,c) are broadly correlative, the possibility exists that the three units of the Fitchburg complex are members of a cognate differentiation series related by fractional crystallization from a mantle-derived basaltic magma. The main problem with this hypothesis concerns the absence of the large amount of relatively mafic material necessary to differentiate and produce the volumes of felsic material presently exposed. Current understanding of the structure of the Merrimack synclinorium does not allow for such volumes of mafic material to occur at shallow depth in proximity to the complex. It is possible that the large volumes of mafic differentiates are located at considerable depth beneath the complex or that they have been eroded away, but there is no compelling evidence to support either of these alternatives. The felsic nature of the complex precludes the possibility that it represents an undifferentiated, mantle-derived partial melt.

Source in deep continental crust. The Fitchburg plutonic complex is a metamorphosed set of intrusions of varied composition. To satisfy current understanding of the relationships among the units of the complex, it appears that it was necessary to have had three separate magmas, one for each major unit in the complex. Magmas corresponding to the granodiorite gneiss and the granite gneiss were coeval but not necessarily consanguinous. A third, corresponding to the granite, was generated sometime afterwards, escaping the majority of pervasive Acadian metamorphism and deformation that affected the other two units.

In the eastern belt of the granodiorite gneiss, the rocks have retained vestiges of their igneous origin in the form of some relict igneous crystal habit. The samples of the common gneiss at South Monoosnoc Hill and at West Sterling are relatively homogeneous in outcrop and have virtually identical chemistries, despite the fact that the two localities are nearly nine kilometers apart. Acadian metamorphism did not cause partial melting in the granodiorite gneiss of the eastern belt as it did in the western belt. In light of these considerations, it is presumed that the composition of one of the common gneiss samples from South Monoosnoc Hill, such as MF-8, represents the best available example of a primary melt. As previously mentioned, application of the two feldspar geothermometer of Stormer (1975) to the feldspar compositions of sample MF-8 yields a temperature of 400°C, a temperature which is indicative of subsolidus reequilibration rather than that of primary crystallization. Using the relations of the system Q-Ab-Or-An-$H_2O$ as a basis for estimation (Figure 22a and b), sample MF-8 would be a

melt at roughly 750°C and $P_{H_2O}$ = 5 kb or contain a significant non-liquid fraction at a lower temperature or lower $P_{H_2O}$.

The choice of a common granodiorite gneiss sample as being representative of a primary melt may not be strictly correct and may be misleading. The granodiorite gneiss and the tonalite inclusions, in addition to their physical association have close chemical affinities as observed in the Harker variation diagrams (Figure 16 a,b,c). The tonalite inclusions have a relict igneous texture which demonstrates that they crystallized from a melt. This evidence suggests that the tonalite inclusions are early differentiates of the granodiorite melt, representing settled crystals with interstitial melt or accumulations of crystals and liquid on the magma chamber walls. The coarse-grained, poikilitic biotite grains suggest adcumulus crystal growth. Crystallization of the tonalite from the magma appears to have changed the bulk composition of the melt, enriching it in K and $H_2O$, causing the instability of hornblende as a primary crystallization phase, and preventing further crystallization of hornblende in the granodiorite gneiss. Crystallization and removal of a significant amount of material similar in composition to the tonalite inclusions would alter the original melt composition. The small number of inclusions can be construed to indicate that the differentiation process was not extensive or that few of the products travelled up the vent at the time of sill intrusion. If the amount of differentiated material which forms the tonalite inclusions was small in comparison to the entire granodiorite gneiss body as is thought, then the effect of differentiation in changing the composition of the melt may have been minor. If most of the separated tonalite stayed below, any

attempt at estimating the conditions of generation for this melt using the typical granodiorite gneiss composition as a basis would be in substantial error.

In the presence of excess water, temperatures of approximately 950°C are necessary to sustain a melt of granodiorite-tonalite composition, having biotite and hornblende in solution (Wyllie, 1977). Assuming the hornblende and biotite in the tonalite inclusions crystallized from the melt, and considering that water-saturated conditions are not necessarily the case, as is implied by the former presence of clinopyroxene, temperatures may have been even higher during the generation of that magma. Because these temperatures are substantially above those normally associated with regional metamorphism, a remote source for the melt would have been necessary.

Experimental data and relations in the system Q-Ab-Or-An-$H_2O$ indicate that a granodiorite gneiss melt would have had to contain a significant non-liquid fraction, probably relict source material, if it were generated in the upper crust during regional metamorphism. Because petrographic evidence to support such a conclusion is scant and because this unit was present at the onset of metamorphism, the magma probably originated from some deeper, remote source. Compositional and temperature constraints previously discussed suggest deep continental crust as a likely source.

Due to its relatively homogeneous character in outcrop and lack of obvious contaminating material, sample MW-2 is thought to be the most representative of a primary melt for the granite gneiss unit. Having

been subjected to sillimanite-muscovite grade metamorphism, the granite gneiss has a recrystallized texture and strong foliation.

The composition of MW-2 plots adjacent to the ternary minimum of the system Q-Ab-Or (Figure 20) at approximately 4 kbar but is displaced toward greater Or content. Relative to the more granitic samples from this unit, it appears that it was generated at higher pressure or is the product of more extensive partial melting. In the system Q-Ab-Or-An-$H_2O$ (Figure 22a and b) MW-2 plots essentially on the plag + qz + L + V cotectic surface at approximately 675$^{o}$C. Considering the peraluminous and high potassic chemistry of this unit and the location of MW-2 on the plag + qz + L + V cotectic surface, non-minimum melt conditions are indicated.

Approximately 15 km west of the Fitchburg complex in the Barre area, conditions of sillimanite-K-spar metamorphism have been estimated at an average of 650$^{o}$C, 5.5 kbar (Tucker, 1977). These as well as the relatively lower sillimanite-muscovite grade metamorphic conditions in the area of the Fitchburg complex would be insufficient to generate the postulated granite gneiss magma. This conclusion coupled with the fact that the granite gneiss was present at the beginning of Acadian deformation suggests a remote source for the granite gneiss. A deep continental crust source similar to that of the granodiorite gneiss appears likely.

Field evidence and the non-minimum compositions expressed by the granodiorite gneiss and the granite gneiss indicate a remote deep crustal rock source. This conclusion is in accord with the tectonic

model of southern New England of Robinson and Hall (1980) where crustal rocks were involved in a westward-dipping subduction zone during Early Devonian (Acadian) time. High temperatures associated with subduction undoubtedly caused partial melting in the subducted crustal rocks, and these partial melts were probably intruded into higher structural levels as subduction continued.

In contrast to the granodiorite gneiss and the granite gneiss, the granite has a generally massive character and its map pattern is discordant with respect to the surrounding metamorphosed sedimentary rocks. These criteria are the basis for concluding that the intrusion of the granite postdates the majority of Acadian deformation (Peper and others, 1978).

In the system Q-Ab-Or (Figure 20) the samples from Rollstone Hill and MWN-2 from Malden Hill plot in a cluster that is suggestive of minimum melting, but the cluster is displaced from the experimentally determined minimum toward the Or apex. MWN-1, the other sample from Malden Hill, and the sample from Princeton plot very close to the experimentally determined minima. Relations in the system Q-Ab-Or-An-$H_2O$ (Figure 22a and b) indicate that most of the granite samples could exist as magmas in the range of 670 to 680$^{o}$C at $P_{H_2O}$= 5 kb. Relations in the systems Q-Ab-Or and Q-Ab-Or-An-$H_2O$ as well as the relatively homogeneous character of these samples suggest that they are minimum or near-minimum melts. The regular chemical trends observed in Figures 16a, b, and c suggest that the source rocks of the granite may have been similar to that of the granodiorite gneiss and the granite gneiss.

Melting in situ. The center of the complex appears to have been a thermal high during Acadian metamorphism with conditions reaching sillimanite-muscovite-K-spar grade (Figure 3). As seen in Figure 19, the curve for the breakdown of muscovite plus quartz (Day, 1973) intersects that for the minimum melt of granite (Tuttle and Bowen, 1958) at approximately 660°C, 3 kbar $P_{H_2O}$. The occurrence of sillimanite rather than andalusite as the stable aluminosilicate polymorph implies a pressure in excess of approximately 2 kbar in the temperature range for the breakdown of muscovite plus quartz (Holdaway, 1971), and suggests that the muscovite + quartz breakdown may have occurred within the P-T realm of the minimum melting of granite.

Because evidence suggests that the granite gneiss was emplaced prior to the peak of metamorphism (Tucker, 1978; Field, 1975), and because the metamorphic regime may have been suitable for minimum melting in the granite gneiss, the granite may have been generated by in situ melting of the granite gneiss. Such an origin would help explain the correlation between the chemistries of the granite and the granite gneiss.

The intrusive nature of the granite has not been conclusively demonstrated but has been inferred on the basis of its discordant map pattern. At the Metropolitan District Commission gauging station in Barre, sequential samples collected during the building of the Quabbin aqueduct were examined. Samples collected in the vicinity of the inferred contact between the granite gneiss and the granite are not unequivocally distinct as to their affinity and thus, the contact appears to be gradational at this location. Strongly foliated, biotite-rich

gneisses are also present and may represent residual material remaining from the separation of a granitic minimum melt from the granite gneiss. These observations support an *in situ* melting of the granite gneiss as the origin for the granite.

## Evolution of Melt

*Fractional crystallization*. Studies of the various plutons which comprise the Sierra Nevada batholith show that the rocks are predominantly granite to granodiorite in composition, although compositions from diorite through leucogranite may be present. Zoned plutons are characteristic of the Sierra Nevada (Wones, 1980), and much of the zonation occurs independent of the wall rock composition, indicating the operation of some differentiation process (Bateman and others, 1966). In their study of the Tuolumne intrusive series, a concentrically zoned granitoid body in the Sierra Nevada, Bateman and Chappell (1979) analyzed samples collected along a traverse through the series and examined chemical variation with respect to position along the traverse. Bateman and Chappell observed a nearly continuous range of compositions from quartz diorite through granite in the series and concluded that crystal accretion to the magma chamber walls and/or crystal settling on the magma chamber floor were the primary processes which could account for the zoning.

This systematic spatial arrangement of rocks having regular chemical variation has not been found in the Fitchburg complex. No tenable combination of circumstances involving "in situ" fractional crystallization as the principal method of generating variation could result in the observed

distribution of rock compositions within any of the units of the complex. Thus, this type of fractional crystallization is not considered to be important in understanding the chemical variation of the complex.

Although the process is thought to be peripheral to the understanding of the complex as a whole, fractional crystallization may have bearing on the origin of the tonalite inclusions. The petrographic and chemical reasons for this conclusion have already been discussed on page 105. Petrographic evidence suggests that the tonalite inclusions probably formed by the segregation of hornblende, plagioclase and biotite crystals along with some interstitial melt which eventually crystallized more plagioclase, biotite, and quartz. Crystallization of the tonalite appears to have changed the bulk composition of the magma, making hornblende unstable and preventing further crystallization of hornblende in the granodiorite gneiss body.

Multistage intrusive origin of individual units. Generation of compositional variations could have occurred for each unit at a remote location by multistage fractional crystallization or progressive partial melting, and the sequential products of either process could then be individually intruded into their present positions. Such a mechanism may be responsible for the origin of the modally and chemically disparate samples.

At South Monoosnoc Hill, samples MF-11 and 16, a tonalite and a granite respectively, are intrusive into the common granodiorite gneiss, and all of these rock types are cross cut by pegmatite dikes. Although the mechanism(s) for the production of these two rock types is not certain,

their chemistries do not preclude the possibility that they are genetically related to the granodiorite gneiss.

Similarly, the granite gneiss sills on Wachusett Mountain (samples MW-11, 14, 18) appear to be the result of discrete intrusions into the common gneiss prior to the majority of Acadian deformation. Their chemistries are in some aspects discordant to the trends of variation noted in the common granodiorite gneiss and thus were probably not generated in the same manner and/or not of the same parentage as the common gneiss.

The variation observed in the granodiorite gneiss at Wachusett Mountain and the granite gneiss at Crow Hills occurs as rapid changes in grain size, mafic mineral content, and amount of pegmatitic stringers. This variation is well documented at Wachusett Mountain in modal and chemical data. Although Acadian metamorphism could have obscured some evidence of multiple intrusion it is unlikely that a multiple intrusion mechanism would produce variation on the small physical scale that is observed.

Incorporation of xenolithic material. The presence of inclusions of country rock and their possible contaminating effects in granitoids has been noted in the past, but only recently has the importance of cognate xenoliths and xenocrysts and their relation to chemical variation in granitoids been recognized. Through their work with S- and I-type granitoids, White and Chappell (1977) have made a significant contribution to the understanding of granitoid genesis by elucidating the relationship between granitoids and their inclusions as products of ultra-metamorphism.

In the model system for the generation of granitoids (White and

Chappell, 1977), a source rock will produce a minimum melt and residual material (restite) under the appropriate conditions, and chemical variation can be generated by the progressive separation of these two components. The range of compositions which can be produced in this simple two component mixing (or segregation) system is expressed as a straight line between "pure restite" and "pure minimum melt" compositions when plotted on standard Harker diagrams.

Wide ranges of compositional variability have been found in the granitoids of the Lachlan fold belt of eastern Australia, and the majority of this variation has been ascribed to the process of mixing variable amounts of restite with a minimum melt. In the field the granitoids have variable amounts of xenoliths, and the increasing amount of xenoliths is correlated with the increasingly mafic character of the granitoids. Typically, the xenoliths are megascopic clots of predominantly mafic minerals which are distinctly different in appearance from the host granitoid. All stages of xenolith disintegration are observed from sharp, angular contacts to rounded, diffuse contacts with the host granitoid. In thin section individual mineral grains can be identified as being xenocrysts (Rhodes, 1969; Chappell and White, 1974; Griffin and others, 1978; Hine and others, 1978; Chappell, 1978).

Whole rock chemical variation of the granitoids of the Lachlan belt closely approximates the model system. Linear variation of elements against silica is observed in contrast to the commonly curvilinear variation trends associated with igneous bodies which have been differentiated through fractional crystallization (White and Chappell, 1977).

Similar to the granitoids of the Lachlan belt, whole rock chemical data from the Fitchburg complex vary in a linear manner when plotted against silica, but nothing similar to the nature and distribution of restite material within the Lachlan belt has been recognized in this area.

Metamorphic Effects Including Local Melting

Structural evidence indicates that the granodiorite gneiss and the granite gneiss were emplaced before or during the first phase (nappe phase) of Acadian deformation (Tucker, 1978). The granodiorite gneiss at South Monoosnoc Hill was subjected to sillimanite-staurolite grade metamorphism which partially recrystallized the rock, but some minerals have relict igneous crystal habit. The granodiorite gneiss at Wachusett Mountain and the granite gneiss were subjected to sillimanite-muscovite and local sillimanite-muscovite-K-spar grade metamorphism which has completely recrystallized these rocks and formed a strong foliation.

Mehnert (1968) defines migmatite as a "megascopically composite rock consisting of two or more petrographically different parts, one is the country rock in a more or less metamorphic stage, the other is of pegmatitic, aplitic, granitic, or generally plutonic appearance". The granodiorite gneiss at Wachusett Mountain is migmatitic in outcrop (Figure 8) being a strongly foliated gneiss with variations in grain size, mafic mineral content, and amount of pegmatitic stringers occurring throughout the sequence. Although some of the leucocratic/pegmatitic material appears to be intrusive in origin, the nature and distribution of much of the leucocratic/pegmatitic material appears as if it is the result of

partial melting of the gneiss. High temperatures associated with the peak of metamorphism and excess water derived from prograde dehydration reactions in the surrounding metamorphosed sedimentary rocks may have provided a suitable environment for some amount of partial melting to occur.

That the average composition of the granodiorite gneiss at South Monoosnoc Hill is situated roughly in the middle of the range of compositions found at Wachusett Mountain could be interpreted to indicate that a minimum melt-restite type of process was responsible for generating the chemical variation. Thus at the time of emplacement, the average bulk composition in both areas could have been the same, but the subsequent partial melting during continued Acadian metamorphism may have generated a wide compositional range in the gneiss at Wachusett Mountain.

Although superficially the minimum melt-restite model may appear to be the panacea for the problems of generating the observed variation in the granodiorite gneiss, there are complications. The most glaring of these complications is the behavior and distribution of potassium.

Brown and Fyfe (1970) conducted melting experiments on a wide variety of quartz-feldspar-hydrous phase (e.g. muscovite, biotite, hornblende) mixtures and found that the first liquids generated in such fusion experiments were granitic in composition. Thus, it appears that minimum melting of a bulk composition similar to sample MF-8, the commom gneiss sample from South Monoosnoc Hill and postulated initial bulk composition for the granodiorite gneiss unit, would be granitic in

composition also. Progressive separation of a melt from residuum would lead to potassium enrichment on the felsic end, but the trend exhibited by the granodiorite gneiss at Wachusett Mountain is toward a slight decrease in potassium with increasing felsic character of the granitoids. The K trend probably reflects the decrease of biotite with increasing felsic character of the gneiss.

In addition, the $K_2O$ content of the granodiorite gneiss at Wachusett Mountain is on the average one % lower than comparable samples from South Monoosnoc Hill, a fact which is not readily explained by the minimum melt-restite model. General differences in element distribution occur in Na, Rb, Pb, Ga, and Y, but their significance is not understood.

A minimum melt-restite mechanism may account for the type of variation observed in the granite gneiss. As previously discussed, sample MW-2 from Princeton appears to be the best choice available for a representative of an initial composition, due to its homogeneous character in outcrop. In contrast, the gneiss at Crow Hills is heterogeneous and migmatitic, suggestive of some sort of partial melting. Some particularly leucocratic samples of the granite gneiss plot in a cluster on the Q-Ab-Or plot (Figure 20), which could indicate formation by minimum melting. Relatively mafic specimens of the granite gneiss plot away from the plag + qz + L + V cotectic surface (Figure 22a and b) as if some portion of their granitic components had been removed. Although the Crow Hills locality is inadequately sampled and thus poorly documented, the range of variation there is comparable to that found in the granodiorite gneiss at

Wachusett Mountain, and sample MW-2 is situated approximately in the center of the two extremes in variation.

Although the minimum melt-restite mechanism appears to explain some of the broad chemical aspects of the granite gneiss, the reason for the variation in the granite gneiss is difficult to determine because the pattern of variation is not completely systematic. In the typical gneiss, there are substantial chemical differences in specimens having similar silica contents (e.g. K, Na, Total Fe, Pb, Th, Ga, Y in samples MW-1, 2, and MF-22).

This manner of generating variation is attractive because it creates both more mafic and more felsic compositions than the starting material, a situation which appears to have occurred at Wachusett Mountain and Crow Hills. In theory, the resulting variation of elements is linear with respect to silica, as is the pattern observed for most of the element plots against silica at both areas.

Extraction of a minimum or near minimum melt from the "primary" granodiorite gneiss or granite gneiss could have produced the more mafic specimens of their respective variation series. Formation by this process would explain the location of the more mafic samples in a high temperature area of the system Q-Ab-Or-An-$H_2O$ plots (Figures 22a and b). The more felsic compositions could have resulted from progressively more effective separation of melt from the residual material.

The minimum melt-restite model for generating variation in the granodiorite gneiss at Wachusett Mountain and in the granite gneiss at Crow Hills appears to explain some of the observed variation, but

obviously does not resolve all of the problems concerning the evolution of these rocks.

## SUMMARY OF CONCLUSIONS

1) Petrographic and geochemical data for the Fitchburg plutonic complex show that there is a range of compositions present within each of its three units: a wide, nearly continuous, series of compositions in the granodiorite gneiss, a wide but sporadic range in the granite gneiss, and a relatively narrow range in the granite. This variation is due to systematic change in the relative proportions of the major rock-forming minerals as well as compositional changes in some of these minerals.

2) Field, petrographic, and chemical evidence indicate that the granodiorite gneiss and the granite gneiss were generated by partial melting of some remote crustal rock source, probably continental crust in an Acadian subduction zone. Evidence suggests that the granite gneiss and the granodiorite gneiss are non-minimum, partial melts of very similar source materials, but the degree of melting necessary to produce the granite gneiss was less extensive than that needed for the granodiorite gneiss. The tonalite inclusions in the granodiorite gneiss appear to be differentiates of the granodiorite magma, formed by the segregation of early crystallization products. The granite may have been generated by minimum melting of crustal materials similar to the source rocks of the granodiorite gneiss and the granite gneiss, or it may be the product of

*in situ* melting of the granite gneiss.

3) After the emplacement of the granodiorite gneiss and the granite gneiss, continued Acadian metamorphism caused partial melting in the granodiorite gneiss at Wachusett Mountain and in the granite gneiss at Crow Hills. By a minimum melt-restite segregation mechanism (White and Chappell, 1977), chemical variation may have been generated in these gneisses. Although the total chemical behavior of the units in the complex is not adequately explained by any single process, the minimum melt-restite mechanism is currently the most satisfactory explanation for much of the observed variation within these units. The pattern of variation of these rocks indicates a complex history, where a number of processes influenced the distribution of the elements.

# REFERENCES CITED


Aleinikoff, J.N., 1978, Structure, petrology, and U-Th-Pb geochronology in the Milford (15') quadrangle, New Hampshire: Ph.D. thesis, Dartmouth College, Hanover, New Hampshire, 247 p.

Ashwal, L.D., 1974, Metamorphic hydration of augite-orthopyroxene monzodiorite to hornblende granodiorite gneiss, Belchertown batholith, central Massachusetts: M.S. thesis, Contribution No. 18, Department of Geology, University of Massachusetts, Amherst, 124 p.

Bateman, P.C., and Wahrhaftig, C., 1966, Geology of the Sierra Nevada, in Bailey, E.H., ed., Geology of Northern California, California Division of Mines Geological Bulletin, v. 190, p. 107-172.

_____, and Chappell, B.W., 1979, Crystallization, fractionation, and solidification of the Tuolumne intrusive series, Yosemite National Park, California: Geological Society of America Bulletin, v. 90, p. 465-482.

Belvin, I.E., and Tollo, R.P., 1977, Unpublished data on the Paxton quadrangle, University of Massachusetts, Amherst, Massachusetts.

Billings, M.P., 1956, The geology of New Hampshire, part II-bedrock geology: New Hampshire Planning and Development Commission, 203 p.

Brown, G.C., and Fyfe, W.S., 1970, Production of granitic melts during ultra-metamorphism: Contributions to Mineralogy and Petrology, v. 28, p. 310-318.

Chappell, B.W., and White, A.J.R., 1974, Two contrasting granite types: Pacific Geology, v. 8, p. 173-174.

_____, 1978, Granitoids from the Moonbi district, New England batholith, Eastern Australia: Journal of the Geological Society of Australia, v. 25, 267-283.

Chayes, Felix, 1956, Petrographic modal analysis: John Wiley and Sons, 113 p.

Dale, T.N., 1923, The commercial granites of New England: United States Geological Survey Bulletin 738, 488 p.

Day, H.W., 1973, The high temperature stability of muscovite plus quartz: American Mineralogist, v. 58, p. 255-262.

Deer, W.A., Howie, R.A., and Zussman, Jack, 1966, An introduction to the rock-forming minerals: Longmans, 528 p.

Dixon, H.R., 1968, Bedrock geology of the Danielson quadrangle, Connecticut: United States Geological Survey Quadrangle Map GQ-696.

_____, and Lundgren, L.W., Jr., 1968, Structure of eastern Connecticut, p. 203-218, in Zen, E-an, White, W.S., Hadley, J.B., and Thompson, J.B., Jr., eds., Studies of Appalachian geology, Northern and Maritime: Wiley, 475 p.

Emerson, B.K., 1898, Geology of old Hampshire County, Massachusetts: United States Geological Survey Monograph 29, 790 p.

_____, 1917, Geology of Massachusetts and Rhode Island: United States Geological Survey Bulletin 597, 289 p.

Evans, B.W., 1965, Application of a reaction rate method to the breakdown equilibrium of muscovite and muscovite plus quartz: American Journal of Science, v. 263, p. 647-667.

Fahlquist, R.R., 1935, Geology of region in which Quabbin Aqueduct and Quabbin Reservoir are located; Appendix to report of Chief Engineer: Annual Report of the Metropolitan District Water Supply Commission, Commonwealth of Massachusetts, Public Document No. 147, 47 p.

Field, M.T., 1975, Bedrock geology of the Ware area, central Massachusetts: (Ph.D. thesis) Contribution No. 22, Geology Department, University of Massachusetts, Amherst, 186 p.

Flanagan, F.J., 1976, 1972 compilation of data on U.S. Geological Survey standards, p. 131-183, in Descriptions and analyses of eight new U.S.G.S. rock standards, United States Geological Survey Professional Paper 840, 192 p.

Fleischer, M., 1969, U.S. Geological Survey standards-I, additional data on rocks G-1 and W-1, 1965-1967: Geochimica et Cosmochimica Acta, v. 33, p. 66-79.

Greene, R.C., 1970, The geology of the Peterborough quadrangle, New Hampshire: New Hampshire Department of Resource and Economic Development Bulletin, No 4, 88 p.

Grew, E.S., 1970, The geology of the Pennsylvanian and pre-Pennsylvanian rocks of the Worcester area, Massachusetts: Ph.D. thesis, Harvard University, Cambridge, Massachusetts, 263 p.

Griffin, T.J., White, A.J.R., and Chappell, B.W., 1978, The Moruya batholith and geochemical contrasts between the Moruya and Jindabyne suites: Journal of the Geological Society of Australia, v. 25, p. 235-247.

Guidotti, C.V., and Sassi, F.P., 1976, Muscovite as a petrogenetic indicator mineral in pelitic schists: Neues Jahrbuch fuer Mineralogie, Abhandlungen, v. 127, p. 97-142.

Hall, A.J., 1941, The relation between color and chemical composition in biotites: American Mineralogist, v. 26, p. 29-33.

Hayama, Y., 1959, Some considerations on the color of biotite and its relation to metamorphism: Journal of the Geological Society of Japan, v. 65, p. 21-30.

Hepburn, J.C., 1976, Preliminary bedrock geologic map of the Sterling quadrangle, United States Geological Survey, open file report.

_____, Unpublished data, United States Geological Survey, (Worcester North quadrangle).

Hine, R., Williams, I.S., Chappell, B.W., and White, A.J.R., 1978, Contrasts between I- and S-type granitoids of the Kosciusko batholith: Journal of the Geological Society of Australia, v. 25, p. 219-234.

Holdaway, M.J., 1971, Stability of andalusite and the aluminum silicate phase diagram: American Journal of Science, v. 271, p. 97-131.

James, R.S., and Hamilton, D.L., 1969, Phase relations in the system $NaAlSi_3O_8$-$KAlSi_3O_8$-$CaAl_2O_8$ at 1 kilobar water vapor pressure: Contributions to Mineralogy and Petrology, v. 21, p. 111-141.

Kerrick, D.M., 1972, Experimental determination of muscovite plus quartz stability with $P_{H_2O}<P_{Total}$: American Journal of Science, v. 272, p. 946-958.

Luth, W.C., Jahns, R.H., and Tuttle, O.F., 1964, Granite system at 4 to 10 kilobars: Journal of Geophysical Research, v. 69, p. 759-773.

Mehnert, K.R., 1968, Migmatites and the origin of granitic rocks: Elsevier Publishing Company, 393 p.

Norrish, Kenneth, and Chappell, B.W., 1967, X-ray fluorescence spectrometry, p. 201-272, in Zussman, Jack, ed., Physical methods in determinative mineralogy: Academic Press, 514 p.

Osberg, P.H., Moench, R.H., and Warner, Jeffrey, 1968, Stratigraphy of the Merrimack synclinorium in west-central Maine, p. 371-383, in Zen, E-an, White, W.S., Hadley, J.B., and Thompson, J.B., Jr., eds., Studies of Appalachian geology, Northern and Maritime: Wiley, 475 p.

_____, 1979, Geologic relationships in south-central Maine, p. 37-62, in Skehan, J.W., and Osberg, P.H., eds., The Caledonides in the U.S.A., Weston Observatory, Department of Geology and Geophysics Boston College, Weston, Massachusetts, 250 p.

Peacock, M.A., 1931, Classification of igneous rocks: Journal of Geology, v. 39, p. 54-67.

Pease, M.G., and Peper, J.D., 1968, The Brimfield (?) and Paxton (?) formations in northeastern Connecticut: New England Intercollegiate Geological Conference, 60th Annual Meeting Guidebook, New Haven, Connecticut, Section F-5.

Peper, J.D., and Wilson, F.A., 1978, Reconnaissance bedrock geologic map of the Fitchburg quadrangle and part of the Ashby quadrangle, north-central Massachusetts: United States Geological Survey Miscellaneous Field Studies Map MF-959.

_____, Wilson, F.A., and Robinson, G.R., 1978, Emplacement of the Fitchburg granite in the Fitchburg-Ashby area, Massachusetts: Geological Society of America, Abstracts with Programs, v. 10, p. 79-80.

Pomeroy, J.S., 1973, Preliminary bedrock geologic map of the Warren quadrangle, Worcester, Hampden, and Hampshire counties, Massachusetts: United States Geologic Survey, open file report.

_____, 1975, Preliminary bedrock geologic map of the East Brookfield quadrangle, Worcester County, Massachusetts: United States Geological Survey Open-File Report 75-530.

Presnall, D.C., and Bateman, P.C., 1973, Fusion relations in the system $NaAlSi_3O_8$-$CaAl_2Si_2O_8$-$KAlSi_3O_8$-$SiO_2$-$H_2O$ and generation of granitic magmas in the Sierra Nevada batholith: Geological Society of America Bulletin, v. 84, p. 3181-3202.

Rhodes, J.M., 1969, The geochemistry of a granite-gabbro association at Hartley, New South Wales: Ph.D. thesis, Australian National University, Canberra, Australia, 315 p.

Robinson, G.R., 1978, Bedrock geologic map of the Pepperell, Shirley, Townsend quadrangles and part of the Ayer quadrangle, Massachusetts and New Hampshire: United States Geological Survey Miscellaneous Field Studies Map MF-957.

Robinson, Peter, 1967, Gneiss domes and recumbent folds of the Orange area, west-central Massachusetts: New England Intercollegiate Geological Conference, 59th Annual Meeting, Guidebook, Amherst, Massachusetts, p. 114-127.

_____, and Tucker, R.D., 1976, Unpublished reconnaissance data on Winchendon, Ashburnham, Templeton, and Paxton quadrangles: University of Massachusetts, Amherst.

_____, and Belvin, I.E., 1977, Unpublished reconnaissance data on Paxton and Worcester North quadrangles: University of Massachusetts, Amherst.

_____, and Hall, L.M., 1980, Tectonic synthesis of southern New England, p. 73-82, in Wones, D.R., ed., Proceedings: the Caledonides in the USA; IGCP Project 27: Caledonide orogen: Department of Geological Sciences Memoir 2, Virginia Polytechnic Institute and State University, Blacksburg, Virginia, 329 p.

Rodgers, John, 1972, Latest Precambrian (post-Grenville) rocks of the Appalachian region: American Journal of Science, v. 272, p. 507-520.

Skehan, J.W., Murray, D.P., Palmer, A.R., Smith, A.T., and Belt, E.S., 1978, Significance of fossiliferous Middle Cambrian rocks of Rhode Island to the history of the Avalonian microcontinent: Geology (Boulder), v. 6, p. 694-698.

Streckeisen, A.L., 1973, Plutonic rocks - classification and nomenclature recommended by the I.U.G.S. subcommission on the systematics of igneous rocks: Geotimes, v. 18, p. 26-30.

Thompson, J.B., Jr., Robinson, Peter, Clifford, T., and Trask, N.J., Jr., 1968, Nappes and gneiss domes in west-central New England, p. 203-218, in Zen, E-an, White, W.S., Hadley, J.B., and Thompson, J.B., Jr., eds., Studies of Appalachian geology, Northern and Maritime: Wiley, 475 p.

Troger, W.E., 1971, Optiche Bestimmung der gesteinsbilden Minerale, Teil 1, Bestimmungstablellen: 4th edition, E Schweitzerbart'sche Verlangsbuchhandlung, Stuttgart, 181 p.

Tucker, R.D., 1976, Unpublished reconnaissance data on Templeton, Barre, and Wachusett Mountain quadrangles: University of Massachusetts, Amherst.

_____, and Robinson, Peter, 1976-1977, Unpublished reconnaissance data on Gardner quadrangle: University of Massachusetts, Amherst.

_____, 1977, Bedrock geology of the Barre area, central Massachusetts: M.S. thesis, Contribution No. 30, Department of Geology, University of Massachusetts, Amherst, 132 p.

_____, 1978, Contact relations and deformation of the west margin of the "Fitchburg pluton", Wachusett Mountain area, central Massachusetts: Geological Society of America, Abstracts with Programs, v. 10, p. 89-90.

Tuttle, O.F., and Bowen, N.L., 1958, Origin of granite in the light of experimental studies in the system $NaAlSi_3O_8$-$KAlSi_3O_8$-$SiO_2$-$H_2O$: Geological Society of America Memoir 74, 153 p.

Van Der Plas, L., and Tobi, A.C., 1965, A chart for judging the reliability of point-counting results: American Journal of Science, v. 263, p. 87-90.

White, A.J.R., and Chappell, B.W., 1977, Ultrametamorphism and granitoid genesis: Tectonophysics, v. 43, p. 7-22.

_____, Williams, I.S., and Chappell, B.W., 1977, Geology of the Berridale, 1:100,000 sheet (8625): Memoir of the Geological Survey of New South Wales, 138 p.

Wilson, A.D., 1955, A new method for the determination of ferrous iron in rocks and minerals: Bulletin of the Geological Survey of Great Britain, v. 9, p. 56-58.

Winkler, H.G.F., 1979, Petrogenesis of metamorphic rocks, 5th edition: Springer Verlag, 347 p.

Wones, D.R., 1980, A comparison between granitic plutons of New England, USA and the Sierra Nevada Batholith, California, p. 123-130, in Wones, D.R., ed., Proceedings: the Caledonides in the USA: IGCP Project 27: Caledonide orogen: Department of Geological Sciences Memoir 2, Virginia Polytechnic Institute and State University, Blacksburg, Virginia, 329 p.

Wyllie, P.G., Huang, W.L., Stern, C.R., and Maaloe, Sven, 1976, Granitic magmas: possible and impossible sources, water contents and crystallization sequences: Canadian Journal of Earth Science, v. 13, p. 1007-1019.

_____, 1977, Crustal anatexis: an experimental review: Tectonophysics, v. 43, p. 41-71.

Zen, E-an, 1968, Introduction, p. 1-5, in Zen, E-an, White, W.S., Hadley, J.B., and Thompson, J.B., Jr., eds., Studies of Appalachian geology, Northern and Maritime: Wiley, 475 p.

# ADDENDUM

<u>More Precise Locations for Samples of Hornblende Tonalite</u> (see page 33)

MW-4 and MW-5 Collected along the 1050-foot contour on a mound 100 feet north of state highway 62, at a point 1.4 miles west of the junction of highways 62 and 31.

MW-8 Collected along the 940-foot contour, 800 feet due west of a point on calamint Hill Road, that is 0.9 miles south of the junction of Calamint Hill Road and state highway 62.